UNIVERSITÀ DELLA CALABRIA

Scuola di dottorato in "Scienza e tecnica"

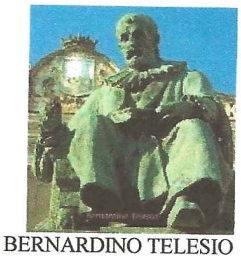

BERNARDINO TELESIO

UNIVERSITA' DEGLI STUDI DELLA CALABRIA

Scuola di Dottorato B. Telesio

Dottorato in:

Scienze e Tecnologie delle Mesofasi e dei Materiali Molecolari

Ciclo XXIII

Settore Scientifico Disciplinare FIS01

TiO_2 NANOTUBES IN THE NANOTECHNOLOGY

PHD. STUDENT:
LETICIA JIMENEZ

COORDINATOR
PROF. CARLO VERSACE

SUPERVISOR
PROF. CARLO VERSACE

Abstract

During the last years the nanotechnology is currently field of research, demand for new sources of energy, the control of modulation of the light is a challenger for a researches, in this way, the applications in this field are broad and multidisciplinary. Due to the wide range of applications interesting field of a research.

Anodically fabricated TiO_2 nanotube arrays have attracted significant attention in the scientific community because it has proven to be a robust and cost-effective functional material, widely investigated in many applications especially those related to energy conversion such as photoelectrochemical water splitting and solar cells. However, the properties of this material must be modified in order to increase its energy conversion efficiency. For example, the wide band-gap of TiO_2 (~ 3.0 eV for rutile and 3.2 eV for anatase).

My challenger in this research, was found to apply in the nanotechnology as metamaterials, surface plasmon polariton(SPP) also I tried to improved the TiO_2 nanotubes changing the temperature for example more long or short, depend if, I need full with different materials LC, or metals, depending on the size of the molecule.

Contents

INTRODUCTION

Materials consisting of nanostructures or possessing morphology at the nanoscale are commonly found in nature. The reader's body contains nanomaterials such as proteins and DNA.

Nanomaterials are also found in smoke from fires, in volcanic ash, in sea spray.

But what is the different the past two or three decades, is an explosive increase in our ability to fabricate nanostructures and nanosystems with a great grade of control.

Our system very simple, and versatile Titanium oxide TNA(Titanium nanotubes arrays), although relatively recently discovered [1], Ti spattered in glass slides for obtain an transparent area by anodic chemical process, we obtained a high order or nanotubes, have already shown great promise regarding solar energy harvesting application[17,12,80,90], as well as in the hot subject of investigation exhibiting very good photocatalytic, photovoltaic and optical properties. By chemical process anodization we used viscous electrolytes for made up nanotubes.

Varying the temperature, sputter deposition anodization time, we observed as this system is very sensitive at changes in the shapes TiO_2 nanotubes.

Because a TNA is highly porous and anisotropic, and its nanostructure can be engineered to form a variety of useful shapes, there has been recent interest in these new materials. They can be infiltrated with[102] liquids, liquid crystals, organic monomers etc, and these infiltrated media can alter the host optical properties predictably. Thus, they can act as optical sensors for the detection and quantification of chemical, biological, and nuclear media. Other envisioned

In 1999, Zwilling and co-workers achieved self-organized porous TiO_2 by anodizing a Ti-based alloy in an acidic, fluoride-based electrolyte [49,50]. In 2001, Gong and co-workers fabricated self-

organized, highly uniform TiO_2 nano- tube arrays by anodizing Ti in aqueous dilute HF electrolyte [41, 42]. Maximum nanotube lengths in this first synthesis generation were approximately 500 nm. In subsequent work, the second-generation, the nanotube array length was increased to approximately 7mm by proper control of the anodization electrolyte pH thereby reducing the chemical dissolution of TiO_2 during anodization [43, 46]; the pH should be high but remain acidic. In later work, the third-generation, TiO_2 nanotube arrays with lengths of up to approximately 1000mm were achieved using a non-aqueous, polar organic electrolyte such as formamide, dimethylsulfoxide, ethylene glycol or diethylene glycol [44, 51–54].

Other interesting working publication about the news use and shapes Ursaki [104],TiO_2 nanotubes with high aspect ratio were successfully fabricated by using anodization of Ti foils in ethylene glycol based electrolytes. By tailoring the anodization voltage and the electrolyte composition, TiO_2 NTs with different inner and outer diameters can be produced, however, the spatial density of nanotubes is also changed in these processes.

It has been recently shown that the variation of electrolyte temperature allows the controlled modification of the inner diameter of the TiO_2 NTs in the range from several tens to hundreds of nanometers, while maintaining a nearly constant density and outer diameter . The production of NT arrays with a controlled (e.g.modulated) inner diameter is of considerable interest for the elaboration of photonic crystals[104]. In addition to traditional applications of titania nanostructures, it has been recently proposed to explore possibilities for photonic applications of titania nanotube arrays.

In this decade there have been many studies about tailoring, TiO_2 whit different metals, or vise-versa i.e, for different uses, the research study different shapes from TiO_2 nanotubes, in this way their possible applications, in the hot topics, surface plasmonics Huang[105] Plasmonics, an emerging branch of nanophotonics, concerns properties of collective electronic excitations(known as surface plasmons) in films or nanostructures of noble metals (especially Au and Ag).

Based on the interactions between light and conduction electrons at the metal thin films or in the

metal nanostructures, the surface plasmons lead to nearfield localization of the light into subwavelength dimensions.

The strong spatial localization of light enables many important applications of surface plasmons: nanophotonic devices and circuits; molecular-specific biological sensing, imaging, and photothermal therapy; nanolithography; surface plasmon tweezers; and metamaterials.

The surface plasmon-based nanophotonic circuits can carry optical and electric signals through the same thin metal circuitry. This feature makes it possible to combine the superior technical advantages of both photonics and electronics, and allows.

Metal nanostructures can be coated with an additional layer of a different material (metal, dielectric, or semiconductor) to form core/shell structures.

We[104] produced Au/TiO_2 core/shell nanoprism arrays by depositing conformal TiO_2 shells onto the surfaces of the Au nanoprisms With a high refractive index that depends on the crystal structure, TiO_2 is a commonly used optical material.

We present also the preparation of SiK nanotubes or macrotubes by easy form.

Dimensionality plays a critical role in determinating the properties of materials due to, for example, the different ways that electrons interact in three dimensional, two dimensional, and one dimensional structure.

CHAPTER 1

Carbon nanotubes

Carbon nanotubes are molecular-scale tubes of graphitic carbon with outstanding properties. They are among the stiffest and strongest fibres known, and have remarkable electronic properties and many other unique characteristics. For these reasons they have attracted huge academic and industrial interest, with thousands of papers on nanotubes being published every year. Commercial applications have been rather slow to develop, however, primarily because of the high production costs of the best quality nanotubes.

Structure

The bonding in carbon nanotubes is sp^2, with each atom joined to three neighbours, as in graphite. The tubes can therefore be considered as rolled-up graphene sheets (graphene is an individual graphite layer). There are three distinct ways in which a graphene sheet can be rolled into a tube, as shown in the diagram below.

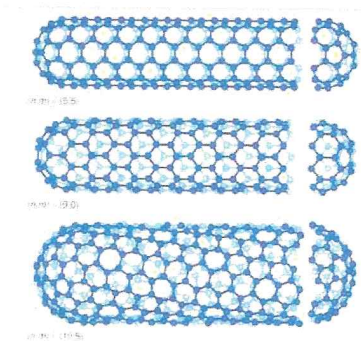

The first two of these, known as "armchair" (top left) and "zig-zag" (middle left) have a high degree of symmetry. The terms "armchair" and "zig-zag" refer to the arrangement of hexagons around the circumference. The third class of tube, which in practice is the most common, is known as chiral, meaning that it can exist in two mirror-related forms. An example of a chiral nanotube is shown at the bottom left.

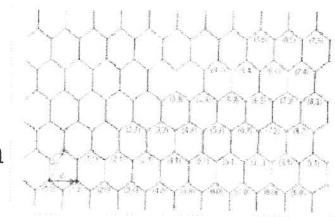

The structure of a nanotube can be specified by a vector, (n,m), which defines how the graphene sheet is rolled up. This can be understood with reference to figure on the right. To produce a nanotube with the indices (6,3), say, the sheet is rolled up so that the atom labelled (0,0) is superimposed on the one labelled (6,3). It can be seen from the figure that m = 0 for all zig-zag tubes, while n = m for all armchair tubes.

Synthesis

The arc-evaporation method, which produces the best quality nanotubes, involves passing a current of about 50 amps between two graphite electrodes in an atmosphere of helium. This causes the graphite to vaporise, some of it condensing on the walls of the reaction vessel and some of it on the cathode. It is the deposit on the cathode which contains the carbon nanotubes. Single-walled nanotubes are produced when Co and Ni or some other metal is added to the anode. It has been known since the 1950s, if not earlier, that carbon nanotubes can also be made by passing a carbon-containing gas, such as a hydrocarbon, over a catalyst. The catalyst consists of nano-sized particles of metal, usually Fe, Co or Ni. These particles catalyse the breakdown of the gaseous molecules into carbon, and a tube then begins to grow with a metal particle at the tip. It was shown in 1996 that single-walled nanotubes can also be produced catalytically. The perfection of carbon nanotubes produced in this way has generally been poorer than those made by arc-evaporation, but great improvements in the technique have been made in recent years. The big advantage of catalytic synthesis over arc-evaporation is that it can be scaled up for volume production. The third important method for making carbon nanotubes involves using a powerful laser to vaporise a metal-graphite target. This can be used to produce single-walled tubes with high yield.

Properties

The strength of the sp^2 carbon-carbon bonds gives carbon nanotubes amazing mechanical properties. The stiffness of a material is measured in terms of its Young's modulus, the rate of change of stress with applied strain. The Young's modulus of the best nanotubes can be as high as 1000 GPa which is approximately 5x higher than steel. The tensile strength, or breaking strain of nanotubes can be up to 63 GPa, around 50x higher than steel. These properties, coupled with the lightness of carbon nanotubes, gives them great potential in applications such as aerospace. It has even been suggested that nanotubes could be used in the "space elevator", an Earth-to-space cable first proposed by Arthur C. Clarke. The electronic properties of carbon nanotubes are also extraordinary. Especially notable is the fact that nanotubes can be metallic or semiconducting depending on their structure. Thus, some nanotubes have conductivities higher than that of copper, while others behave more like silicon. There is great interest in the possibility of constructing nanoscale electronic devices from nanotubes, and some progress is being made in this area. However, in order to construct a useful device we would need to arrange many thousands of nanotubes in a defined pattern, and we do not yet have the degree of control necessary to achieve this. There are several areas of technology where carbon nanotubes are already being used. These include flat-panel displays, scanning probe microscopes and sensing devices. The unique properties of carbon nanotubes will undoubtedly lead to many more applications.

Review TiO_2 nanotubes

Si nanotubes

SURFACE PLASMON POLARITON

Titanium was discovered in 1791 by W. Gregor[25], identified and named in 1794 by H. Klaproth, and

isolated in an impure form by Berzelius in 1825. The metal was purified in 1910 by Hunter but substantial quantities of metallic titanium became available only after the industrial adoption of the Kroll process, in 1949. High-purity titanium has been prepared in small amounts since 1925 by the so called "iodide process" (thermal dissociation of titanium iodides) [26].

In view of its position in the periodic table and its electrochemical behaviour, titanium was classified as a "film-former", i.e., a metal whose surface is always covered with natural oxide film when exposed to air, water or other oxygen containing media. Titanium shares that classification with many other metals notably Ta, Nb, W, Al, etc. The natural oxide film on titanium ranges in thickness from 5 to 70 A, depending on the composition of the metal and the surrounding medium ,the maximum temperature reached during the working of the metal, [27,28].The nature of that oxide film is controversial; it has been reported to consist of TiO_2 rutile [26], anatase [29], or lower amorphous oxides [26]. Different conditions, and the oxide composition may also depend on the purity of the metal.

Titanium is a very reactive metal; nevertheless, it exhibits a high resistance to corrosion, which

should be attributed to the protective effect of the surface oxide films, and in particular TiO_2, are inert with respect to most natural environment and many chemicals

Corrosion is believed to occur through "weak spots in the oxide; a forced increased in films thickness(e.g., by electrolytic or thermal oxidation) would eliminate such weak spots and could increase the corrosion resistance.

Many electrolytes, under different condition, have been used for the anodic oxidation of titanium and its alloys; data on the electrolyte,use of viscous electrolytes.

Although the general rules governing the anodic oxidation of titanium are roughly the same as for other valve metals (i.e., the ionic current during anodic polarization leads to film formation, and the relatively great contribution, of ionic current is probably associated with the high heats of formation of the respective oxides [30,31]) the controversial data on the composition and structure of the anodic films on titanium.

The exact nature of the breakdown of anodic oxide films, which occurs above certain critical potentials, is controversial, but in all cases it involves a loss of passivity and in certain cases it leads to pitting of the metal.

Titanium is different in this respect; breakdown voltages are spread over a wide range, reproducibility is poor even if great care is take similarity condition, in the case of titanium the breakdown voltage is strongly affected by the nature of the electrolyte [32,33,34].

Metallic titanium exists in the close-packed hexagonal ("alpha-phase") or body-centredcubic("beta-phase") forms. In alloys, aluminium and tin as well as oxygen and nitrogen stabilize the cph structure, while V, Cr, Mn, Fe, Mo, Si, Zr and Nb stabilize the bcc form. Titanium dioxide has tree known modifications (rutile,anatase,and brookite), and there are a number of lower oxides, notably TiO and Ti2Oa.

Agree that the anodic film on titanium consistsof TiO_2; however, it has been reported that the anodic oxide is oxygen-deficient [35, 36, 37],while some authors believe that oxygen is in excess.

The refractive index of the film depends on its structure, and generally corresponds to that of the observed crystalline modification of TiO_2 Koyama [135] reports a value of 2.2 to 2.5.

The film exhibits intense interference colours, which depend on the formation voltage, the composition composition of the metal, the formation voltage, the composition of the metal, the formation temperature, etc.[38].

Anodic oxidation is a commonly used surface treatment, especially on aluminium alloys for structural applications. Its aim to improve the corrosion or wear resistance, the external aspect, and ability for adhesive bonding. The formation and structure of the anodic films on those alloys has been extensively studied[39,40], and even if the detailed mechanism are still under discussion, the different steps involved during their electrochemical construction are well defined. The application of anodic oxidation to the surface preparation Since Zwilling [1], and co-workers have shown for the firsttime the ability to grow self-organizedIn CA electrolytes, addition of fluoride ionic species to the electrolyte is necessary to obtain porous structure on Ti and TA6V.The respective thickness of both layers is different for the two materials: the compact layer is very thin on aluminium alloys, but may reach more than 50 nm on alloyed titanium.

nanotubes by anodic oxidation of polycrystalline Ti-foils and its alloys , several electrochemical approaches have been investigated to improve the structure as well as the functionality of TiO_2. Other researches P. Schmuki and co-workers have made a extensive research, many about the growing eletrochemical formation, properties and application, [3] particularly the case of TiO_2 stimulated significant research activity as TiO_2 is a material with a number of almost unique properties used for many years in various functional applications.

For Ti and other so-called valve metals it has been known for more than 50 years that it is possible to grow compact oxide layers of considerable thickness by anodization in aqueous electrolytes [41,42].The structure of the as grown oxide can be amorphous or crystalline, strongly depend on the specific electrochemical parameters such such as the applied potential, the time anodization, or the sweep rate of the potential ramp.

Depending on the anodizing conditions the crystal structure has been reported to be anatase [43–44], a mixture of anatase and rutile[43–44], or rutile.

A completely different growth morphology can be obtained, if fluoride ions are present in

electrolytes and suitable anodization condition are used. Ordered nanotubular/nanoporous structure of TiO_2 or other transition metal oxides can be formed, in general, the morphology and the structure of the porous layers are affected strongly by the electrochemical conditions (particularly the anodization voltage) and the solution parameters (in particular the HF concentration, the pH and the water content in the electrolyte).

The first generation of the TiO_2 nanotube arrays was grown in HF electrolytes or acidic HF mixtures[1–46].The key factor controlling the tube diameter is the anodization voltage [46,47]. Particularly in the case of TiO_2 nanotubes layers, a wide variety of nanotube diameters can be achieved.For anodization experiments carried out in 1 MH3PO4 + 0.3 wt% HF it has been shown that the tube diameter can be grown in the range of 15–120 nm in the potential range between 1 and 25 V [46].Recently, for mixed glycerol–water electrolytes containing 0.27 M NH4F, the tube Diameter range was further extended from 20 up to 300 nm in the potential range between 2 and 40 V [47].

Crystallographic [3]structure As-formed TiO_2 tubes typically have an amorphous structure. Several studies show that the tubes can be converted structure. Several studies show that the tubes can be converted 280°C in air [48–50] or a mixture of anatase an drutile at temperatures higher than approximately 450°C [48,49]. Most recently, there are indications that already in the as-formed tubes under certain conditions nano-crystallitescan be present [47,51].

Recently, it has been reported that the nanotube layers have an unusually high reactivity [52,53], i.e. the TiO2nanotube system intrinsically is active toward oxygen adsorption [52]a feature not observed on other, pure anatase or rutile material.

Particular advantages [3]of regular tube arrays, the defined geometry result in a narrow distribution of diffusion paths. Certain TiO_2 applications require specific crystallographic structure for an optimized performance
structures for an optimized performance. For example anatase form of TiO_2 shows the highest solar energy conversion efficiency [54,55] and has also the highest activity for catalysis [56,57]. A main challengeregarding the exploitation of TiO_2 in photochemical applications is the large band gap of

TiO_2 making photoinduced reactions only possible at excitation <400 nm.Two key approaches to achieve this are dye-sensitization [54,55]and so-called doping with species that essentially reducethe band gap of the material [58].

the TiO_2 nanotubes, but this researches made too differents architectures[4]Ti metal sheet in dilute fluoride electrolytes at a certain voltage for a given time. Novel morphologies such like bamboo-type

reinforced nanotubes and two-dimensional(2D) nanolace sheets can be obtained if the anodization process is carried out under specific alternating-voltage. The key to this approach is exploiting the fact that, during the initial stages of anodization, two fundamentally different oxide morphologies grow successively on the Ti surface. In the first stage, a compact anodic oxide is formed, and only after a certain period of time does the grown of order nanotubular structure take place.

Very interesting geometric modifications of the tube geometry (tube diameter, wall morphology) could be obtained[5],in order to maximize the aspect ratio of the nanotubes using ethylene glycol based electrolytes and investigate the morphology dependence on the applied potential, concentration of fluoride ions and time.

The resulting geometry of the nanotubular layer depends strongly on the applied potential and the HF concentration.

It was found that the formation mechanism of TiO_2 nanotubes is similar to the porous alumina case

under high electrical field. As a result, combining the electrochemical parameters in an optimal way, ordered TiO_2 nanotube layers.

The similar work nanotubes with a so-called bamboo type morphology can substantially increase the conversion efficiency of NT-based DSSCs.

Bamboo-type tubes[8] as well as conventional smooth-walled tubes were prepared

electrochemically by controlled anodization of Ti, using appropriate alternating voltage cycling allows a switch between condition that enable tube growth and condition leading compact layers Essentially, at each voltage step can compact connecting layer is formed in between the tubes and a bamboo type of structure can be grown. Thus by using different AV pulse duration the

distance between the stratification layers can be adjust.

In order tomaximize the aspect ratio of the nanotubes[5].Using ethylene glycol based electrolytes

and investigate the morphology dependence on the applied potential, concentration of fluoride ions and time

The interesting result show that the growth of more than 250 μmthick self-organized TiO_2 nanotube layers is possible, using an electrochemical approach in organic electrolytes. The tubes can grown as a hexagonal close packed pore arrays Crucial parameters that decide on the dimensions are the fluoride ion concentration, the voltage and the anodization time. Self organized tube formation restricted to a critical parameter range.

The applications for the nanotechnologies, medicine, biology, for environment for uses as solar cell, for her the most active photocatalytic properties.

In her worker about this researches TiO_2 nanotubes her study the properties with different annealing temperatures shows the photoresponse [6], From the SEM pictures it is clear that no morphological changes appear in the porous structure after a thermal treatment for 1 s at 450 °C in air or dry Ar. However, if the anneling treatment is carried at 450°C in Ar and the sample is held at this temperature, the morphology changes. Such changes are not observed when the annealing procedure is carried out in air.

process, and when the temperature change the structure amorphous to crystalline anatase or rutile depend of the temperature anneling.

Also to study the wetting behaviour in this case, change the properties of the TiO_2 nanotubes uses a Electrochemical treatment. Technological applications of self-organized porous media target the use of the high order or the high surface area of the structures in the optical field or for catalysis. Another potential application is based on controlling the surface wettability and has attracted significant scientific interest particularly for biological systems. The reason for this interest is that adsorption[6], DNA and proteins as well as cell adhesion on the surface.

The possibility to modify and control the surface wettability of different materials has attracted significant scientific and technological interest.

were mechanically ground, lapped and finally mirror[7].Schmuki and ko-workers also study the alloys with metals end TiO_2 nanotubes [9]for enhanced photocatalytic activity, as is influenced the morphology of TiO_2 nanotubes with of quantity of water content in the electrolyte on nanotubes morphologies and the mechanism of rib formation[10,11].

Titanium was anodized in 0.2M NH_4 F/glycerol electrolytes containing between <1 and 50% by volume of water.

The increase in current density for anodizing in electrolytes with water contents >10 vol.% is at least partially due to oxygen gas generation at the anode. The oxygen evolution reduces the charge available for film grown, resulting in shorter nanotubes.

Grimes made up nanotubes [12]. Innovations in materials technology in the fields of photovoltaics and photocatalysis play a key role in the paradigm shift from fossil fuels to renewable sources. Economically viable and stable Titania nanotube arrays for dye-sensitized solar cells

Others[1,2,3,4,6] have shown thatdye-sensitized solar cells DSCs, fabricated using titania nanotube arrays (TNAs) grown on titanium foil, have charge-collection and light-harvesting efficiencies 25 and 20% higher, respectively, corresponding nanoparticle-based DSCs.

Efforts to fabricate [12], transparent nanotube arrays for DSC applications have been limited to short nanotube arrays using titanium deposited at high temperatures. Although transparent nanotube arrays of extended length, that is, lengths.

with a lengths about 0.3 and 33.0 μm, by sputtering on FTO glass, in the first time Grimes started this investigation only sputtering on glass [13] with successful.

And her extensive research Grimes [14], reported ultra long nanotubes about 1000μm grown in foils of Ti, of electrolytes containing different concentrations of NH_4F and H_2O in EG at 60 V.optimum concentration of water for achieving the highest growth rates for different NH_4F concentration. Also Grimes' group[15], make up different dimension nanotubes pore size, wall thickness, different diameter, using different cations [16] they found the cation choice to be a key

parameter influencing both the nanotube length, with the length and aspect ratio of the nanotubes increasing cation size.

In this way Grimes' group concentrate in the solar cell, in the work about nanotubes review[17], The key processes responsible for anodic formation of nanoporous titania appear to be the same, and are fundamental to the formation of straight.

The key processes are: (1) Oxide growth at the surface of the metal

(2) Metal ion (Ti4+) migration from the metal at the metal/oxide interface; Ti4+ cations will be ejected from the metal/oxide interface under application of an electric field that move towards the oxide/electrolyte interface. (3) Field assisted dissolution of the oxide at the oxide/electrolyte interface. Due to the applied electric field the Ti–O bond undergoes polarization and is weakened promoting dissolution of the metal cations. Ti^{4+} cations dissolve into the electrolyte, and the free O_2-anions migrate towards the metal/oxide interface, to interact with the metal[59,60]. (4) Chemical dissolution of the metal, or oxide, by the acidic electrolyte also takes place during anodization. Chemical dissolution of titania in the HF electrolyte plays a key role in the formation of nanotubes rather than a nanoporous structure.

The properties of titania depend on the crystallinity and isomorphs type. Anatase phase is preferred in charge separation devices such as DSSCs, while rutile is used predominately in gas sensors and as dielectric layers. Rutile has minimum free energy in comparison to other titania polymorphs hence given the necessary activation energy all other polymorphs including anatase transform into rutile through first-order phase transformation.

However, the temperature at which metastable anatase to stable rutile transformation takes place depends upon several factors, including impurities present in the anatase, primary particle size, texture and strain in the structure. In the diffraction patters, the anatase phase starts appearing at a temperature of 280°C. As the 250°C annealed sample, it is clear that tha sample was crystallized in anatase phase at a temperature between 250 and 280°C. At a temperature near 430°C rutile phase appears in the X-ray diffraction pattern.

Beyond this temperature, the rutile (1 1 0) peak grows whereas the anatase (1 0 1) peak diminishes. Complete transformation to rutile occurs in the temperature range 620–680°C. 580°C and they fully vanish at around 680°C. This shows that the oxidation followed by crystallization of titanium support takes place at these temperatures.

.With respect to variation of the size of the anatase and rutile crystallites with temperature, it was found that the anatase grain size initially increases

with temperature but between 480 and 580°C the grain size decreases to increase again after 580°C. At the same time the grain size of rutile progressively increases with temperature after its nucleation. At 430°C a rutile fraction of 31% compared to anatase was formed. It increased to 75% at 480°C and further to 92% at 580°C on annealing for 3 h at this temperature. It was observed that at temperatures in the range 550–580°C depending on the sample, small protrusions come out through the porous structure. Above this temperature the tubular structure completely collapsed leaving dense rutile crystallites.

The as-anodized titania films fabricated from a Ti thin film deposited on glass, having an extremely thin discontinuous metal layer underneath the nanotubes, were anneled at 260°, 280° and 500°C for 6 h in dry oxygen ambient.

Their GAXRD patterns showed only one exception, the absence of rutile phase in the thin film samples annealed at 500°C [19]. This result is in striking contrast to that found with nanotube arrays formed from Ti thick-film foils, where an earlier study noted that rutile phase appears at 430°C and both rutile and anatase co-exist till around 620°C. However, we find that thin film samples with a continuous metal layer underneath the nanotubes behave in way similar to that the foil samples,with both rutile and anatase phases co-existing at 480 1C. These results support the hypothesis that rutile grows at the interface between the barrier layer and titanium metal where the metal is thermally oxidized. The constraints imposed by the nanotube walls make it difficult for the anatase crystals situated there to undergo phase transformation to rutile.

Optical properties of titania nanotube arrays[62]. The titania nanotube arrays can be grown over a

wide range of pore diameters, wall thicknesses, lengths, and chemical composition with each topology showing different light absorption and photocatalytic properties leading to different values of photoconversion efficiency. It became evident that knowledge of the light-absorbing behaviour of the various nanotube array geometries prior to sample fabrication would be desirable. Therefore, the computation electromagnetic technique finite difference time domain (FDTD) [63] was used to simulate the light-absorbing properties of the nanotube arrays as a function of feature size [64]. The simulations were performed for titania nanotube array films with no metal layer underneath the nanotubes (transparent, Type-I) and also for the nanotubes grown on titanium foil (opaque, Type-II). Note that in the former case, Type-I, the glass substrates were not included in the simulations and hence the nanotubes film can be considered self-standing. The FDTD space was terminated with an absorbing boundary condition (ABC) made of a uniaxial perfect matching layer [65] to eliminate field reflection from the computational boundaries. The Type-II model contains a perfect electrical conductor layer at the bottom of the nanotube array to represent the titanium layer. Therefore, in the case of Type-I, transmittance and in the case of Type-II, reflectance are used to determine the absorbance of light by the nanotube array. In all simulations reported to date the distance between two adjacent tubes was taken as 10 nm.
The validity of the FDTD simulations were established by comparison of the calculated and experimentally measured transmittance of a Type-I film of different porosity.
The tube length, pore diameter, wall thickness, and barrier layer thickness are, respectively, 1000, 100, 20, and 100 nm. shows the wave originating from the source and moving towards the nanotubes. When the wave front hits the top surface of the nanotube array, most of the incident energy is transmitted into the nanotubes with a negligible portion reflecting back.
nanotube array to reach the barrier layer, show the wave reflecting back from the conducting Ti layer at the bottom of the nanotube array. Note that the reflected wave contains multiple wave

fronts as the derivative Gaussian pulse contains radiation over a wide frequency range; the individual frequencies travel at different velocities through the barrier layer and nanotube array due to the frequency-dependent variation in the titania permittivity. The measured absorbance spectrum of a titania nanotube array (length—200 nm, pore size—22 nm, wall thickness—13 nm and barrier layer thickness—100 nm) was compared with the simulated results [120]. Both curves were found similar except that the absorption edge of measured spectra is shifted slightly to the higher wavelength region compared to the simulated spectra. This is due to the fact that the barrier layer has rutile crystallites and the nanotube walls consist of anatase crystallites.

The band gap of the rutile is lower (3.0 eV) compared to the anatase (3.2 eV). The rutile phase at the barrier layer leads to the shifting of the absorption edge to higher wavelength, a property not taken into account by the FDTD simulations.

With respect to the applied properties of Type-II samples, it should be noted that to induce crystallinity the nanotube array samples are annealed at elevated temperatures in an oxygen environment. The diffusion of oxygen into Ti foil is consistent with the Fick's second law, hence a gradient in the oxide composition exists from the top of the barrier layer to the Ti metal . Consequently there is a gradient in the complex permittivity spectrum of the oxide layer underneath the nanotubes and hence light is bent before it is reflected back from the metal. This gradient was considered during the simulation process by linearly increasing the permittivity values of the barrier layer so the permittivity at the

The transmittance of light through self-standing titania nanotube array films (Type-I) are calculated as a function of tube length while keeping wall thickness, pore diameter, and barrier layer thickness constant. The transmittance reaches a value over 95% at wavelengths greater than 380 nm.

The optical behavior of the TiO_2 nanotube arrays is quite similar to that reported for mesostructured titanium dioxide. The difference in the envelope magnitude encompassing the interference fringe

maxima and minima is relatively small compared to that observed in titania films deposited by RF sputtering, e-beam and sol–gel methods.

The absorbance (or optical density) of the films were estimated from the transmittance 'T' using the relation: $A=-\alpha\log(T)$. Here them assumed that all the incident light is either transmitted or absorbed, reflection or scattering being negligible. The Napierian absorption coefficient of the sample was calculated using Lamberts law, a $\alpha=2.303(A/d)$

used this information Grimes' group calculate too, the refraction index,the porosity of the nanotube array with this information. A profound research about[17], nanotubes arrays.

In this work explain as, improves the starting titanium material. As by restricting the solid angle through which light can be reflected restricting from the surface and leave the device one can imagine that a certain fraction of the reflected light, and be available again for the electron-hole generation.

Grimes explain[18], about the last resourches, and application of nanotubes, for uses in the solar cells.

[19], calculated the optical properties constants through of the transmission analysis, thickness of film, refraction index, absorbance with Manifacer's method [21].

Other interesting work has been madding for Krishnan[22]And Co-workers, them made TiO2 nanotubes with a pulses voltages, and her results, with this changes her nanotubes are formed in better self-organized arrays under pulse anodization than their counterparts grown at constant anodization voltage, this better nanotubes morphology have to better photoelectrochemical response, the photocurrent densities for the nanotubes of TiO_2 films obtained by pulse anodization. Grimes' group too make divers experiment with dimethyl sulfoxide (DMSO), showing as is possible make very easily long nanotubes [23,24].To increase the nanotubes length, it is necessary to both reduce the chemical dissolution of the oxide at the pore mouth The presence of DMSO modifies the space charge region in the pores.

Also explain as the longer depend of the voltage, but the result in this work, if the voltage is high Ti 70 or 80V, films dissolve into the electrolyte after 24 h.

Depending upon the anodization voltage, the inner pore diameters of the resulting nanotubes arrays

range from 20 to 150nm.

Z. Sadek Abu published a work about nanotubes [66] obtained with successful TiO_2 nanotubes by sputtering on glass/ITO/Ti for anodization chemical process,

the use of foil limits their potential applications, particularly in the fabrication of microscale devices. The type of substrate is an important factor in the morphological formation and lattice orientation of Ti films. In the deposition temperature, the stress mismatch of the substrate and Ti films, and the type of deposition all affect the films which in return a morphologic.

About this take advantage of, TANG Yu-xin [69] and co-workers by RF magnetron sputtering on glass substrate at room temperature, Anodization was conducted in different HF concentrations ranging from 0.1% to 1.0% (mass fraction).

Effect of sputtering parameters on microstructure of titanium films.In order to find out the suitable deposition parameters to fabricate dense and uniform titanium film by the RF, we found that thickness of Ti films increases gradually, while the dense of Ti films decreases with the increase of sputtering pressure (pw).

The usage of multistep anodization or altering the water contentTiO_2 nanotubes for uses as the fabrication of microscale devices solar cell, if as the nanotubes are anchorage her uses is better for uses as solar cell the advantage in the production energy[12], conversation efficiency ranged from 70 to 80% for wavelengths between 450 and 650 nm.

Others researches groups as Wilaiwan [67] and co-workers made experiments used few organic, obtaining with successful oriented nanotubes, used pulse anodization, they reported effect of pulse anodization,In this paper, pulse anodization is show to result in better-defined nanotube

Another finding was that the nanotubes prepared by pulse anodization were shorter than those under constant voltage.

These results demonstrate that, at 0 V, the main effect is that of fluoride ions at the outer interface

by formation of highly soluble TiF6 effect is that of fluoride ions at the outer interface (oxide/electrolyte) that dissolve the TiO_2 surface by formation of highly soluble $TiOF_6$,

It is worth noting that long t_0 periods promote the increase of the barrier layer that in turn decrease the growth rate of the nanotubes arrays.

Morphologies than in the constant voltage growth mode. The resultant TiO_2 nanotube arrays show a higher quality of photoresponse than those grown via the continuous anodization route. Important mechanistic are also furnished by this data. Careful tuning of the pulse duty cycle end the negative voltage limit point toward the importance of chemical (corrosion) processes during nanotubes growth as well as surface passivation effects introduced by the adsorption of electrolyte species processes during nanotube growth as well as surface

M. M Hasan [2], and co-workers made study about TiO_2 films sputtering by RF magnetron, sputtering, in this paper the authors, uses different technical for analyser.

Her studies about this film, we explain how a variation of the index diffraction with the annealing to different temperature, and to made the spectroscopy analysis, of X rays for analyser the phases anatase, and rutilo and her properties.

In her conclusion: he explain when the temperature changes the properties of TiO_2 and calculation the band gap, and the variation with the temperature increase from 3.39 to 3.42 eV with increase of the annealing temperature.

Other works about naotube, but in this case Xiaofen [68] obtained nanotubes and nanoporus by Ti sputtering on silicon. Ti film (~100 nm) was deposited on a silicon wafer substrate by DC magnetic sputtering. Anodization in neutral electrolyte was conduced at room temperature.

changed remarkably with the anodization time, concentrations for the electrolytes and applied voltage amplitude.

The porous surface exhibits connecting pores with the average diameter of 25 and interpore distance fo 40 nm. The porous titanium film on silicon substrate formed

average diameter of 25 nm and interpore distance of 40 nm.

The formation mechanism[70], of a thin film of self organized TiO_2 nanotube arrays prepared by

anodic oxidization of a pure titanium sheet in electrolyte solutions containing potassium fluoride and sulphate was investigated though near-real time monitoring the anode mass, the current density, and the surface topography during anodization

electrolyte solutions containing potassium fluoride and sulfate was investigated through near-real time monitoring the anode mass, the current

With the protection of the oxide layer, long nanotubes could be formed in electrolyte solutions with relatively high pH. The surface composition analysis indicates that the nanotubes were not totally oxidized to TiO_2.

In order to investigate the influence of the water content in the organic electrolyte[71], we have carried out a detailed investigation of the effect of water content on the electrochemical anodization of Ti in electrolytes consisting of ammonium fluoride, water, and ethylene glycol.

The mechanisms of the effect of the water content on the diameter and growth rate revealed here should establish a basis for further optimization.

In the last time, focused for others, structure [103], used the same principle chemistry, anodization of Ti sheets in an ethylene glycol an HF containing electrolyte allows one prepare TiO_2 TNs (Titania nanotubes) with controlled inner diameter. The diameter can be varied in a controlled fashion in the range from 10nm to more than 250nm through the change of the electrolyte temperature from -20 °C to +50°C. The anodization process with the electrolytes temperature below 0°C result in the production of closely packed TiO_2 TNs with hexagonal transverse section

An important feature of the Ti anodization process at electrolyte temperature under 0°C is the self – arranged ordered porous structure at the top surface.

In the last time other news experiment for improve the TiO_2 nanotubes, in this way Grimes' group[106], made up the news, development of various methods for the synthesis of crystalline TiO_2 nanoarchitectures. Among the widely used processing routes to fabricate crystalline TiO_2 are hydrothermal, sol-gel, and calcination processes. However, crystallizationby hydrothermal

treatment is not convenient, as it leads to a strong reduction of the textural properties due to excessive coalescence of the inorganic framework, and structural damage results when hydrothermal

treatment is performed on mesostructured titania. With calcination, the thusgeneratedTiO_2 crystals are usually too large to be accommodated with in mesopore walls, resulting in structural collapse. In alternative strategies, organic additives were extensively used to control the morphology and growth mechanisms of various crystalline nanoarchitectures.

This relative gradual improvement in crystallinity and morphology as we go from EG to EG encouraged us to investigate an even higher molecular weight polyol compound. The nanotubearrays fabricated in PEG-containing electrolytes showed the formation of crystalline nanotube arrays over the whole entire range of applied voltages (40-80 V),

Themorphology of the nanotube arrays fabricated at 80 V (1.05 μmlong) Note that the poremouths of the as-fabricated tubes were completely free of precipitate often seen some time or another.

The nanotube length was found to decrease with increasing chain length of the polyol Electrolyte. This can be related to the increase in viscosity of the electrolyte as its molecular weight increases which in turn results in slower reaction kinetics. However, on the

positive side, the high viscosity of these electrolytes improves the quality of the resulting nanotube films by affecting the degree of oxide dissolution at these high positive potentials.

The intensity of the anatase (101) reflection was found to increase with increasing the molecular weight of the electrolyte.

Effect of Water Content.

the amount of water added to the solvent during the fabrication of TiO_2 using various routes, but not yet the anodization route, is crucial in promoting the formation of anatase phase. To explore the validity of this assumption too ur fabrication route and to understand the possible role of H_2O in the synthesis of anatase TiO_2 nanocrystals, we systematically

changed the amount of H_2O added in the reaction system and characterized the corresponding final nanoarchitectures.

The effect of water can be understood on the basis of the mechanistic formation of TiO_2 crystal structure. Water is the predominant source of O2- ions in the anodic films, especially when fabricated in organic electrolytes. All TiO_2 crystal structure sare built up of TiO62- octahedra, which share corners and edges in different manners, resulting in the formation of different crystalline phases. Using the two lone pairs of electrons on the oxygen, water molecules might form bridges between surface OH groups of different octahedra that share only one common vertex. Consequently, dehydration occurs and the structure of two octahedra sharing one edge is formed.

Because of the interesting morphology and the potential applications, the formation of smooth TiO_2 nanotubes using the protic non-aqueous[107] organic media could be a process for further research. It was observed that the reproducibility of the formation of well ordered nanotubular arrays using a two-electrode configuration was affected by the experimental conditions, especially water content of the electrolyte. This aspect has not been addressed in the available reports mainly because a three electrode configuration.

The formation of the ordered TiO_2 nanotubes with smooth surface, was affected by the initial water content of the polyhydric alcohol, relative humidity, exposure time of the electrolyte to the atmosphere and anodization duration.

The news efforts for applications in the nanoteccnology, TiO_2 has been extensively used and investigated as an excellent photocatalyst because of its exceptional properties. [110]However, a large intrinsic band gap of TiO_2 (3.2 eV for anatase and 3.0 eV for rutile) allows only a small portion of solar spectrum in the ultraviolet (UV) light region to be absorbed. Therefore, the effective utilization of visible light has become one of the most important goals in photocatalytic applications. Various methods have been developed to reduce the band gap of TiO_2 via, for example, substitutional doping (N, C, F, etc.) and combing TiO_2 with organic dyes or narrow-gap semiconductors quantum dots(QDs), such as CdS, CdSe, InP, and PbS QDs. Noble-metal nanoparticles (NPs) show strong visible-light absorption because of size- and shape-dependent

plasmon resonance, which has a wide variety of applications such as colorimetric sensors, photovoltaic devices, photochromic devices, and photocatalysts. Plasmon-based photochemical and photothermal reactions have been used for preparation of Ag nanoprisms and Au nanorods and irreversible and reversible photoimaging. In particular, silver NPs show efficient plasmon resonance in the visible region, which has been utilized to develop a plasmonic photocatalyst.

we present also the preparation of SiO_x nanotubes or macrotubes or easy form.

Dimensionality plays a critical role in determinating the properties of materials due to, for example, the different ways that electrons interact in three dimensional, two dimensional, and one dimensional structure.

The study of dimensionality[111], has a long history and chemistry and physics, although this has been primarily with the prefix quasi added to the description materials. Dimensionality plays a critical role in determining the properties of materials due to, for example,

the different ways that electrons interact in three-dimensional, two dimensional (2D), and one-dimensional (1D) structures.

The study of dimensionality has a long history in chemistry and physics, although this has been primarily with the prefix "quasi" added to the description of materials.

interesting and important as 2D and 0D systems. 1D systems are the smallest dimension structures that can be used for efficient transport of electrons and optical excitations, and are thus expected to be critical to the function and integration of nanoscale devices. However, little is known about the nature of, for example, localization that could preclude transport through 1D systems.

In addition, 1D systems should exhibit density of states

singularities, can have energetically discrete molecular like states extending over large linear distances, and may show more exotic phenomena, such as the spin-charge separation predicted for a Luttinger liquid. There are also many applications where 1D nanostructures could

be exploited, including nanoelectronics, superstrong and tough composites, functional nanostructured materials, and novel probe microscopy tips.

To address these fascinating fundamental scientific issues and potential applications requires answers to two questions at the heart of condensed matter chemistry and physics research: (1) How can atoms or other building blocks be rationally assembled into structures with nanometer-sized diameters but much longer lengths? (2) What are the intrinsic properties of these quantum wires and how do these properties depend, for example, on diameter and structure?

How can atoms or other building blocks be rationally assembled into structures with nanometer-sized diameters but much longer lengths (1D nanostructures)? There are now well-developed methods for the synthesis of 0D nanoclusters, such as arrested precipitation, and for the growth of 2D layers using molecular beam epitaxy. General methods for the growth of 1D nanostructures have not been available, although a number of strategies have been pursued. For example, multiwalled carbon nanotubes (MWNTs) have been obtained from hot carbon plasmas. Si:catalyst composition, and temperature for nanowire growth can be determined by examining the Si-rich region of binary metal-Si phase diagrams. For example, the Fe-Si phase diagram tells us that there is a broad area above 1200 °C in the Si-rich region where $FeSi_2$(l) and Si(s) coexist. Within the framework of our approach, Si nanowire synthesis is achieved by laser ablation of a Si0.9Fe0.1 target at temperatures 1200 °C. Laser ablation of the $Si1\text{-}_2Fe_2$ target produces a vapor of Si and Fe that rapidly condenses into Si-rich liquid Fe-Si nanoclusters, and when the nanoclusters become supersaturated in Si, the coexisting pure Si phase precipitates and crystallizes as nanowires.

Detailed studies[112] of the morphology and growth of silicon whiskers have led to a new concept of crystal growth from the vapor, which we call here the vapor-liquid-solid (VLS) mechanism. From these and subsequent studies, in which *Si* whiskers were grown by the disproportionation of SiI_2 or by the hydrogen reduction of $SiCI_4$, three important facts emerged: (a) silicon whiskers do not contain an axial screw dislocation; (b) an impurity is essential for whisker growth; (c) a small globule *is* present at the *tip* of the whisker during growth. From fact (a) and related evidence, *it* became clear that growth from the vapor did not occur by the Frank screw dislocation mechanism.

From facts (b) and (c), and much additional evidence, the VLS mechanism emerged. In *this* mechanism, the role of the impurity is to form a liquid alloy droplet of relatively low freezing temperature. The liquid droplet *is* a preferred *site* for deposition from the vapor, which causes the liquid to become supersaturated with *Si.* The whisker grows by precipitation of *Si* from the droplet. Since the whisker grows from the liquid, a screw dislocation *is* unnecessary.

Self-assembled nanowires offer the prospect of accurate and scalable device engineering at an atomistic scale for applications in electronics, photonics and biology. However, deterministic nanowire growth and the control of dopant profiles and heterostructures are limited by an incomplete understanding of the role of commonly used catalysts and specifically of their interface dynamics. Although catalytic chemical vapour deposition of nanowires below the eutectic temperature has been demonstrated in many semiconductor–catalyst systems, growth from solid catalysts is still disputed and the overall mechanism is largely unresolved. Here, [113]we present a video rate environmental transmission electron microscopy study of Si nanowire formation from Pd silicide crystals under disilane exposure. A Si crystal nucleus forms by phase separation, as observed for the liquid Au-Si system, which we use a comparative benchmark. The dominant coherent Pd silicide/Si growth interface subsequently advances by lateral propagation of ledges, driven by catalytic dissociation of disilane and coupled Pd and Si diffusion.

The catalytic chemical vapour deposition (CVD) of nanowires occurs by several sequential processes: (1) gas precursor transport, (2) precursor adsorption and dissociation at the catalyst surface, (3) material diffusion across the catalyst particle and (4) precipitation of nanowire material. The often cited vapour–liquid–solid (VLS) mechanism refers to catalyst liquefaction during nanowire CVD, typically by alloying with the substrate or during steps (2) and (3). High aspect-ratio nanowires are formed because of a higher reactive sticking probability of the gas on the catalyst surface and precipitation at the catalyst–nanowire interface. Nevertheless, the present atomic-level understanding of nanowire growth is incomplete, in particular for technologically

relevant nanometre-sized catalysts. Post-growth analyses lead to contradictory explanations as to the state of the catalyst, the role of melting point depression and the rate-limiting step. In situ electron microscopy for the Au–Ge system has shown that the state of the catalyst alloy can be either liquid or solid, and that a large undercooling relative to the bulk eutectic can occur owing to Ge supersaturation. However, for either a VLS or a vapour–solid–solid(VSS) framework, there has been no discussion of the catalyst interface dynamics and the initial phases of nanowire formation. It is known that, in general, interfacial roughening determines the crystal growth mode. Atomic steps are also known to play a central role in heterogeneous nucleation and interface propagation for thin films and nanostructures such as quantum dots.

Silicon nanowires have been identified as important components [114], for future electronic and sensor nanodevices. So far gold has dominated as the catalyst for growing Si nanowires via the vapour–liquid–solid (VLS) mechanism. Unfortunately, gold traps electrons and holes in Si and poses a serious contamination problem for Si complementary metal oxide semiconductor (CMOS) processing.

From a technological standpoint, a much more attractive catalyst material would be aluminium, as it is a standard metal in Si process lines. Here we report for the first time the epitaxial growth of Al-catalysed Si nanowires and suggest that growth proceeds via a vapour–solid–solid (VSS) rather than a VLS mechanism. It is also found that the tapering of the nanowires can be strongly reduced by lowering the growth temperature.

Semiconductor wires, in particular Si nanowires, have been studied for more than forty years. Si nanowires can be synthesised by coating a Si substrate with a thin Au film and annealing the substrate in a vacuum chamber to obtain Au–Si catalyst particles. When a vapour-phase Si precursor is introduced at a substrate temperature above the eutectic point (that is, the lowest temperature at which the Au–Si mixture will melt, the catalyst particles become supersaturated with Si and crystalline Si nanowires will nucleate out of the melt and grow. In this vapour–liquid–solid (VLS) growth mechanism, proposed by Wagner and Ellis, the Au catalyst particle, located at the tip

of the nanowire, is in a liquid state during growth. This liquid particle serves as the preferential site for adsorption of the Si from the vapour precursor species. In addition to VLS growth, vapour–solid–solid (VSS) growth via a solid catalyst particle is also possible.

In this paper[114], we use an ultra-high vacuum chemical vapour deposition system to grow Si nanowires epitaxially on a Si (111) substrate using Al catalyst particles. Figure 1 shows the Al-rich part of the Al–Si binary phase diagram. As indicated there in different growth modes are possible depending on temperature:

VLS and VSS. For VLS growth, the growth temperature has to be higher than the eutectic temperature of 577°C so that the Al–Si catalyst particle is liquid. Due to the supersaturation of Si. Al-catalysed non-epitaxial VLS growth of Si wires has been reported by Osada and Whang, even though Al as the catalyst for S nanowire growth has proven to be difficult. In addition to the VLS growth of Si nanowires, VSS growth using temperatures below 577 °C also may be possible. In this case, the catalyst particle remains in its solid a-Al phase.

Surface plasmons (SPs) are of interest to a wide spectrum of scientists, ranging from physicists, chemists and materials scientists to biologists. Renewed interest in SPs comes from recent advances that allow metals to be structured and characterized on the nanometre scale. This in turn has enabled us to control SP properties to reveal new aspects of their underlying science and to tailor them for specific applications. For instance, SPs are being explored for their potential in optics, magneto-optic data storage, microscopy and solar cells, as well as being used to construct sensors for detecting biologically interesting molecules.

SPs were widely recognized in the field of surface science following the pioneering work of Ritchie in the 1950[117].

SPs are waves that propagate along the surface of a conductor, usually a metal[118]. These are essentially light waves that are trapped on the surface because of their interaction with the free electrons of the conductor (strictly speaking, they should be called surface plasmon polaritons to reflect this

hybrid nature). In this interaction, the free electrons respond collectively by oscillating in resonance

with the light wave. The resonant interaction between the surface charge oscillation and the electromagnetic field of the light constitutes the SP and gives rise to its unique properties.

For researchers in the field of optics, one of the most attractive aspects of SPs is the way in which they help us to concentrate and channel light using subwavelength structures.

This could lead to miniaturized photonic circuits with length scales much smaller than those currently achieved.

Such a circuit would first convert light into SPs, which would then propagate and be processed by logic elements, before being converted back into light. To build such a circuit one would require a variety of components: waveguides, switches, couplers and so on. Currently much effort is being devoted to developing such SP devices; one example is the 40 nm thick gold stripe that acts as a waveguide for SPs. An appealing feature is that, when embedded in dielectric materials, the circuitry used to propagate SPs can also be used to carry electrical signals. Developments such as this raise the prospect of a new branch of photonics using SPs, sometimes called plasmonics.

The use of SPs to help us concentrate light in subwavelength structures stems from the different (relative) permittivities, ε, of the metals and the surrounding non-conducting media. (ε is the square of the complex index of refraction.)

Concentrating light in this way leads to an electric field enhancement that can be used to manipulate light–matter interactions and boost non-linear phenomena. For example, metallic structures much smaller than the wavelength of light are vital for the massive signal enhancement achieved in surface-enhanced Raman spectroscopy (SERS)—a technique that can now detect a single molecule Furthermore, the enhanced field associated with SPs makes them suitable for use as sensors, and commercial systems have already been developed for sensing biomolecules. SP-based sensing applications and SERS.

The interaction between the surface charges and the electromagnetic field that constitutes the SP has two consequences. First, the interaction between the surface charge density and the electromagnetic field results in the momentum of the SP mode, $\hbar k_{SP}$, being greater than that of a free-space photon

of the same frequency $\hbar k_0$. ($k_0 = \omega / c$ is the free-space wevector.) Solving Maxwell's equations under the appropriate boundary conditions yields the SP dispersion relation, that is, the frequency-dependent SP wave-vector, k_{SP}. The frequency-dependent permittivity of the metal, ε_m, and the dielectric material, ε_d, must have opposite signs if SPs are to be possible at such an interface. This condition is satisfied for metals because ε_m, is both negative and complex (the latter corresponding to absorption in the metal). As an example, using equation , the SP wavevector for a silver–air interface in the red part of the visible spectrum is found to be $k_{SP} \approx 1.03.k_0$. This increase in momentum is associated with the binding of the SP to the surface, and the resulting momentum mismatch between light and SPs of the same frequency must be bridged if light is to be used to generate SPs.

The second consequence of the interaction between the surface charges and the electromagnetic field is that, in contrast to the propagating nature of SPs along the surface, the field perpendicular to the surface decays exponentially with distance from the surface. The field in this perpendicular direction is said to be evanescent or near field in nature and is a consequence of the bound, non-radiative nature of SPs, which prevents power from propagating away from the surface.

There are three main techniques by which the missing momentum can be provided. The first makes use of prism coupling to enhance the momentum of the incident light. The second involves scattering from a topological defect on the surface, such as a subwavelength protrusion or hole, which provides a convenient way to generate SPs locally. The third makes use of a periodic corrugation in the metal's surface1. Indeed, over 100 years ago, Wood[119] reported anomalous

behavior in the diffraction of light by metallic diffraction gratings— some of these phenomena are now known to arise from coupling to SPs. The diffraction (scattering) of light by a metallic diffraction grating allows incident light to be momentum matched and thus coupled to SPs. Importantly the reverse process also allows the otherwise non-radiative SP mode to couple with light in a controlled way with good efficiency, which is vital if SP-based photonic circuits are to be developed.

Once light has been converted into an SP mode on a flat metal surface it will propagate but will gradually attenuate owing to losses arising from absorption in the metal. This attenuation depends on the dielectric function of the metal at the oscillation frequency of the SP.

In the past, absorption by the metal was seen as such a significant problem that SPs were not considered viable for photonic elements; the SP propagation length was smaller than the size of components at that time. This view is now changing thanks primarily to recent demonstrations of SP-based components that are significantly smaller than the propagation length.

Such developments open the way to integrate many SP-based devices into circuits before propagation losses become too significant.

In addition to dealing with the problem of loss owing to absorption in the metal, there is another key loss mechanism that must be considered: unwanted coupling to radiation. To build SP-based circuits one will need components that convert one SP mode into another, for example, a switch to re-route SPs without scattering the SP mode in such a way as to lose its energy to freely propagating light.

Optical properties

TiO_2 thin films and TiO_2 nanotubes

The nanostructure, is a technology versatile and very sensible at the all types of changes, K. Narasimrh[94]. Structure and optical properties of TiO_2, films are very sensitive to deposition parameters, Titanium dioxide films are extensively used in optical thin film device applications because of their desirable optical properties and good stability in adverse environments. Optical losses, laser-induced damage and durability of the films depend on the preparation technique. Substrate temperature, starting material and enhanced reactivity control the stoichiometry and structure of the films.
Extensive investigations have been made on optical and structural properties of TiO_2 films using a variety of deposition techniques sol gel, PVD, DC magnetron and taking various deposition parameters into consideration.
For low Ar/O_2 ratio the band gap is 3.13 eV, while for higher values of the Ar/O_2 the TiO_2 band gap increases up to 3.38 eV. The properties of TiO_2 thin films[95] deposited by DC magnetron procedure are reported. There was shown that it is possible to grow films with different band gap. The method is suitable for the preparation of separate films with different band gap width or for TiO_2 sandwich based structures, with different band gap width films for optical or electrical purposes.
There was shown that important changes in optical parameters e.g. (refractive index and extinction coefficient) are related to the films deposited at low oxygen partial pressure (10% oxygen and 90% argon), a refractive index of 2.8 at 400 nm being a typical value for TiO_2. The refractive index increases for TiO_2 thin films deposited at higher value of gas flowing rate. The extinction coefficient increases when the films are deposited at lower gas flowing rate.

In order to prepare high quality TiO_2 thin films it is necessary to use a flowing gas mixture with a higher proportion in oxygen. A high gas flowing rate is recommended in order to get films with reproducible and controlled parameters.
The optical properties of TiO_2 thin films have been ex- tensively investigated. A postdeposition annealing of TiO_2 films leads to densification of the deposited layers, ac- companied by a microstructural coarsening i.e., grain growth and phase transformation. Therefore, a decrease in optical transmittance and an increase in refractive index of the TiO_2 thin films are frequently observed as annealed at higher temperatures. In addition to the optical properties, several attempts e.g., by doping have been employed to structural evolution of the sputtered Ti films after high- temperature oxidation at various temperatures.
The optical properties of TiO_2 nanotubes in general , the properties of titania can vary considerably with fabrication procedure.

Grimes group [96] has measured the optical properties of the nanotubes using by Ellipsometric measurements, from transmittance spectrum of a transparent titania nanotubes array film on glass substrate. The absorbance (or optical density) of the films were estimated from the transmittance T using the relation: A=–log(T).
The Napierian absorption coefficient of the sample was calculated using Lambers law,α=2.303(A/d), were d is the thickness of film, which can be determined using the relation

$$d = \frac{\lambda_1 \lambda_2}{2[\lambda_2 n(\lambda_1) - \lambda_1 n(\lambda_2)]}$$

whereλ_1 and λ_2 are the wavelengths corresponding to the two adjacent maxima or minima, and $n(\lambda_1)$ and $n(\lambda_2)$ are the refractive indices at λ_1 and λ_2, respectively. The refractive indices of the titania nanotube film were calculated using the transmit- tance spectrum in the range 380–1,100 nm by employing Manifacier's envelope method [97].
The porosity of the nanotubes array determined from the relation[98] where n(=1.66) and n (= 2.5) are the refractive indices of the nanotube structure (annealed at 450°C) and nonporous anatase films, respectively. The low refractive index is due to the high porosity of the nanotube architectures, with nanotube diameters much less than the wavelength of light in the visible range, which reduces the light reflection from the surface of the array. The absorption coefficient and the band-gap Eg are related through the equation

$$(\alpha h\nu)^s = h\nu - E_g$$

The solid state TiO_2 nanotubes

The solid state the most structure diversity, is a material that retains shape and volume over time. If a solid possesses long range, regularly repeat units, it is classified as a crystalline material. Crystalline solids are only produced when the atoms, ions, or molecules have opportunity to organize themselves into regular arrangement, or lattices.
In fact, a solid product generated from many chemical reactions will be amorphous by the, unless special procedures are used ordering. Although the crystalline state is more thermodynamically favourable than the disorder disordered state.

TYPES OF BONDING IN SOLIDS

Depending on the nature and strength of these interactions a variety of physical optical, and electronic properties are observed. It is convenient to considerer three types of chemical bonds:

Electrostatic bonds, covalent bonds, and metallic bond.This classification not rigorous.

The covalent bond.

Following Lewis[77], we interpret all of the ordinary valence bonds, as involving the sharing of a pair of electrons by the two bonded atoms. A double bond and a triple bond between two atoms can be represented respectively by four and six shared electrons.

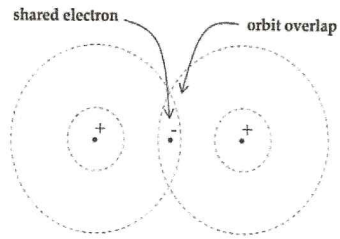

Lewis-type Chemical bond

Metallic bond

The most striking [77], characteristic of the bond that holds atoms together in a metallic aggregate is the mobility of the bonding electrons, which gives rives to the high electric end thermal conductivity of metals.

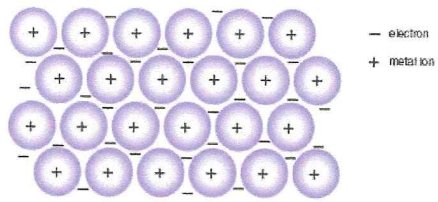

Ionic bond

The most important electrostatic bond is the ionic bond[77], resulting from the Coulomb attraction of the excess electric, charges of oppositely charged ions.
The atoms of metallic elements lose their outer electrons easily, whereas those of nonmetalic elements tend to add additional electrons; in this way stable cations and anions may be formed, which may essentially retain their electronic structure as they approach one another to form a stable molecular or crystal.
The melting points of this solids are extremely high, as very strong electrostatic attractions between countering must be overcome.

Ionic solid are only soluble in extremely polar solvents due to dipole-dipole interactions between component ions and the solvents. Since the lattice energy of the crystal must be overcome in this processes, the salvation

Structural Properties of Titanium Dioxide

TiO_2 in phase anatase and rutile is a highly anisotropic crystal. It has a hexagonal close-packed structure with
c/a = 1.861. TiO_2 therefore shows highly anisotropic behaviour in its various physical properties such as mean square displacement (MSD), mean square velocity, coefficient of thermal expansion and Gruneisen parameters. The values of these parameters along the c axis and perpendicular to it, i.e. in the basal plane are quite different. Further, recent measurements (Potzel et al 1983, 1984, Obenhuber et al 1987) of the Lamb.

The electronic properties of titania have made it an attractive material for applications in various systems such as photocatalysis, solar cells, sensors, etc. TiO2 can exist in both crystalline and amorphous forms. The amorphous form of TiO2 is photocatalytically inactive. The superior electronic properties of TiO2 depend on its crystal structure, and can be changed by doping titania with different elements. In some cases this doping changes the local atom distribution, and in some others it changes the electron transfer without altering this distribution. Therefore, to understand the electronic properties of titania, it is necessary to have some information regarding its crystal structure.

There are three crystalline phases of TiO2; anatase, rutile and brookite. Both anatase and rutile have been extensively studied for photocatalytic applications with the former found to be the most suitable for photocatalytic reactions. Brookite is not commonly available and has not, apparently, been tested for photocatalysis.
Anatase and rutile are both tetragonal in structure while the brookite structure is orthorhombic. All consist of TiO_6^{2-} octahedral with different manner of arrangement/bonding. In rutile, two (out of twelve) edges are shared forming a linear chain.[120] If each titanium octahedron (TiO_6^{2-}) was represented by a building block, then the basic structural unit of rutile can be represented by **Figure 1.1a**. For rutile, the linear chains are then joined to each other by the sharing of corner oxygen atoms, producing the overall rutile structure[120], **Figure 1.1b**

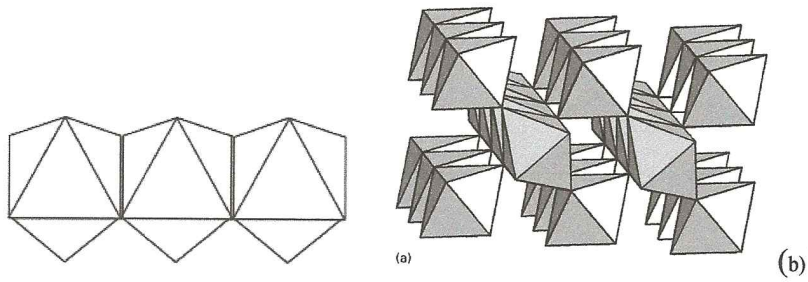

Anatase has four edges shared per octahedron and no corner oxygen sharing.[121] The basic growth units possible for anatase are shown in **Figure 1.1**.This figure shows (a) two edges are shared per octahedron forming a right-angled configuration and (b) the third and fourth edges are shared into and out of adjacent layers. Effectively the arrangement of these octahedra gives the overall structure of anatase[120] shown in **Figure 1.2c**.

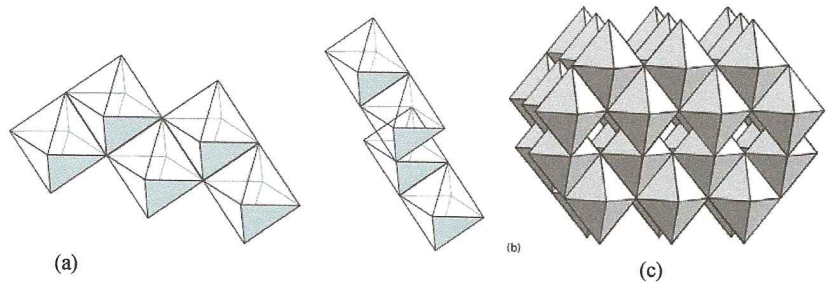

Figure **1-2**: (a), (b) The fundamental structural units and (c) the overall structure of anatase. (a) (b)

The octahedral linkages in brookite are such that three edges are shared per octahedron. The basic unit as well as the overall structures of brookite formed by TiO_6 octahedra are shown in Figure 1.3.

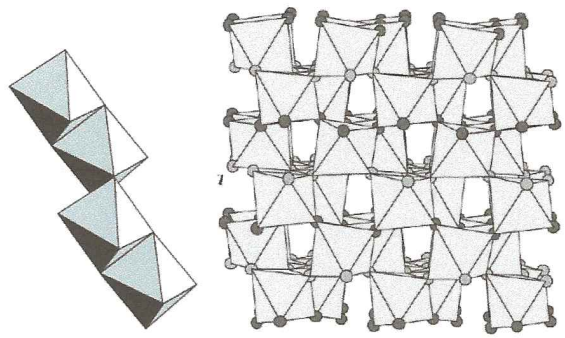

Figure **1-3**: (a) The fundamental structural units and (b) the overall structure of brookite

Crystal structure data of TiO_2

	Rutile	***Anatase***	***Brookite***
Crystal structure	Tetragonal	tetragonal	Orthorhombic
Lattice constans (A)	a=4.5937	a=3.784	a=9.184
	c=2.9587	c=9.515	b=5.447
			c=5.145
Space group	$P4_2/mnm$	$I4_1/amd$	Pbca
Molecule/cell	2	4	8
Volume/molecule(A)	31.2160	34.061	32.172
Density (g/cm)	4.13	3.79	3.99
Ti—O bond length(A)	1.949	1.937	1.87~2.04
O—Ti—O bond angle	81.2°	77.7°	77.0°~105°
	90.0°	92.6°	

Reference[81]

Electrical and Optical properties of Semiconductors

Semiconductors are compounds that show electrical conductivity intermediate between that of metal and insulators.

Semiconductors [75] may be divided into those that show intrinsic conduction and those which are extrinsic: Intrinsic behaviour is shown so-called perfect crystals, whereas extrinsic(or impurity type) Semiconductors contain foreign atoms that present either substitutionally or interstitially in the host crystal.

In the study of transport properties of solids, two types of charge carriers can be present within the crystal, namely, electrons and holes.

However, two processes are possible, the excess electron moves from site to site and this electron flow gives rise to n-type behaviour, where there is a deficiency of electrons each electron jumps in turn so that it appears that hole is moving continuously. This apparent movement of holes can be described as hole conduction, and is called p-type.

The existence of forbidden energy gaps permitted resulted from the continuity required by periodic boundary conditions, the presence of bangap in a semiconductors means the electrical conductivity of a semiconductor is low. The bangap also increase the minimum energy of electron-hole pair formation from zero to $>E_g$. What distinguishes a semiconductor from a insulator is that E_g in a semiconductor, the bangap for semiconductor are typically in the range 150-290 kJ mol (i.e.,1-4eV).

Light exhibit both wave and particle-like behaviour. This duality may be expressed by the de Broglie equation, which equates the wavelength and momentum, p, of a particle (Eq.1). the potential energy of an electron in a crystal lattice depends on its location, end will be periodic due to the regular array of lattice atoms

$$\lambda=h/p \quad (1)$$

the periodic wavefunctions that result from solving Schrodinger equation are referred to a Bloch wavefunctions.
Each wavefunction represents the energy of an electron at a specific location in the lattice.
The wavevector represents a change in momentum on electron.
The new materials called nanomaterials are in this time a currently attention, Alivisatos [108,109] In the nanocrystals did special attention in this semiconductors and her characteristics.
First, the fundamental variation of fundamental electrical and optical properties with the reduction size. In semiconductors this transition occurs for a given temperature, the Fermi levels lies between two bands, denominate low-energy optical and electrical. Therefore, optical excitation depend strongly on size for clusters as 10,000 atoms. Electrical transport also depends strongly on size,
A second important characteristic of semiconductors concerns the influence of the surface on optical and electrical properties, and the need to embed semiconductors clusters in a passivating medium.
The properties of crystalline solids are ordinarily catalogued [109]without reference to their size. It is only in the regime below10 nm where this variable comes into play. In the past decade, tailoring of materials characteristics by size control has been demonstrated in many inorganic solids belonging to one of the most technologically important classes of materials: semiconductors.
There are two major effects which are responsible for thesesize variations in nanocrystal properties.
First, in nanocrystals the number of surface atoms is a large fraction of the total.
Second, the intrinsic properties of the interior of nanocrystal sare transformed by quantum size effects. In any material, surface atoms make a distinct contribution to the free energy, and the large changes in thermodynamic properties of nanocrystals(melting temperature depression, solid-solid phase transition elevation) can ultimately be traced to this. The surfaces of nanocrystals have until recently been thought of as largely disordered, yielding spherical or ellipsoidal shapes.

Quantum Size Effects

The most striking property of semiconductor nanocrystals isthe massive changes in optical properties as a function of the size. As size[109] is reduced, the electronic excitations shift to higher energy, and there is concentration of oscillator strengthinto just a few transitions. These basic physical phenomena ofquantum confinement arise by changes in the density ofelectronic states and can be understood by considering therelationship between position and momentum in free andconfined particles:

$$\Delta p \Delta x \geq \hbar/2$$

For a free particle or a particle in a periodic potential, the energyand the crystal momentumħp may both be precisely defined,while the position is not. As a particle is localized, the energymay still be well-defined; however, the uncertainty in positiondecreases, so that momentum is no longer well-defined.

Fermi Level

"Fermi level" is the term used to describe the top of the collection of electron energy levels at absolute zero temperature. This concept comes from Fermi-Dirac statistics. Electrons are fermions and by the Pauli exclusion principle cannot exist in identical energy states. So at absolute zero they pack into the lowest available energy states and build up a "Fermi sea" of electron energy states. The Fermi level is the surface of that sea at absolute zero where no electrons will have enough energy to rise above the surface. The concept of the Fermi energy is a crucially important concept for the understanding of the electrical and thermal properties of solids. Both ordinary electrical and thermal processes involve energies of a small fraction of an electron volt. But the Fermi energies of metals are on the order of electron volts. This implies that the vast majority of the electrons cannot receive energy from those processes because there are no available energy states for them to go to within a fraction of an electron volt of their present energy. Limited to a tiny depth of energy, these interactions are limited to "ripples on the Fermi sea".

At higher temperatures a certain fraction, characterized by the Fermi function, will exist above the Fermi level. The Fermi level plays an important role in the band theory of solids. In doped semiconductors, p-type and n-type, the Fermi level is shifted by the impurities, illustrated by their band gaps. The Fermi level is referred to as the electron chemical potential in other contexts.

In metals, the Fermi energy gives us information about the velocities of the electrons which participate in ordinary electrical conduction. The amount of energy which can be given to an electron in such conduction processes is on the order of micro-electron volts (see copper wire example), so only those electrons very close to the Fermi energy can participate. The Fermi velocity of these conduction electrons can be calculated from the Fermi energy.

This speed is a part of the microscopic Ohm's Law for electrical conduction. For a metal, the density of conduction electrons can be implied from the Fermi energy.

Fermi Function

The Fermi function f(E) gives the probability that a given available electron energy state will be occupied at a given temperature. The Fermi function comes from Fermi-Dirac statistics and has the form

$$f(E) = \frac{1}{e^{(E - E_F)/kT} + 1}$$

The basic nature of this function dictates that at ordinary temperatures, most of the levels up to the Fermi level E_F are filled, and relatively few electrons have energies above the Fermi level. The Fermi level is on the order of electron volts (e.g., 7 eV for copper), whereas the thermal energy kT is only about 0.026 eV at 300K. If you put those numbers into the Fermi function at ordinary temperatures, you find that its value is essentially 1 up to the Fermi level, and rapidly approaches zero above it.

The illustration below shows the implications of the Fermi function for the electrical conductivity of a semiconductor. The band theory of solids gives the picture that there is a sizable gap between the Fermi level and the conduction band of the semiconductor. At higher temperatures, a larger fraction of the electrons can bridge this gap and participate in electrical conduction.

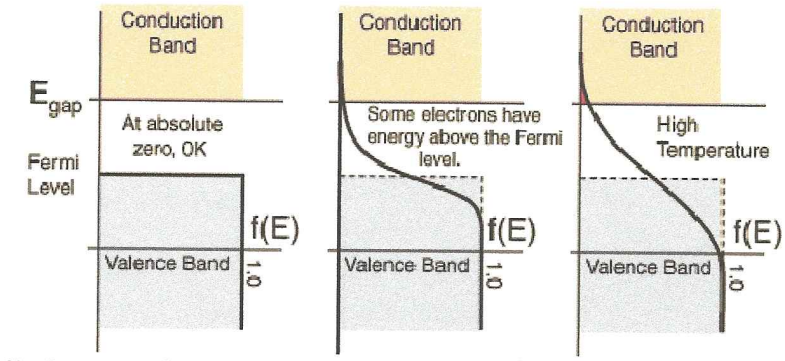

No electrons can be above the valence band at 0K, since none have energy above the Fermi level and there are no available energy states in the band gap.

At high temperatures, some electrons can reach the conduction band and contribute to electric current.

Note that although the Fermi function has a finite value in the gap, there is no electron population at those energies (that's what you mean by a gap). The population depends upon the product of the Fermi function and the **electron density of states.** So in the gap there are no electrons because the density of states is zero. In the conduction band at 0K, there are no electrons even though there are plenty of available states, but the Fermi function is zero. At high temperatures, both the density of states and the Fermi function have finite values in the conduction band, so there is a finite conducting population

OXIDE SURFACES

Oxides are covalent solids[73] that exhibit a range of interesting properties. Most oxides can assume a number structural forms. Metals often have more than one oxidation state, which means that they are able to form oxides of different stoichiometries or even mixed valence compounds in which more than valence state is present. Different crystal structure have different optical and

electronic properties. Defects as well as substitutional or interstitial impurities (dopants) also modify the optical and electronic properties as well as the chemistry of oxides crystal.

The covalent nature of oxides means that certain cleavage planes are much more favoured to form surfaces, that is, there are certain low energy planes that are more much stable and likely to be observed. This is a contrast to metals. Metallic bonding is much more less directional and this means that several planes have similar surface energies and it is easier to make samples of crystalline metals that exhibit a variety of different planes.
Another consequence of directional bonding is that the surfaces of covalent solids are much more susceptible to reconstruction.
As oxide of particular interest is that of TiO_2 the most important crystalline forms of titania are rutile and anatase

Te stability of covalent surfaces[74]. When there is a dipole moment in the repeat unit perpendicular to the surface in an ionic crystal, lattice sums in the electrostatic energy diverge and the calculated surface energy is infinite.
The cause of this divergence is demonstrated and the surfaces of any ionic or partly ionic material are classified into three types. Type 1 is neutral with equal numbers
of anions and cations on each plane and type 2 is charged but there is no dipole moment perpendicular to the surface because of the symmetrical stacking sequence. Both these surfaces should have modest surface energies and may be stable with only limited relaxations of the ions in the surface region. The type 3 have very large surface energies would be unstable.
An oxide of particular interest is that of TiO_2 . The two most important crystalline forms of titania are rutile and anatase. Rutile has a bandgap of ~3.2ev, which means that it absorbs in the near UV by excitation from filled valence band states localized essentially on an O(2p)orbital to the empty conduction band states primarily composed of Ti(3d) states
reconstruction. These conclusions are important for the analysis of the surface structure of ionic crystal.
The surfaces of ionic crystals determine many important properties such as mechanical strength, sintering and shape.
The stability of a surface is determined by the surface energy, E, which can be defined as.
ES = (Cohesive energy of finite crystal) - (Number of atoms)
x (Cohesive energy per atom in infinite crystal)
and is the excess energy associated with the surface. Bertaut (1958) showed that when there is a dipole moment in the unit cell perpendicular to the surface, the surface energy diverges and is infinite.

Rutile (TiO_2)

The rutilo TiO_2 has an electronic configuration of 3d for Ti(IV). The Ti-O σ and π bands are completely filled so that the Fermi level is located at the middle of the energy gap between those bands and the antibonding π^* and cation-cation d-bands
The structure of the rutile(110) surface Titanium dioxide minerals are found in three different crystallographic structure; rutile, anatase, and brookite. Only rutile and anatase surfaces have been studied; brookite transformers into rutile at quiet low temperatures. Rutile is the thermodynamically most stable phase, and the (110) face has the lowest surface energy. The unit cell of the TiO, the (110), (00l), and (100) surface terminations. The structure consists of distorted octahedra, in which Ti is coordinated by 6 oxygen, linked at corners. The unit cell is tetragonal, the space group P4/mnm with lattice dimensions of a=b= 4.59 A, and c= 2.96 A . The (110) surface is perhaps

the best studied of all oxide surfaces, being the most stable of the low index t-utile planes. The accepted model [12,13] for the stoichiometric (1 x 1) surface structure consists of a plane of alternate rows of Ti and O atoms with bridging rows of oxygen on every other row running along the [100] direction.

The surface unit cell is 6.5 A in the [110] direction and 2.96 A in the [110] direction. In this configuration the surface contains Ti in S-fold coordination in the plane and in 6-fold

Mechanistic Model of TiO_2 Nanotube Array Formation

The formation mechanism of the TiO_2 nanotubes is believed to include the following key processes:

1. *Oxide growth* at the surface of the metal substrate as a result of the interaction of the metal with O^{2-} or OH^- ions

2. *Migration of anions* through the oxide layer reaching the metal/oxide interface where they react with the metal.

3. *Migration of metal ions* (Ti^{4+}) from the metal at the metal/oxide interface; Ti^{4+} cations will be ejected from the metal/oxide interface under application of an electric field that move towards the oxide/electrolyte interface.

4. *Field assisted dissolution* of the oxide at the oxide/electrolyte interface; due to the applied electric field the Ti-O bond undergoes polarization and is weakened promoting dissolution of the metal cations. Ti^4+ cations dissolve into the electrolyte, and the free O^{2-} anions migrate towards the metal/oxide interface, to interact with the metal.

5. *Chemical dissolution* of the metal, or oxide, by the acidic electrolyte takes place during anodization. Chemical dissolution of titania in the HF electrolyte plays a key role in the formation of a nanotubular versus nanoporous structure.

Figure 1.2(a,b) shows the formation an growth of an oxide layer atop the metal surface. With the onset of anodization, a thin layer of oxide forms on the titanium surface, Figure 1.2 (b), due to the interaction of the surface Ti^{4+} ions with oxygen ions (O^{2-}) in the electrolyte. The overall reactions for anodic oxidation of titanium can be represented as:

$$2H_2O \rightarrow O_2 + 4H^+ + 4e^- \qquad [1.1]$$

$$Ti + O_2 \rightarrow TiO_2 \qquad [1.2]$$

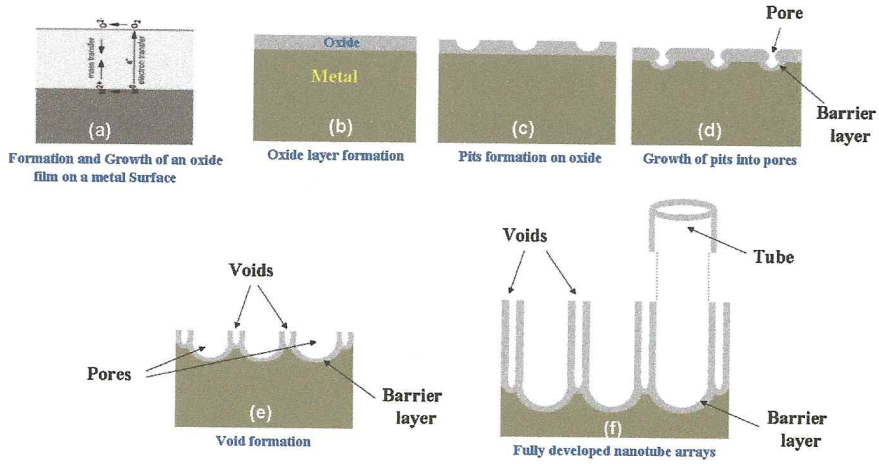

Figure1.1 Schematic diagram of evolution of straight naotubes at constant anodization voltage
See ref.[116]

In the initial stages of the anodization process field-assisted dissolution dominates chemical dissolution due to the relatively large electric field across the thin oxide layer[115] Then, small pits originate in this oxide layer due to the localized dissolution of the oxide, Figure 1.1 (c), making the barrier layer at the bottom of the pits relatively thin which, in turn, increases the electric field intensity across the remaining barrier layer, resulting in further pore growth, as seen in Figure 1.1(d).

$$TiO_2 + 6F^- + 4H^+ \rightarrow TiF_6^{2-} + 2H_2O \qquad [1.3]$$

The pore entrance is not affected by electric field assisted dissolution and hence remains relatively narrow, while the electric field distribution in the curved bottom surface of the pore causes pore widening, as well as deepening of the pore. The result is a pore with a scallop shape. As the Ti-O bond energy is high (323 kJ/mol), in the case of titania it is reasonable to assume that only pores having thin walls can be formed due to the relatively low ion mobility and relatively high chemical solubility of the oxide in the electrolyte, hence un-anodized metallic

portions can initially exist between the pores. As the pores become deeper, the electric field in these protruding metallic regions increases, enhancing the field assisted oxide growth and oxide dissolution. Hence simultaneously with the pores, well-defined inter-pore voids start forming Figure 1.1(e). Thereafter, both voids and tubes grow in equilibrium. The nanotube length increases until the electrochemical etch rate equals the chemical dissolution rate of the top surface of the nanotubes; after this point is reached, the nanotube length will be independent of anodization duration.
The chemical dissolution step, the key for the self-organized formation of the nanotube arrays, reduces the thickness of the barrier layer, keeping the electrochemical etching (field assisted oxidation and dissolution) process active. No nanotubes can be formed if the chemical dissolution is too high or too low.The electrochemical etch rate depends on the anodization potential as well as concentration of electrolytes. If the electrochemical etch proceeds faster than the chemical dissolution, the thickness of the barrier layer increases, which in turn reduces the electrochemical etching process to the rate determined by chemical dissolution. The chemical dissolution rate is determined by the F^- concentration and solution pH, see Eq.1.3. With increasing F^- and H^+ concentrations, chemical dissolution increases. Recent investigations have

shown that only in a certain F^- concentration range can nanotube arrays be achieved.[11,62] The anodic
potential at which nanotubes are formed is related to the F^- concentration, with higher potentials requiring electrolytes of higher F^- concentration.
In polar organic electrolytes such as FA, NMF, DMSO and EG, the water is usually the main source of oxygen in anodizing solutions, atmospheric oxygen is supposed to play lesser role. While the exact mechanism by which water contributes oxygen to an anodic oxide film is not well-understood, it is believed that hydroxyl ion can be injected from the electrolyte into the anodic oxide film during anodization. When a large amount of water is present, hydroxyl ions are injected into the body of the oxide layer and affect the structure sufficiently to impede ion

transport through the barrier layer, which is necessary for further movement of the metal-oxide interface into the metal. However, when less water is present, the difficulty in extracting oxygen and/or hydroxyl ions from the solution limits the rate of growth of the overall oxide film. Also, the barrier oxide layer exhibits increased ionic conductivity caused by the non-stoichiometry induced by the reduced hydroxyl ion availability to the oxide. The amount of hydroxyl ion injection is dependent on the solvent structure.

SURFACE PLASMON POLARITON

SPP

Theory in Brief

The propagation of an SP is easily understood by the solution of the following boundary- value problem. As shown in Figure 1, the plane z=0 separates a metal with complex- valued refractive index n_m from a dielectric sample with complex-valued refractive index n_s. The SP propagates (as an electromagnetic surface wave) parallel to the x-axis, with its magnetic field oriented parallel to the y-axis. The polarization state, thus, is transverse magnetic (TM). Both the metal and the sample are sufficiently thick such that the SP field is confined to the vicinity of the interface.

Let κ be the wavenumber and $\kappa\hat{x}$ be the wavevector of the SP. Then, κ must be the lateral wavenumber of all electromagnetic field phasors. Accordingly, the magnetic field phasors on either side of the interface may be written as

$$\tilde{H} = \hat{y} A_s \exp[i\kappa x + \alpha_s z] \qquad z < 0,$$

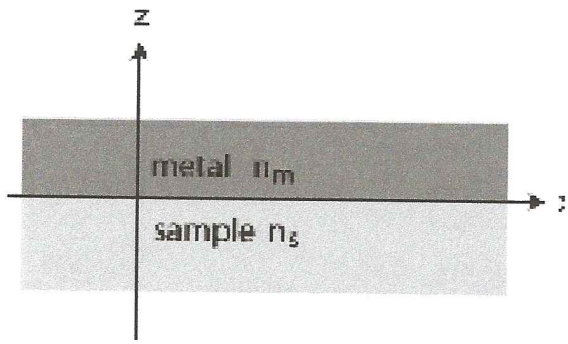

Fig.1

and

$$\tilde{H} = \hat{y} A_m \exp[i\kappa x - \alpha_m z], \qquad z > 0,$$

where $i=\sqrt{-i}$, A_s and A_m are unknown coefficients, the transverse wavenumber α_s and α_m have positive real parts and are to be computed via

$$\alpha_s^2 = \kappa^2 - \left(\frac{2\pi n_s}{\lambda}\right)^2, \qquad \alpha_m^2 = \kappa^2 - \left(\frac{2\pi n_m}{\lambda}\right)^2.$$

Where λ is the free-space wavelengh. Now, the electric field phasors on the two sides of the interface may be obtained though

$$\vec{E} = \frac{i}{\omega\varepsilon_0 n_s^2}\nabla \times \vec{H}, \qquad z < 0 \tag{4}$$

and

$$\vec{E} = \frac{i}{\omega\varepsilon_0 n_m^2}\nabla \times \vec{H}, \qquad z > 0, \tag{5}$$

where ε_0 is the free-space permittivity and ω is the angular frequency. Satisfaction of the usual boundary conditions across the interface z=0 leads to $A_s = A_m$ nad the dispertion relation

$$\alpha_m n_s^2 + \alpha_s n_m^2 = 0, \tag{6}$$

which is often written as

$$\kappa = \frac{2\pi}{\lambda}\sqrt{\frac{\varepsilon_s \varepsilon_m}{\varepsilon_s + \varepsilon_m}}, \tag{7}$$

where $\varepsilon_s = n_s^2$ and $\varepsilon_m = n_m^2$.

Parenthetically, a similar exercise with the electric field polarized to the y-axis quickly shows that SPs cannot have the transverse-electric (TE) polarization state.
Furthermore, the correct name for SPs is actually surface plasmon polaritons because the electrons in the metal are coupled to the photons in the dieletric medium.
Suppose that the imaginary parts of both ε_s and ε_m are small enough to be ignored.
With the usual stipulation that $\varepsilon_s > 0$, Eq. (6) implies $\varepsilon_m < 0$. This condition is often satisfied by metals at optical frequencies. Hence, the first condition for the existence of an SP is to have the real parts of relative permittivities of the metal and sample of opposite signs. Additionally, for κ to be purely real-valued for long-range propagation, the condition

$$\varepsilon_s < -\varepsilon_m \tag{8}$$

must hold by virtue Eq. (7).
Often, the relative permittivity of a metal in the optical regime can be written as

$$\varepsilon_m = 1 - \omega_m^2/\omega^2. \qquad (9)$$

Where ω_m is the plasma frequency. Provided that ε_s is held to be insensitive to frequency and close to unity in magnitude, Eqs. (7) and (9) may be solved to yield
The prism-based excitation of SPR was proposed by Kretschmann and Raether [84] (1968). The Kretschmann configuration is the most common setup, as it provides the most efficient way for generating SPs. In this configuration, a metal film is deposited directly on top of a prism surface. The metal film is illuminated through the prism at an angle of incidence that is greater than the critical angle for total internal reflection (TIR). The light beam undergoes TIR at the interface between the prism coupler and the metal film and excites the SPs at the outer boundary of the metal film by evanescent tunneling.

The original Kretschman fig.2 [85], configuration.

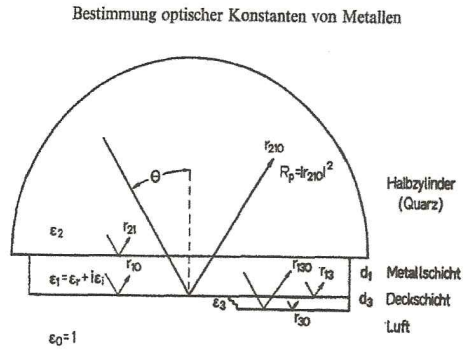

Fig.2

Generating Surface Plasmons

The apparatus used is in the figure 2. Light enters the prism, traveling upwards in the photo. It strikes the base of the prism at an angle controlled by the micrometer at the lower right of the enlarged section. A special coupling fluid allows light to travel through the microscope slide attached to the prism base. The microscope slide effectively becomes the base of the prism.
The surface plasmon travels on the free surface of a thin (60 nm) film of silver that is placed on the far side of the microscope slide. This side is "free," in contact with the air. (The film was fabricated with the department's vacuum deposition system.) Light strikes the base at an angle chosen so that the light is totally reflected.
In this situation, an evanescent wave is also created, extending beyond the surface of the free side of the microscope slide and the silver film. This wave in turn couples to the free side of the metal film

and generates a plasmon wave in the film, propagating along the free surface. The usual material for both prism and slide is "BK-7" glass.
A surface plasmon can be pictured as a traveling charge density wave on the surface of a metal. At a wave crest, electrons bunch, being pulled towards a trough by positive ions that remain in place. The charge density wave is somewhat reminiscent of a longitudinal pressure (sound) wave in air.

Experiment of the Month

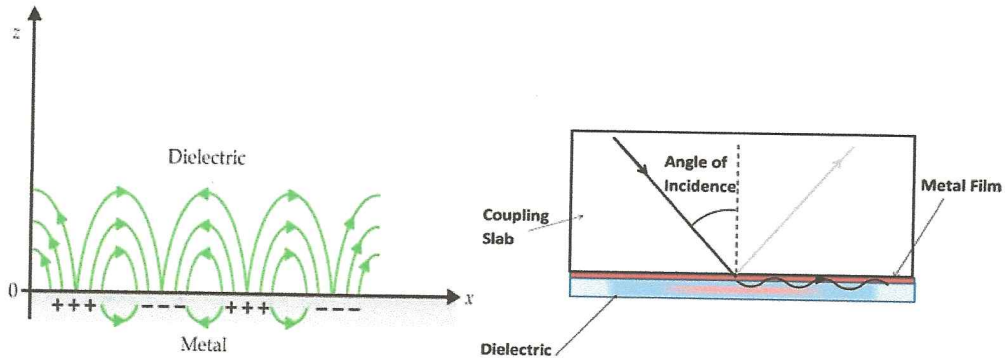

Because the plasmon includes a longitudinal wave character, the incoming light wave is polarized, with its electric field oscillating in the incident plane, defined by the light velocity vector and the normal to the base of the prism. This electric field has a component parallel to the base of the prism. The figure shows a HeNe laser on the left. Its light beam passes through a polarizer to be sure of the polarization before entering one face of the prism.
After reflecting, the light beam exits the other face of the prism and its intensity is detected. When plasmons are generated in the metal film, energy is withdrawn from the beam. The presence and nature of the plasmon is deduced from the resulting dip in the reflected signal strength.
After the incident angle is made large enough to establish total internal refection, the hunt for plasmon excitation begins. The light is "tuned" to generate plasmons by carefully changing the angle of incidence of the light onto the bottom surface of the prism. When the pattern of the light falling on the bottom surface matches the plasmon in both frequency and wavelength, a plasmon is generated. The plasmon velocity at the free surface is higher than for the surface bound to the prism. The plasmon wavelength at the free surface is long enough to match optical wavelengths.

Incoming ray refracts at air-prism interfaceand totally reflects at the microscope slide.

Evanescent disturbance wavelength matches to plasmon wavelength, both at the optical frequency
The silver film is thin compared to the light wavelength so the evanescent electric field penetrates the silver, as sketched above. By changing the angle (fig x), the wavelength of the disturbance in the silver is adjusted to match the plasmon wavelength at the optical frequency.
The plot below shows relative reflected light intensity as a function of the angle of incidence of light on the prism base. The frequency of the HeNe laser light is 4.7×10^{14} Hz. When the separation of light wave crests on the prism base matches the plasmon wavelength at the same frequency, a plasmon is generated and the reflected light shows the characteristic dip in intensity. In this experiment, total reflection began at about 41.0 degrees.

When light enters a transparent dielectric material, a disturbance propagates through the material that is a combination of electromagnetic and electronic waves. The electrons are bound to atoms, and oscillate without significant energy loss in sympathy with the electromagnetic wave, the displacement proportional to the electric field. Their mass slows the progress of the disturbance. Some Background Thoughts:
When light emerges from the material, it is "late" and we say that light traveled slowly in the dielectric. If the dielectric material is opaque, the oscillating bound electrons convert their energy to heat. We say the light is absorbed by the material.
When light strikes a metal, ordinarily the electrons respond in the usual resistive way; the velocity of the conduction electrons is proportional to the electric field. They move to reduce the electric field, driving it to nearly zero, allowing a very short penetration distance.
The conduction electrons are resistive because as they move they collide with ions in the metal and lose kinetic energy to heat. The average time between collisions varies with the metal and the temperature. If the light frequency is high enough, the electric field reverses before most electrons have a chance to collide.
In this situation, the acceleration of the electrons is proportional to the electric field. This means that the displacement of the electrons is proportional to the field, but opposite to the displacement that an electron in a dielectric experiences. Since the dielectric electrons act to reduce the electric field strength inside the material, the conductions in this special situation act to increase the electric field in the metal.
The metal is said to exhibit negative dielectric constant at these high light frequencies. The result is a much stronger electric field at the free surface of the metal in the plasmon generator. The electric field due to the evanescent light is enhanced and couples strongly to the surface plasmon.

In principle, plasmonics deals with the generation, propagation and detection of plasmonic waves, which are collective electronic excitations generated by an electromagnetic field that excites a metal/dielectric interface. As a result of this interaction between matter and radiation, the electromagnetic fields are confined to the surface and propagate along the interface; they are called surface plasmon polaritons (SPP).

Sculptured Thin Films

Sculptured thin films (STFs)[86], are nanostructured inorganic materials with anisotropic and unidirectionally varying a properties that can be designed and realized in controllable manner using physical vapor deposition (PVD).

Introduction

These nanostructured inorganic materials with anisotropic and unidirectionlly varying properties can be designed and fabricated [86], in a controllable manner [87] using PVD, a century-old technique [88]. The ability to virtually instantaneously change the growth direction of their columnar morphology, though simple variations in the direction of the incident vapor flux, leads to a wide spectrum of columnar forms. These forms can be

i) two-dimensional, ranging from the simple slanted columns and chevrons to the more complex C- and S-shaped morphologies[89] or
ii) three dimensional, including simple helixes and super helixes [90]

We observed [91] optical activity in thin solid films composed of nanometre-scale helical columns. These films rotate the plane of the polarization of the light in a manner analogous to the cholesteric liquid crystal and other structurally chiral media. This rotation demostrate the optical activity of the helical structured films and indicates that this films posses other significant optical properties such as circular dichroism. In structurally chiral media, a helical structure creates optical activity.

Chiral STFs

While growing a chiral STF[92], the vapor deposition angle is held fixed as the substrate is rotated about an axis passing nor- mally through it. As the rotation speed is also fixed, helical nanocolumns grow with a certain pitch. We looked for SPP waves over a range of values of the pitch. The metal film is, again, aluminum with a thickness of 15nm, and the chiral STF is made of titanium oxide grown with a vapor depo- sition angle of 10◦. We found five different modes of SPP-wave propagation, with two to four modes present for each value of the pitch investigated. In most cases we found SPP-wave propa- gation possible for a chiral STF that is only two pitches thick, but some modes at some values of the pitch required more pitches in order to efficiently support propagation. Each mode, except mode 5, has a lower bound of the pitch beyond which the mode ceases to exist. It was not possible to discern an upper bound of the pitch for the existence of each SPP wave mode, as serious computational difficulties were encountered at large pitch values.

CHAPTER 2

2.1 EXPERIMENTAL PART

The thin films made up, by DC sputtering technical, with Edwars Auto 306 DC Sputter Coater
The sputtering process: Sputter deposition is a physical vapor deposition (PVD) method of depositing thin films by sputtering, that is ejecting, material from a "target," that is source, which then deposits onto a "substrate,". Sputtered atoms ejected from the target have a wide energy distribution, typically up to tens of eV (10000 K). The sputtered ions (typically only a small fraction (order 1%) of the ejected particles is ionized) can ballistically fly from the target in straight lines and impact energetically on the substrates or vacuum chamber (causing resputtering). Alternatively, at higher gas pressures, the ions collide with the gas atoms that act as a moderator and move diffusively, reaching the substrates or vacuum chamber wall and condensing after undergoing a random walk. The entire range from high-energy ballistic impact to low-energy thermalized motion is accessible by changing the background gas pressure. The sputtering gas is often an inert gas such as Ar. For efficient momentum transfer, the atomic weight of the sputtering gas should be close to the atomic weight of the target.
In the internal part of the sputtering chamber was adapted an oven for to heat the substrate, from at room to 600°C, during the sputtering. Than the sputtered samples are left in vacuum for a long time to insure a slow cooling.
The targets used were Ti 99.999% purity, Ag 99.999% purity, Au 99.99% purity.

Titanium thin films were deposited in two substrates, on substrates glasses[80] (corning 2947) and glass/ITO

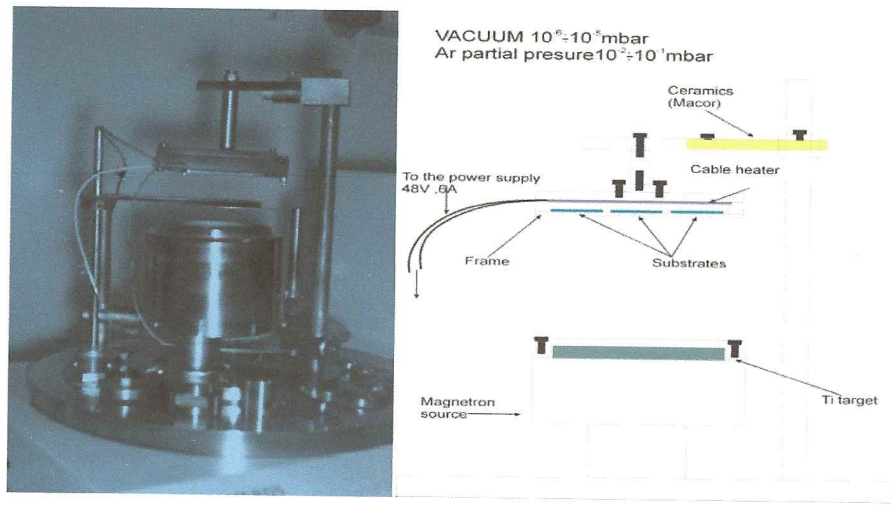

Fig.2.1 left internal part sputterring machine, right

2.2 The Electrochemical Anodization Process

Various techniques have been used to fabricate titania nanotubes of different geometrical shapes and crystallinity such as sol-gel, electrodeposition, sonochemical deposition and chemical treatment of fine titania particles. While many of these fabrication routes are complicated due to the use of templates or the nature of the involved chemical processes, it has recently been demonstrated that self-organized vertically oriented titanium dioxide nanotube arrays can be fabricated using a simple anodization technique. This technique can yield nanotubes of controlled diameters, wall thicknesses and lengths.

Anodization is an electrolytic process that creates a protective or decorative oxide film over a metallic surface. Anodization typically increases both the thickness and density of the oxide layer that forms on any metal surface exposed to the earth's atmosphere. To accomplish it, the conducting piece undergoing anodization is connected to the positive terminal of a (pulses?) power supply and placed in an electrolytic bath where it serves as the anode. The cathode is commonly a plate of platinum. When power is applied electrons are forced from the electrolyte to the positive anode. The process leaves surface metal atoms exposed to oxygen ions within the electrolyte. The atoms react and become an in situ integral part of the oxide layer. The electrons travel through the power source and return to the cathode where, if an appropriate electrolyte is present, they react with hydrogen ions and the combination bubbles off as hydrogen gas.

Since the metal oxide partially dissolves in any electrolyte, it is necessary to use only those electrolytes for which the oxide forms more rapidly than it dissolves. The electrolyte composition is also the primary determinant of whether the oxide film is porous or if it forms a barrier layer. Oxide barrier layers grow in those neutral or slightly alkaline solutions in which titanium dioxide is largely insoluble. Porous oxide layers grow in acidic electrolytes with fluoride or chloride ions in which oxide forms and then rapidly dissolves. The acid cations also affect the resulting nanotube array structures.

A depiction of an electrochemical anodization cell is shown in Fig. 1.2. With a titanium anode and a platinum cathode down in an aqueous electrolyte of dilute

Potentiostatic Anodization

Prior to anodization, substrate slide glass and commercial ITO were ultrasonically cleaned with deionized (D.I.) for 10 minutes followed by ethanol 96% unltrasonically for 10 minutes too, both to 70°C.

The anodization was performed in a two-electrode electrochemical cell with the substrate glass and ITO sputtering with titanium as the working electrode and platinum foil, under applied pulse voltage at room temperature (approximately 25°C) and other varying temperature in either fluoride chloride electrolytes. Keithyley 2612A System Source Meter pulse power supply was used for potentiostatic anodization. The time-dependent current behavior under ()was recorded using a computer controlled multimeter. A schematic representation of the anodization setup is shown in **Figure 2.2.** After anodization, the samples were rinsed thoroughly with (ID)water and then blow-dried with 99.99% pure Ar.

In the fig 2.2.1 shown the classical anodization curve using constant voltage, in fig 2.2.2 the anodization curve obtained using pulse wave forms voltage.

Anodization set-up

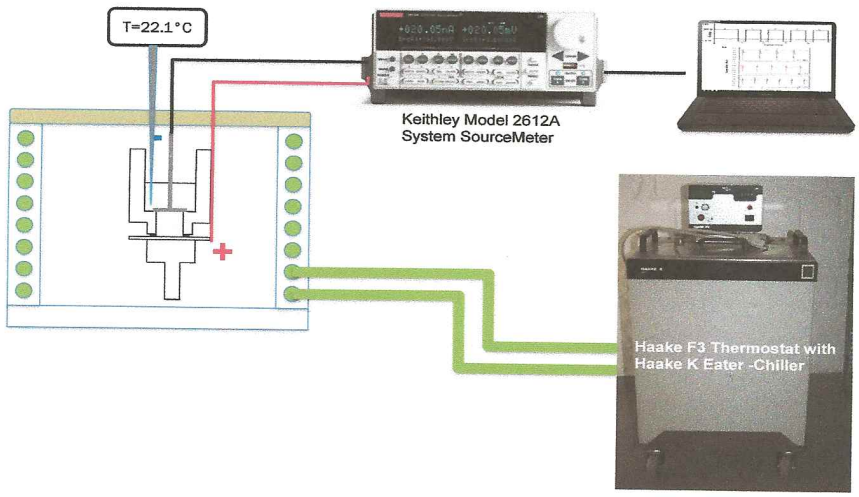

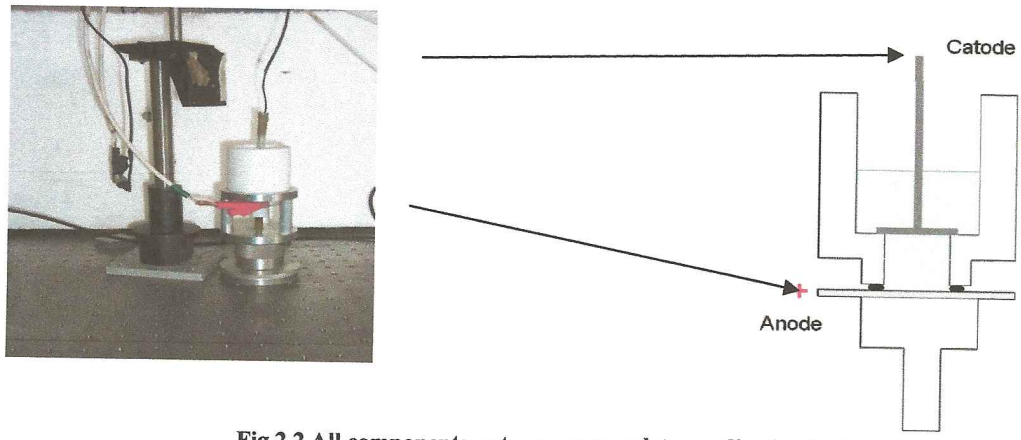

Fig.2.2 All components, set-up, up complete anodization instrumental Down, anodization internal part

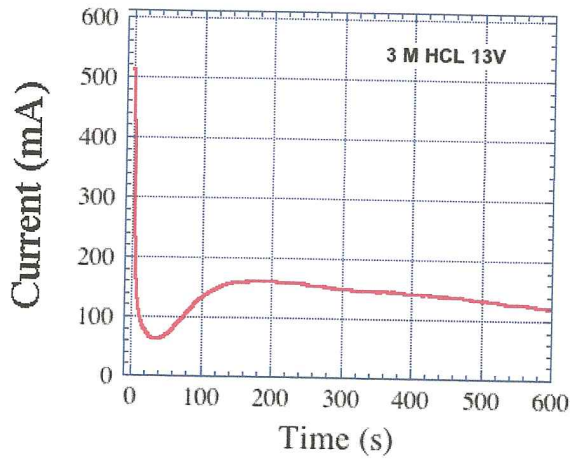

Fig 2.2.1 Typical curve anodization Current vs time DC voltage

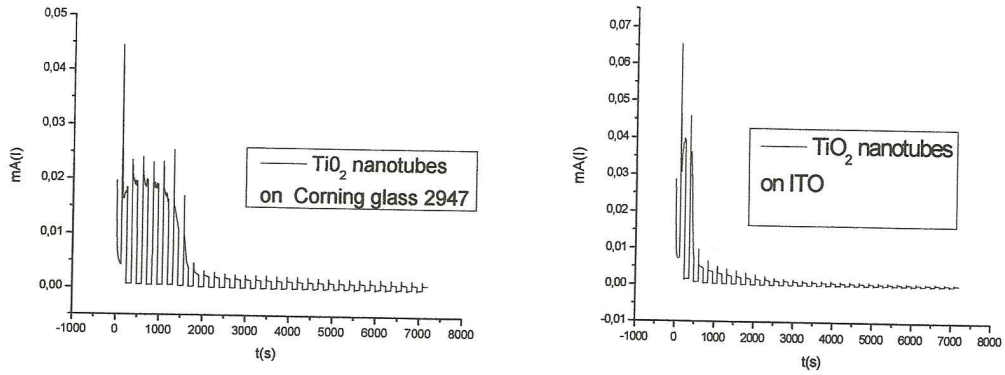

Fig 2.2.2 curve anodization Current vs time pulse waveforms(30,60) voltage

2.3 Crystallisation of TiO_2 nanotubes

However, all the anodically fabricated TiO_2 nanotube arrays to date are amorphous. Before utilization of these amorphous nanotubes in different applications, factors like the crystalline nature of the structure and stability of the desired crystalline phase as well as the stability of the structure itself must be examined.

Titania properties, and hence potential applications, depend on the crystallinity as well as the isomorph present at the desired operating conditions. For example, the anatase phase of titania is preferred in dye sensitized solar cells and catalysis because it is photoactive, whereas rutile is mostly used in the area of dielectrics and high-temperature oxygen gas sensors. In general, crystallization or phase transformations take place through nucleation and growth processes.

Based on the fact that titanium exhibits a capacity for dissolving a considerable amount of oxygen, most of the crystallization methods used for the anodically fabricated TiO_2 nanotubes involve annealing the material at high temperature in oxygen atmosphere.

The most common phase transformation in titania is the anatase to rutile transformation. The mechanisms responsible for this transformation involve breaking two of the six Ti.–O bonds

to form new bonds with the transformation activation energy calculated to be (264 kJ/mol) for the oxygen annealed samples. Nucleation and growth of rutile can occur through different processes.

Nucleation can take place:

1. at the interface of two contacting anatase particles, which results in transforming the anatase grains into a large rutile grain.
2. in the bulk or on the surface of a large anatase grain.

During the nucleation process, the crystallites may rotate and reorient if sufficient volume is available. Hence, rutile nucleation cannot take place easily inside the walls of the nanotube. For example, it was reported that anatase crystallite sizes less than 14 nm are highly stable and will not be converted into rutile[115].

The *growth* of rutile may happen when

1. a rutile crystallite comes into contact with an anatase crystallite forming a larger rutile crystallite; or
2. two rutile nuclei merge together.

As the oxidation proceeds, both titanium and larger anatase crystals at the interface can be directly transformed into rutile at temperatures between 480 and 580°C. However, smaller anatase crystallites grow at higher temperatures (~ 620°C), yielding a larger anatase grain size. Eventually, the anatase crystallites in the walls are consumed by the developing rutile layer complete rutile phase can be seen for sample annealed at 680°C

Although crystallization and phase transformations are essential for many applications, they have adverse effects on the stability of nanoarchitectures, especially when they occur at elevated temperatures. At elevated temperatures, high surface area makes them prone to solid state sintering, which leads to grain growth, densification, and eventually complete collapse of the structure. Such processes are more pronounced during phase transformations when bond breaking and enhanced mass transport take place, which can lead to grain growth and densification.

As showed the R-X **Fig.3.3.1** results after the anodization process, for obtained a crystalline structure: before I cleaned with etanol for 8h, after I put on over 500°C **Fig.2.3.1**, I followed this procedure in all experiments, obtaining the anatase phase.

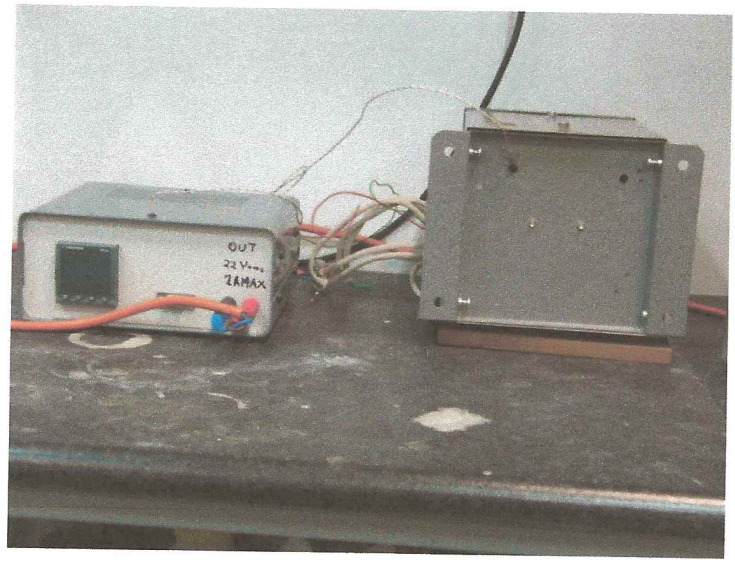

Fig.2.3.1 Over for crystallisation TiO_2 nanotubes

2.4 TiO_2 nanotubes on glass

The parameters in this experiments were: Sputtering parameters, the substrate used in this experiment Corning glass 2947 (75x25) at T=400°C, P=60watts, t= 45minutes, chamb=3.2X10¯2, h=7.9cm.
mixture has the next composition $2MNH_4F$, $2MH_2O$ and Ethylene Glycol, I made a preanodization for cleaned the surface, in this process was used 3%HF, for 5sec with P=60V.
was made a variation in the heating, with a range 15°C even 45°C.
set-up used for anodizing is the same describe in the section 2.2.

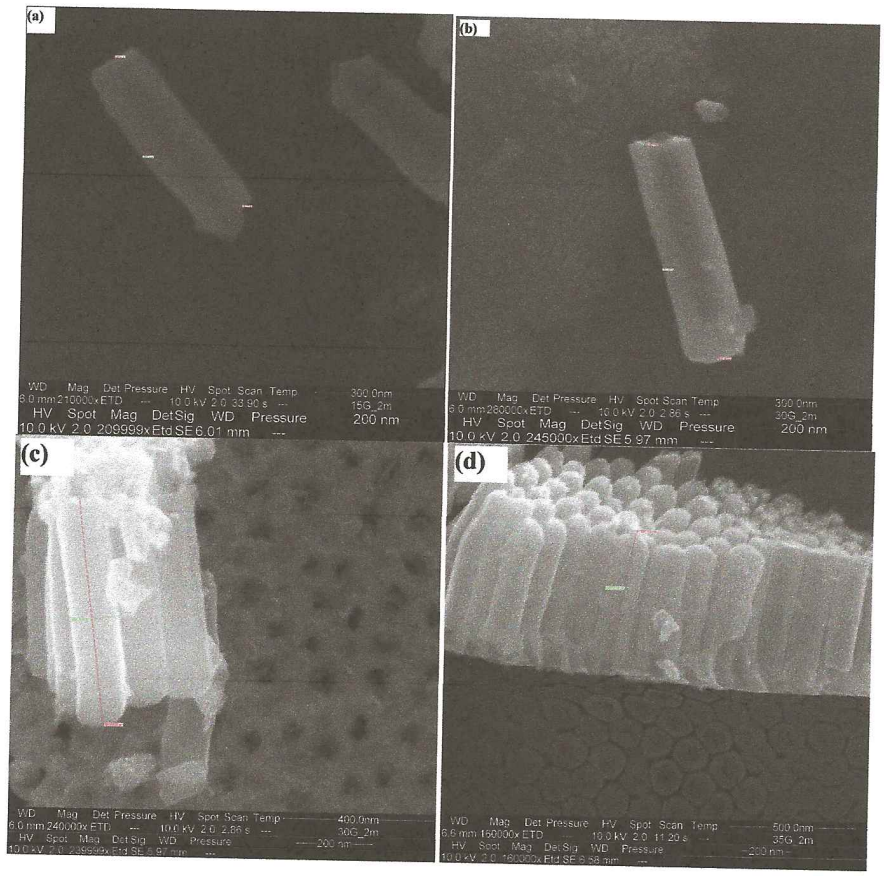

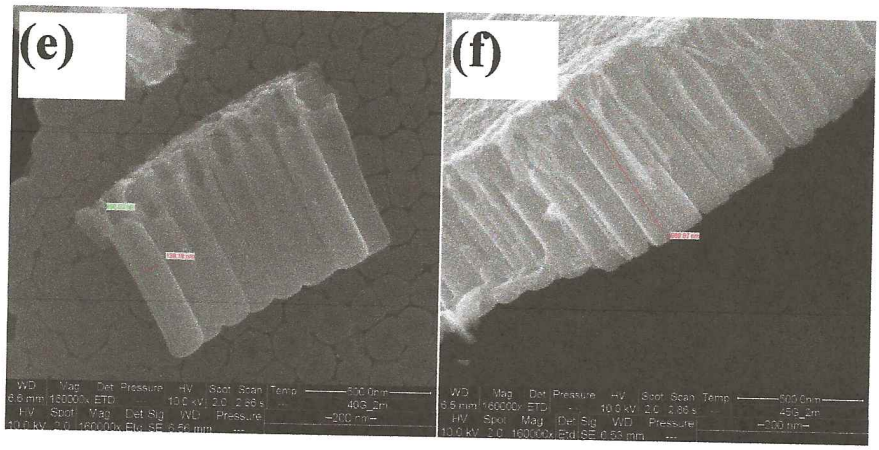

Sputtering parameters. The substrate used in this experiment Corning glass 2947 (75x25) at T=350°C, P=60watts, t= 45minutes, chamb=3.4X10^{-2}, h=7.9cm, Ti 99.999% purity. mixture has the next composition 2MNH_4F, 2MH_2O and Ethylene Glycol, I made a pre-anodization

for cleaned the surface, in this process was used 3%HF, for 15sec with P=30V.
was made a variation in the heating, with a range 25°C even 53°C. anodized was used the set-up describe in 2.2.

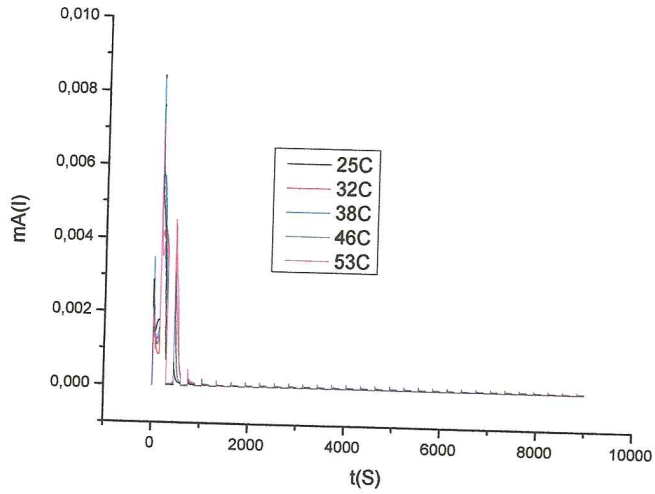

The anodization curve current vs time
varying temperature

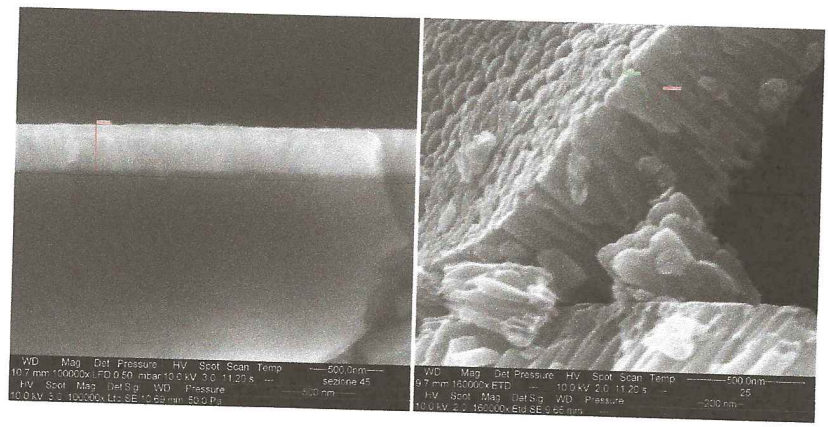

SEM images Left glass/Ti sputtering 45minutes we obtained a thin films ≈300nm, right after to anodization process the thin films glass/TiO_2 nanotubes at T=25° were ≈600nm

2.5 TiO_2 nanotubes on ITO

Experimental part

First step, was cleaned the substrate commercial ITO , with water (ID) sonicated 10minutes, after 10minutes with ethanol 96% at T=70°C dried by Ar gas.
Sputtering parameters. at temperature T=400°C, P=60watts, t= 45minutes, chamb=3.4X10^{-2}, h=7.9cm, Ti 9.999% purirty.
mixture has next composition $NH_4F \cong 0.3\%W$ $H_2O \cong 2\%V$ ID and Ethylene Glycol (ED), I made a preanodization for cleaned the surface, in this process was used 3%HF, for 15sec with P=30V.
the preanodization: using the same set-up
was made a variation in the heating, with a range 25°C even 53°C.
the anodization set-up was description in the seccion 2.2

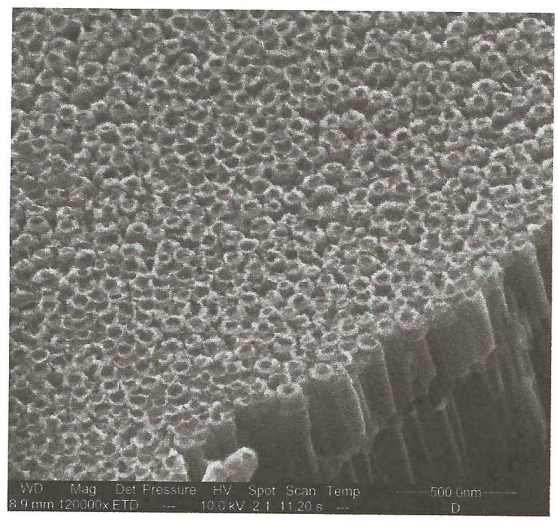

Fig2.5.1 SEM image ITO/TiO_2 nanotubes

We made different measures heated

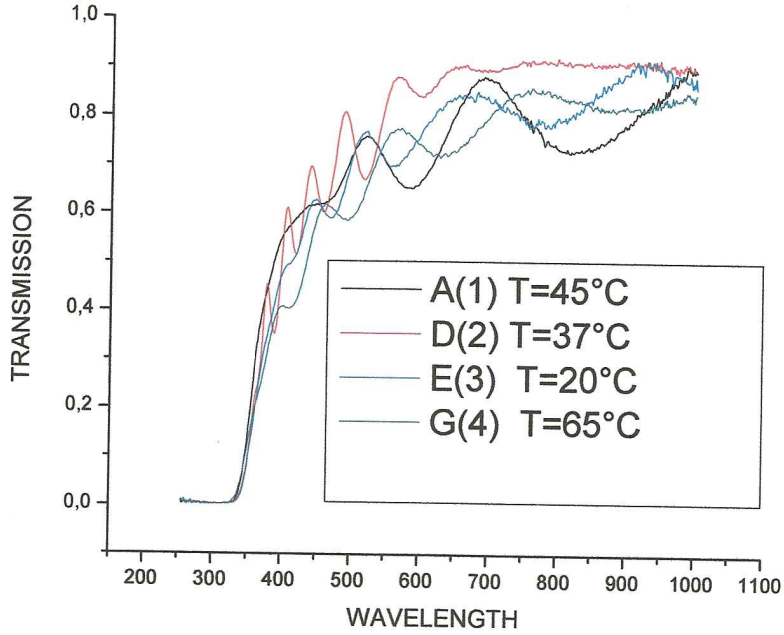

Fig.2.5.2

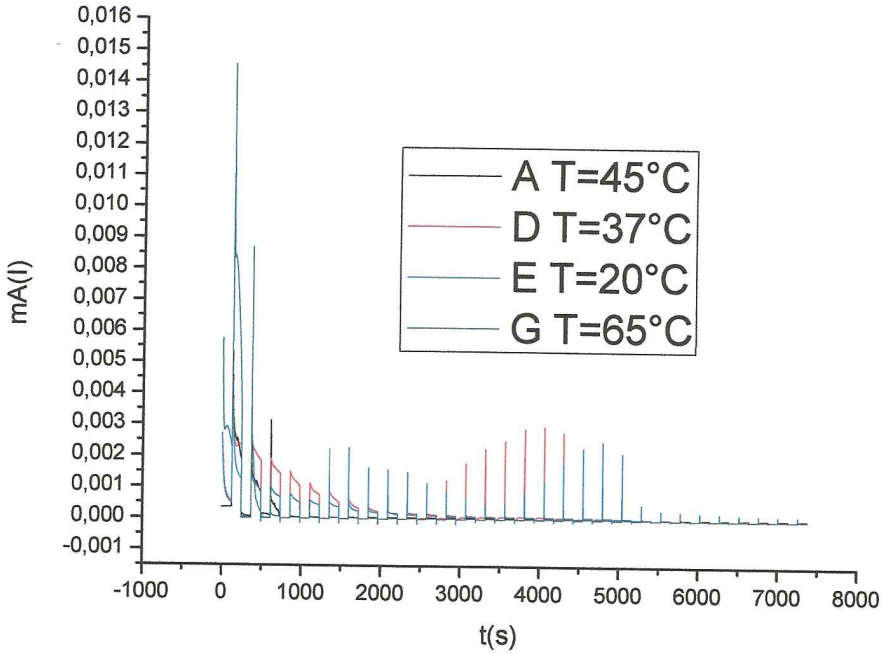

Fig 2.5.3

2.6 ITO/TiO_2 nanotubes sputtering with Ag and Au

First step, was cleaned the substrate commercial ITO with water (ID) sonicated 10minutes, after 10minutes with ethanol 96% at T=70°C dried by Ar gas.
In this experiment were used target to Au of 99.99% purity, Ag of 99.999% purity and Ti of 99.999% purity, in the internal part of the sputtering chamber was adapted an oven for to heat the substrate, from at room to 600°C, Sputtering parameters ITO/Ti, T=350°C, t=30minutes P=60W, Chamber=$3.4x10^{-2}$mb, area Ar. The sputtered samples are left in vacuum for a long time to insure a slow cooling.
Second step, anodization ITO/Ti: before the anodization is necessary to clean the substrates, they are sonicated for 10sec in ethanol and dried by Ar gas flow. The electrolyte is prepared by 2V%H_2O, 0.3%W and Ethylene Glycol, The anodization was performed in a two-electrode electrochemical cell with the substrate ITO/Ti,**Fig.2.2** as the working electrode and platinum foil, under applied pulse voltage at room temperature (approximately 25°C) in either fluoride chloride electrolytes. Keithyley 2612A System Source Meter pulse power supply was used for potentiostatic anodization. The time-dependent current behavior under ()was recorded using a computer controlled multimeter. A schematic representation of the anodization setup is shown in **Figure 2.2.** After anodization, the samples were rinsed thoroughly with deionized water(ID) and then blow-dried with 99.99% pure Ar. After this process, is necessary to cleaning the sample, with toluene about 8h, evaporate in this way the chemical substance, the crystallization process, put in the over **Fig.2.3.1** for 2h at 500°C, with this parameters obtained anatase phase.
ITO/TiO_2 nanotubes were recovered with a thin Ag and Au layer by sputtering deposition technique
We made two experiments one, chamber=3×10^{-2} mb, P=20W, d=5.5cm, t=100sec unheated, this one was done at low power.
In the second experiment were used the following parameters: chamber=3.4×10^{-2} mb, P=180W, d=5.5cm. t=5sec, T=350°C Ar gas area.

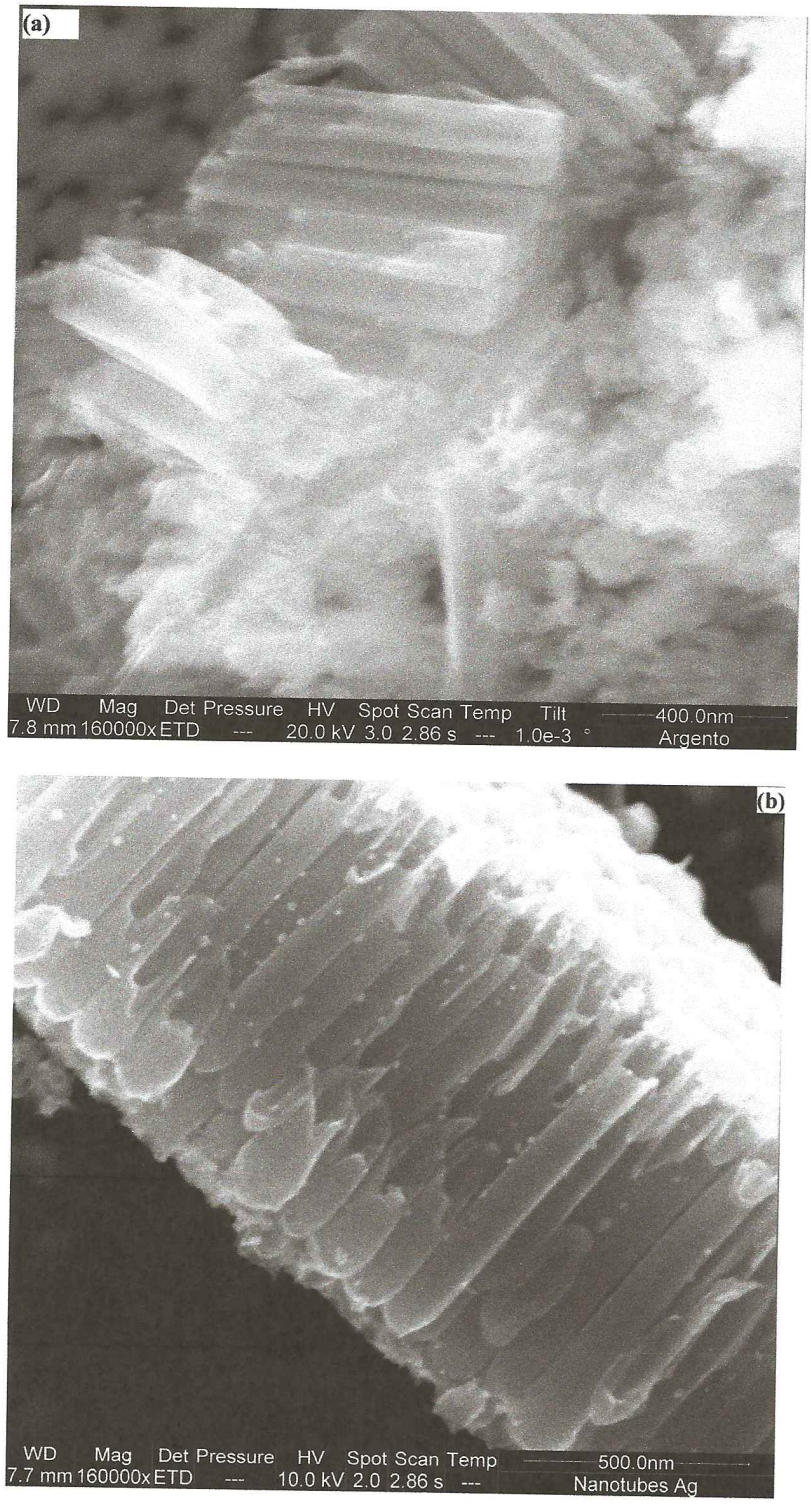

SEM images Sputtering TiO_2 nanotubes with Ag at T=350°C
a) internal part, b) external part.

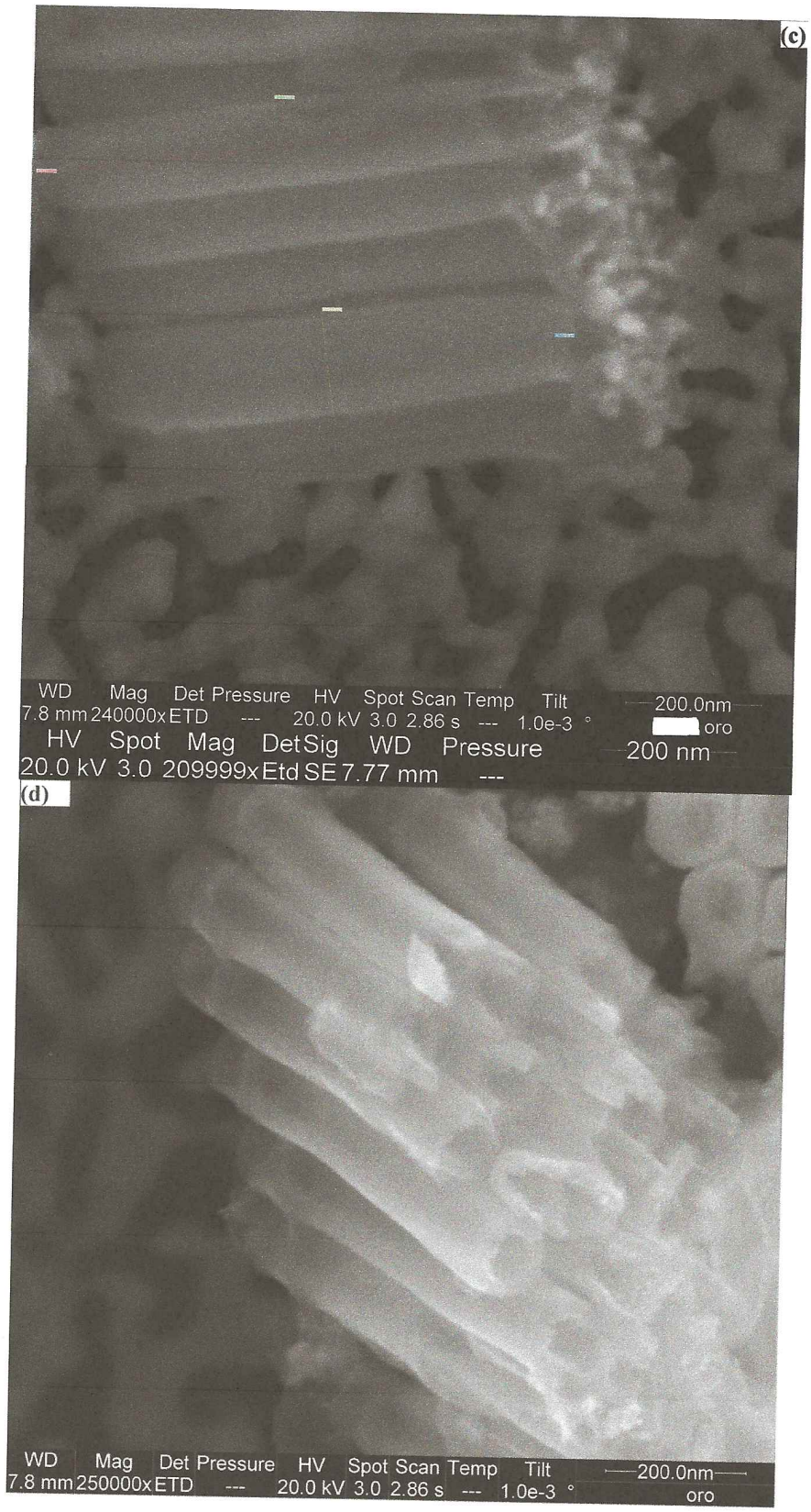

SEM images, sputtering TiO_2 nanotubes with Au at T=350°C 5sec, image (c) size.
Image (d) TiO_2 nanotubes broken, we can inner part impregnate with Au

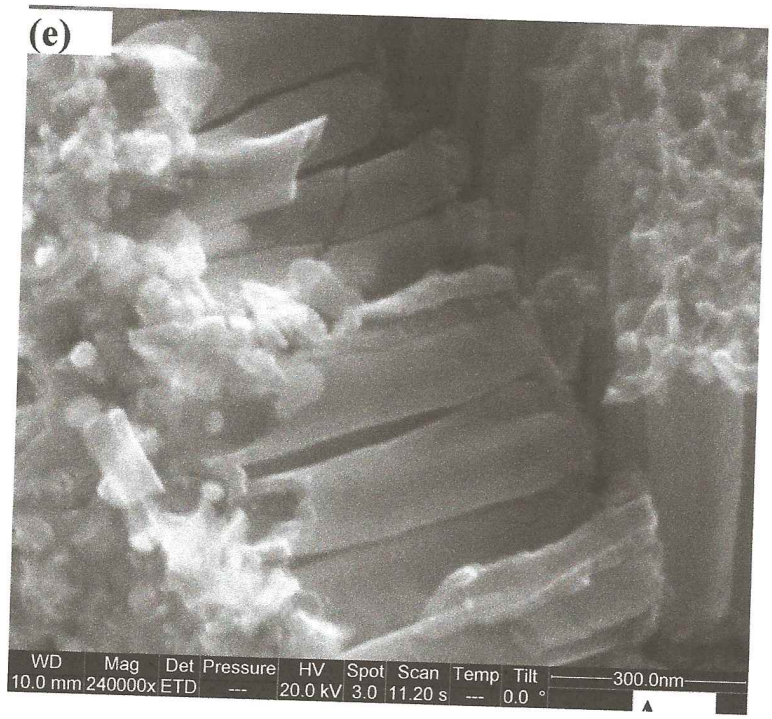

SEM image ITO/TiO_2 nanotubes with Ag sputtering at room in vacuum, left TiO_2 nanotubes broken with twister, Ag entered inner part, Ag particles are larger Those deposited at T=350°C, right TiO_2 nanotubes arrays impregnate in the inner part With Ag particles.

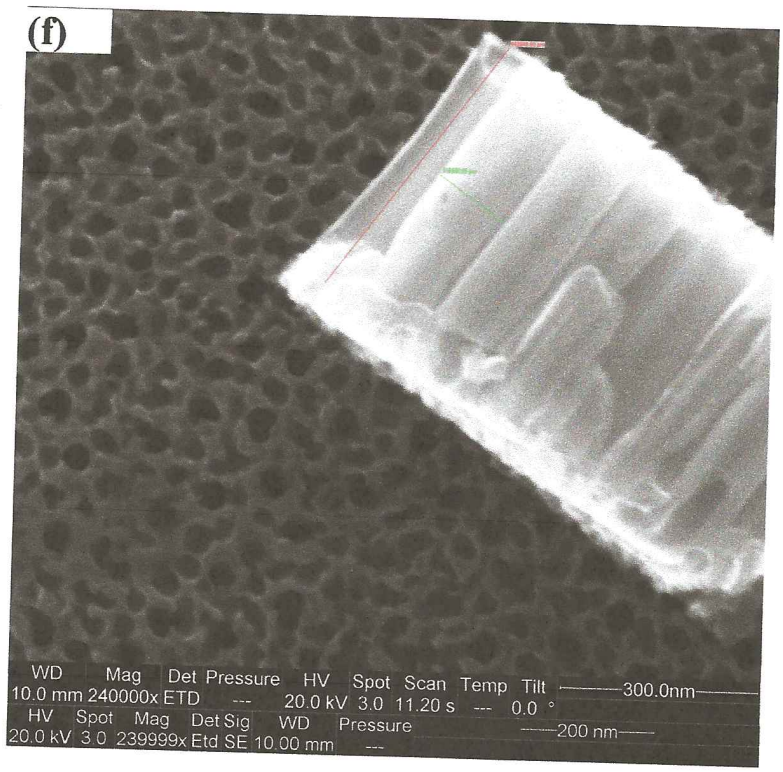

SEM image, **f)** Au sputtering unheated Au particles don't enter

2.7 Glass/Au/TiO_2 nanotubes

First step, was cleaned the substrate slide glass (Carlo Erba code 0893.02010), with water (ID) sonicated 10minutes, after 10minutes with ethanol 96%
In this experiment first was spattered Au, in the second part Ti,
Au sputtering parameters: P=20W, T=350°C, t=100sec, distance target sample d=5.5cm, chamber=$3x10^{-2}$, The sputtered samples are left in vacuum for a long time to insure a slow cooling.
Ti/Au sputtering parameters:T=350°C, t=10minutes P=60W, Chamber=$3.6x10^{-2}$mb, area Ar. The sputtered samples are left in vacuum for a long time to insure a slow cooling.
Second step, anodization: before the anodization is necessary to clean the substrates, they are sonicated for 10sec in ethanol and dried by Ar gas flow. The electrolyte is prepared by 2V%H_2O, 0.3%W and Ethylene Glycol, The anodization was performed in a two-electrode electrochemical cell with the substrate ITO and slide glass, sputtering with titanium as the working electrode and platinum foil, under applied pulse voltage at room temperature (approximately 25°C) in either fluoride chloride electrolytes. Keithyley 2612A System Source Meter pulse power supply was used for potentiostatic anodization. A schematic representation of the anodization setup is shown in **Figure 2.2.** After anodization, the samples were rinsed thoroughly with deionized water(ID) and then blow-dried with 99.99% pure Ar. After this process, is necessary to cleaning the sample, with toluene about 8h, evaporate in this way the chemical substance, the crystallization process, put in the over for 2h at 500°C, with this parameters obtained anatase phase.

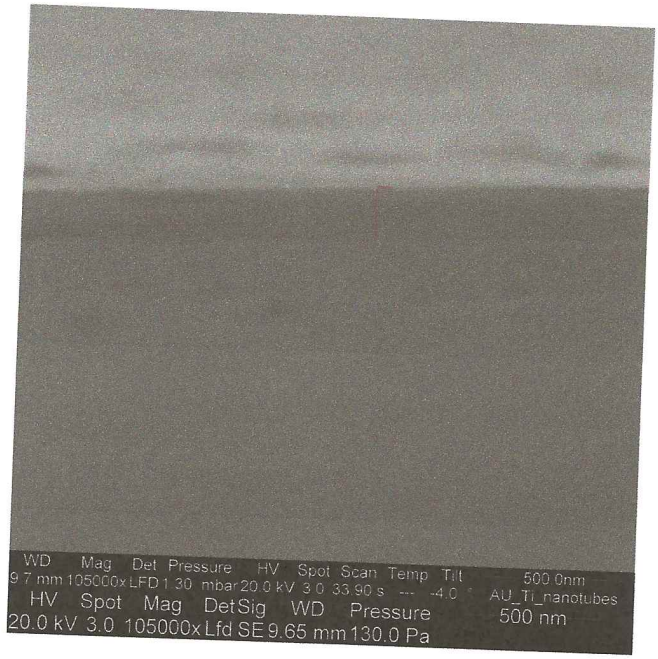

fig.2.7.1 SEM image, thin film gold thickness≈20nm

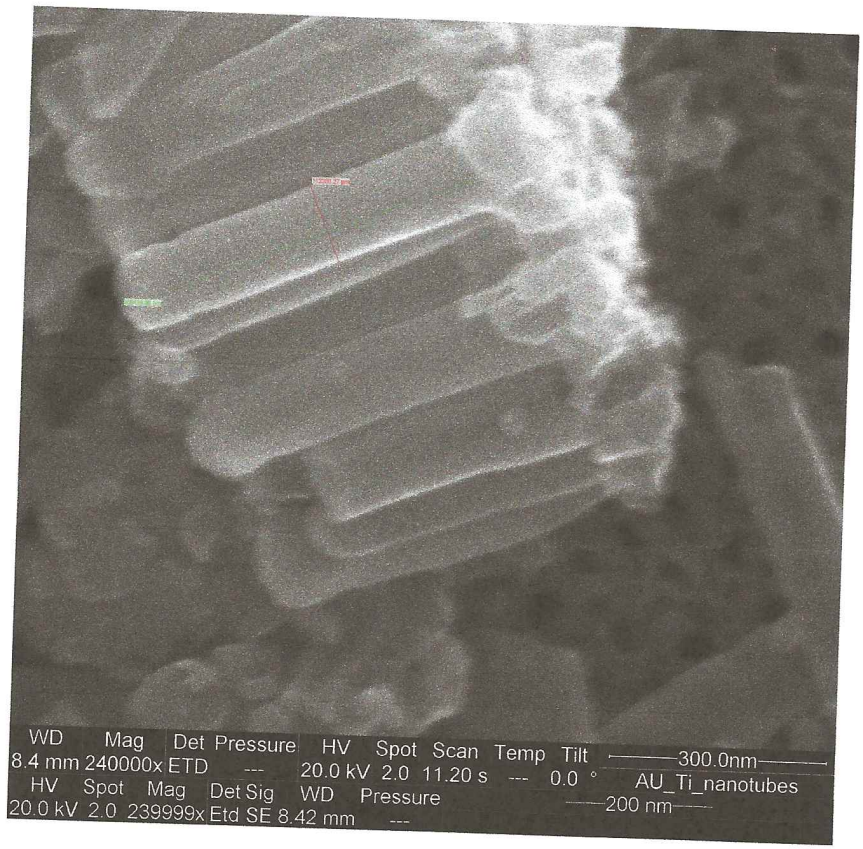

fig.2.7.2 SEM images, TiO_2 grown on thin films Au
0.3%WNH_4F, 2%VH_2O EG

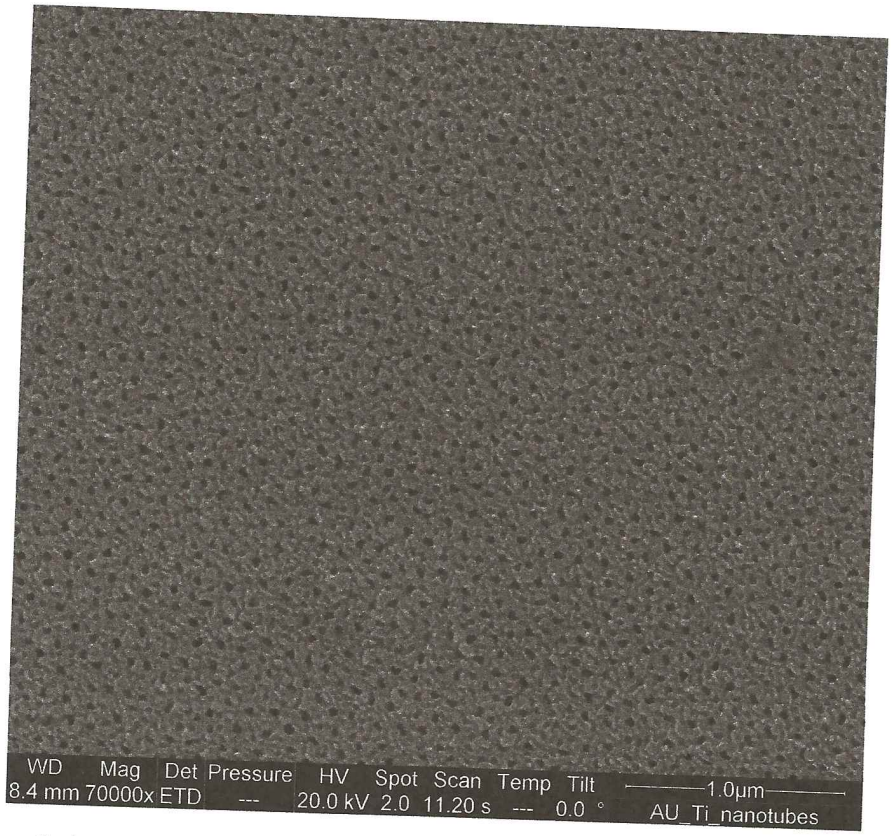

fig.2.7.3 The superficial part, we can see holes, for see the nanotubes and the Au substrate, is necessary to broken the thin film.

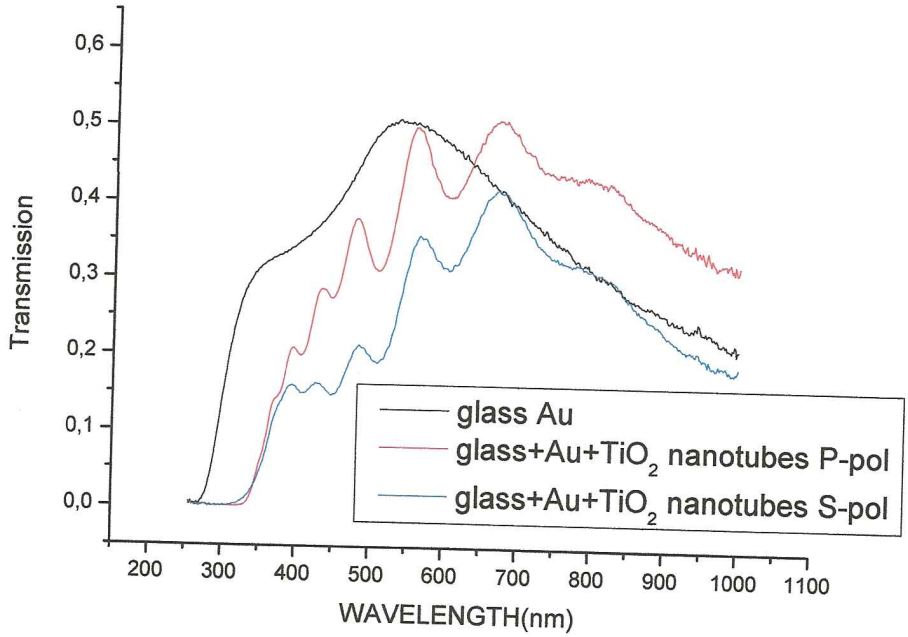

Fig.2.7.4. transmission response.

MICROTUBES

2.7 Describing experimental part of MICROTUBES

First step, was cleaned the substrate slide glass (Carlo Erba code 0893.02010), with water (ID) sonicated 10minutes, after 10minutes with acetone, finally was put in the oven at T=80°C a few minutes.

Second step, sputtering: the sputtering machine was used the same in all experiments Fig.1.2. the parameters were, P=400W, t=30min, area Ar, chamber=3.6×10^{-2}mb distance target sample d=7cm, finally over for 3h, T=400°C.
Third step, Mixture: the mixture was prepared with 400ml EG, 3%WNH_4F, 2% V H_2O (ID) after to prepare the mixture, was put on electromagnetic stirrer with plate at temperature T=80°C for 40minutes, for dissolver NH_4F salt.
The anodization: this experiment was performed see **Fig.2.7.1**, used the classical anodization set-up, in this case was necessary maintain during experiment constant temperature, we used thermostatic bath at T=30°C a constant voltage P=60V.

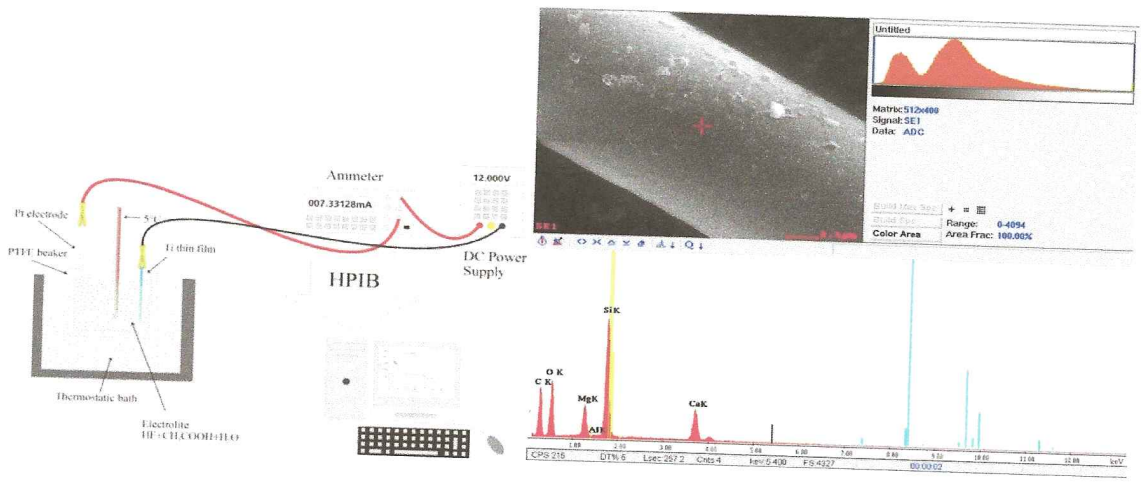

Fig.2.7.1 Left experimental set-up, right microanalysis microtubes

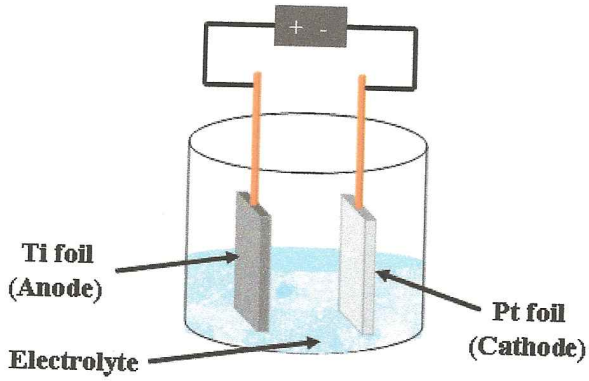

Fig.2.2.7 Schematic of the anodization set-up.

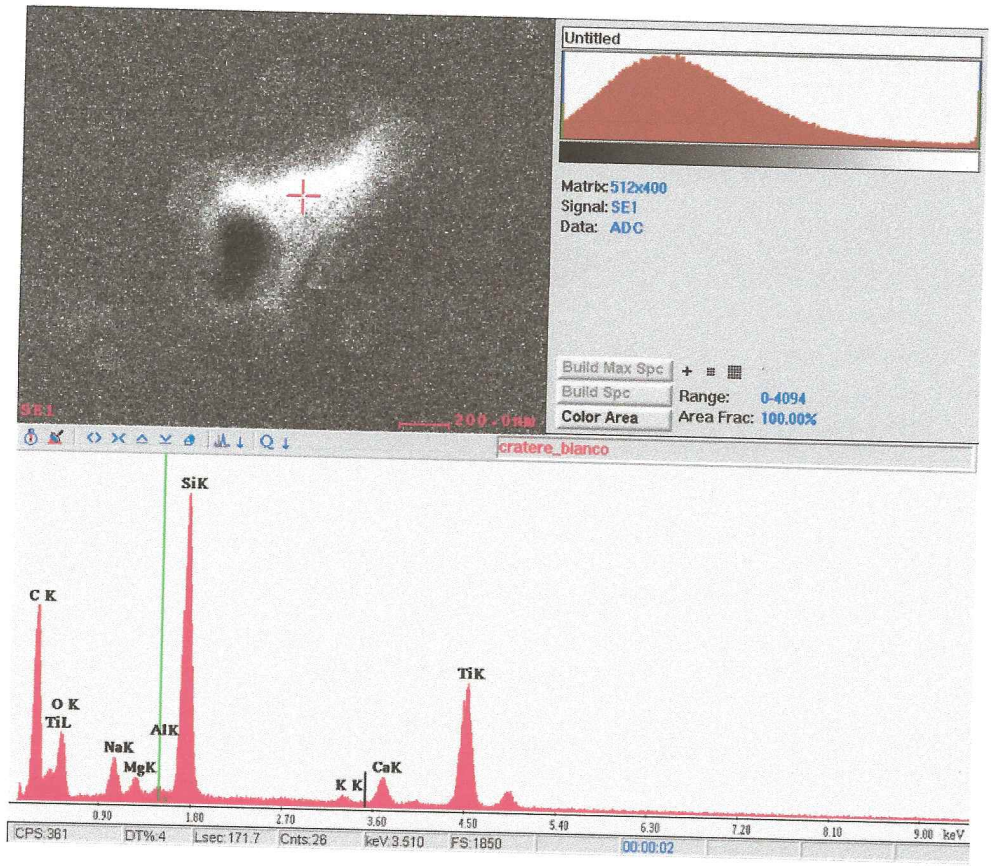

Fig.2.2.8 Microanalysis growing microtubes,

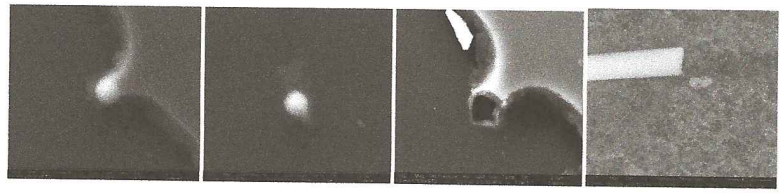

Fig.2.2.9 SEM images, Sequence of growing SiO_X Microtubes

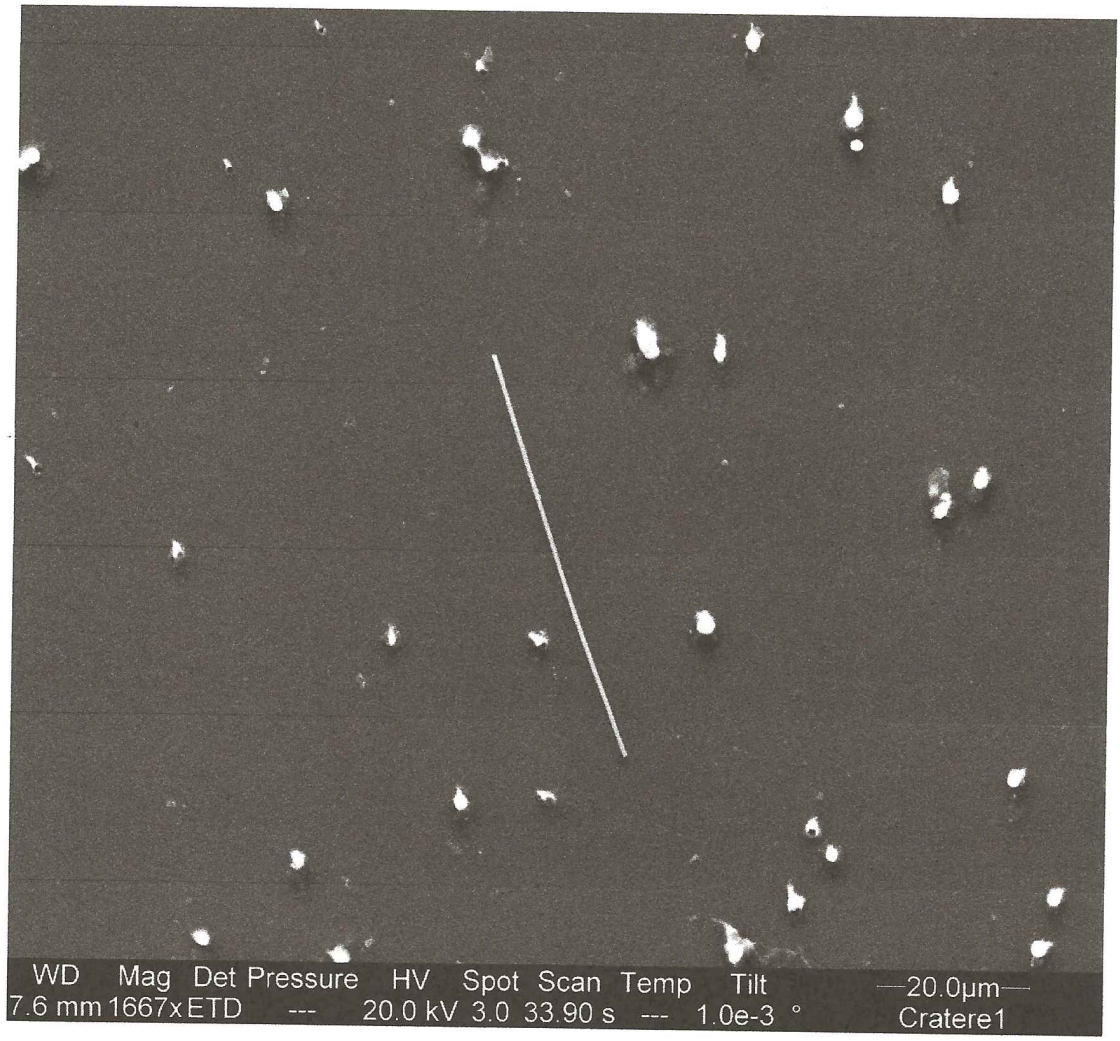

Fig.2.2.10 SEM image, white craters growth of microtubes

2.8. EXPERIMENTAL PART

Surface Plasmon Polariton

SPP

In this part We used the Kretschman configuration **Fig.2.8.1**, Laser LHP-1201 He-Ne $\lambda \approx 633nm$, triangular prism n=1.5 refraction index, circular table with graduation degrees, a detector for measure the energy an oscilloscope, a polarizer, special glasses for eye protection and Microscopy Immersion Oil (n=1.5).
For this study, thin film was made for Drew Pulsifer, in the MRI laboratory State College University, by PVD evaporation, first was evaporated a thin film of Al ≈30nm, next with an angle $\chi=10°$ while the system turned evaporating ZnSe.

In this form hem made sculptured chiral thin films(SCTFs) of three and four pitch.
Only for this thin films Al/ZnSe were made up P-pol polarization S-pol polarization, TS-pol TP-pol.
each 25' it took a lecture, starting with -25 radians until 40 radians.
Also we made for this study, Au thin film 50nm **Fig.2.8.2**, Al thin film **Fig.2.8.3**, 30nm, for these only was take P-polarization
For to convert to radians degrees was used next mathematical expression,

$$\Phi=45°+\text{Arcsin}(\sin\theta / n_{glass})$$

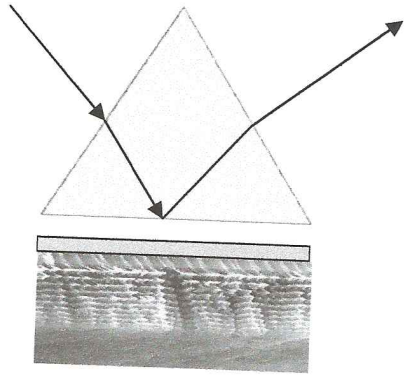

Kretschman configuration, thin film is attached to prism with microscopy immersion oil

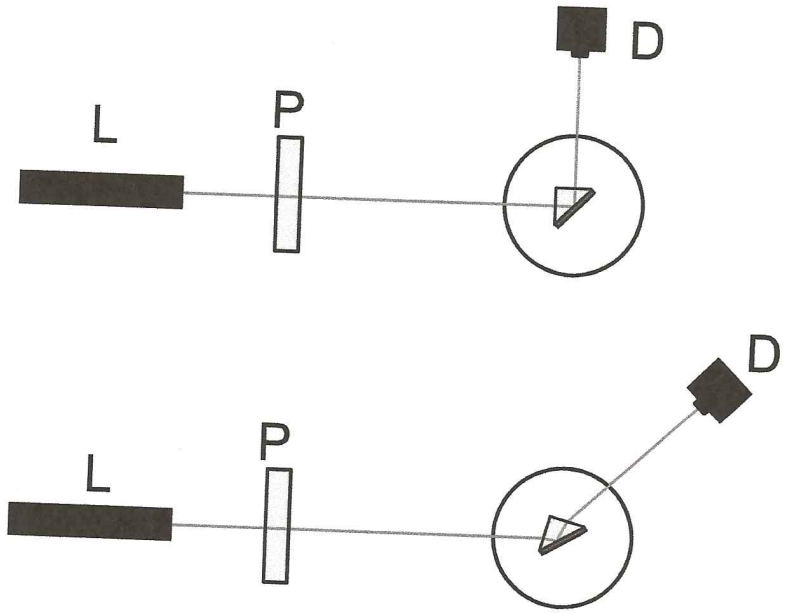

Fig.2.8.1 Total reflection. set-up for generating Surface Plasmon Polariton

CHAPTER 3

RESULTS

We obtained TiO_2 nanotubes arrays by anodization method successfully, we could

The optical properties[96] of the samples have been investigated by variable angle spectroscopic ellipsometry (VASE). Measurements were performed by an Woollam M2000F rotating analyzer ellipsometer, data analysis were accomplished by the VASE software by J.A.Woollam Co.
Ellipsometric angles were acquired for both the annealed and the not annealed sample at 475 wavelength in the range 245nm -1000 nm and fitted by an appropriate optical model . In **figure 3.1a** and **fig 3.2a** we show the experimental data along with them best fit for both the annealed and not annealed sample. In both cases the best agreement were found by the stratified model given in **figure 3.1b** and **3.1c** for the not annealed and the annealed sample respectively. The model of the not annealed nanotube film consists of 6 different layer, the deeper layer consists in a titanium film, whose optical constants (**fig 3.1c**) were found il literature.
On the top of this layer there is a TiO_2 solid layer which is few tens of Angstrom, the optical density of this layer is very high and it is perfectly transparent till 350mn, as shown in **figure 3.1d** and **3.2d**, confirming that at the basis of the nanocolumnar structure there is a solid TiO_2 layer intermixed with titanium atoms.
Then we found the nanotube array modeled by a Burggmann effective media approximation (EMA) layer. This layer consists of TiO_2 and empty space (about 50%), as result its refractive index n undergoes to a strong decrease, see **figure 3.1e** and **3.2e.**
On the top of the structure there is a low dispersing, very transparent Cauchy layer, it might be meso or nano porous titania, whose optical constants are shown in **fig 3.1f** and **3.2f.**
As effect of the annealing process the film becomes most uniform, its roughness decrease and as a whole the refractive index increase, suggesting for the annealed sample an higher crystallinity with respect the not annealed.

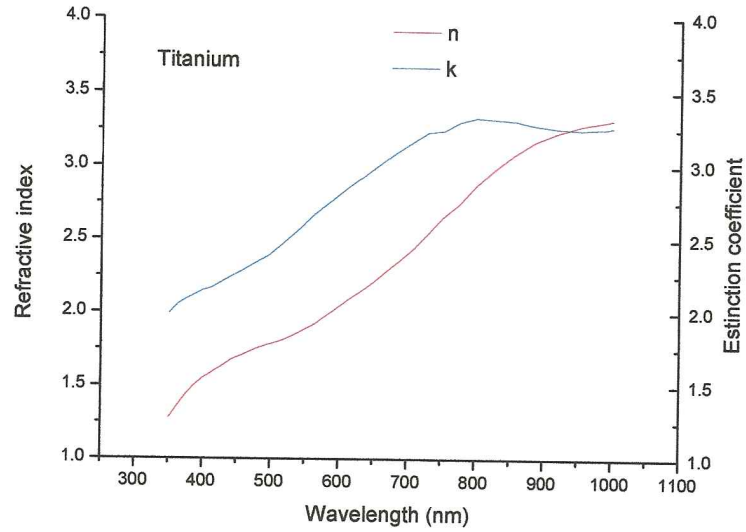

fig. 3.1c

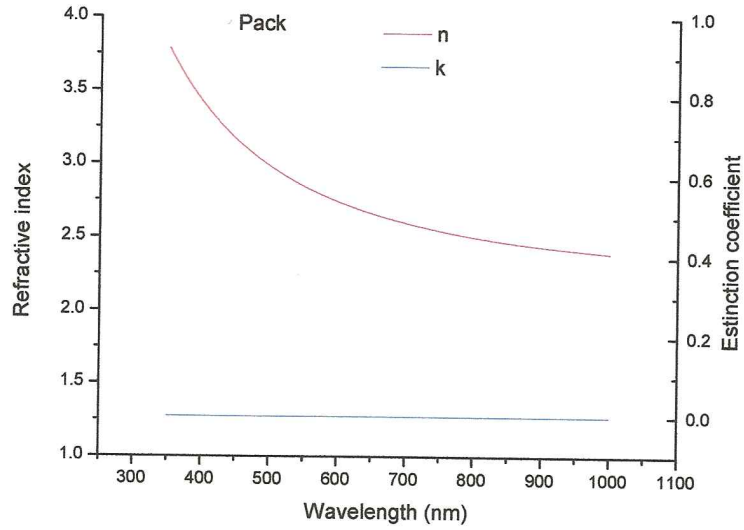

fig. 3.1d

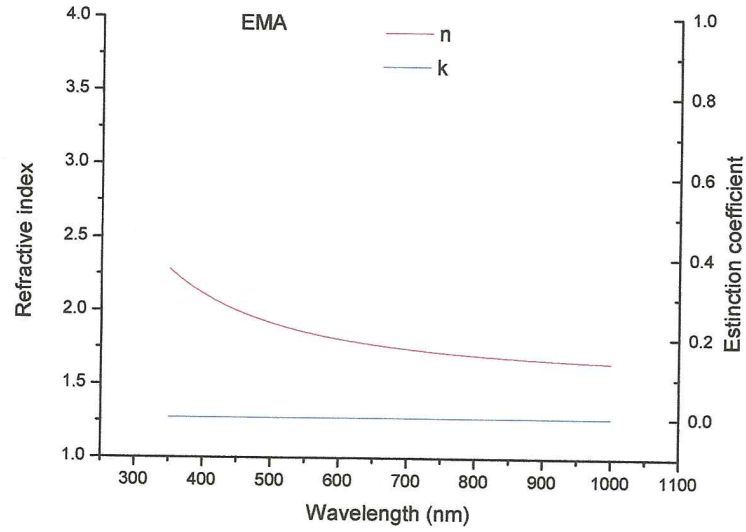

fig. 3.1e

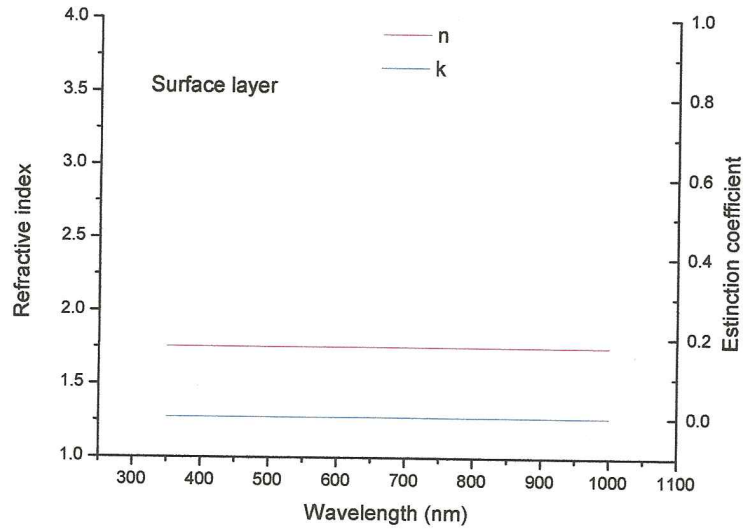

fig. 3.1.f

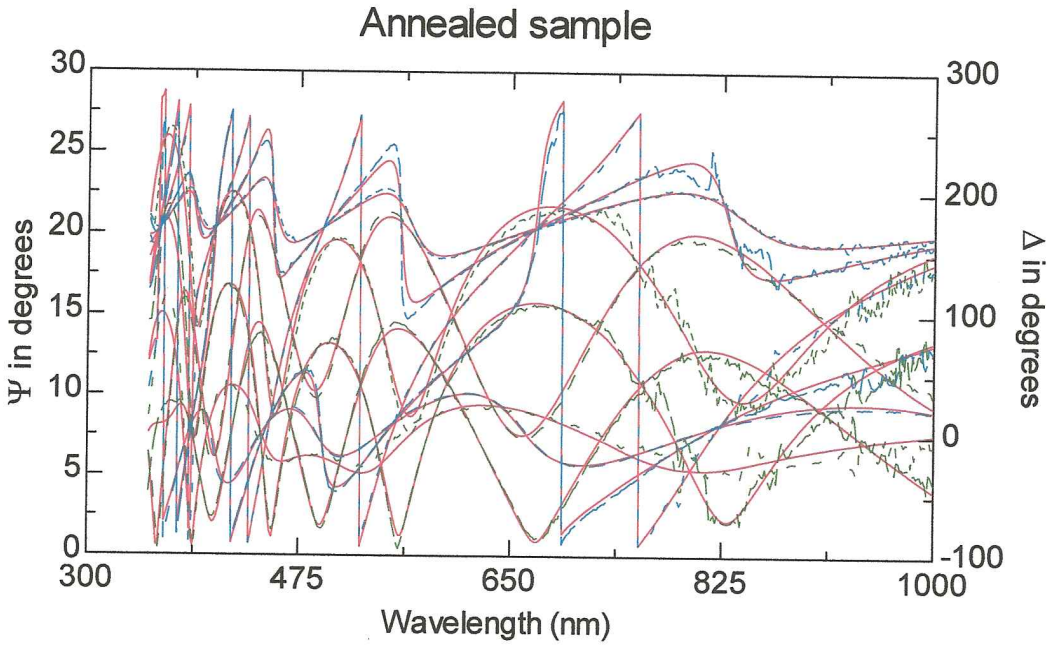

fig.3.2.a

6	srough	8.6534 nm
5	strato superficiale	92.914 nm
4	ema (pack)/50% void	336.64 nm
3	pack	5.4671 nm
2	intermix	7.7315 nm
1	ti	3.3276 nm
0	sodalime carlo erba	1.1 mm

fig.3.2.b

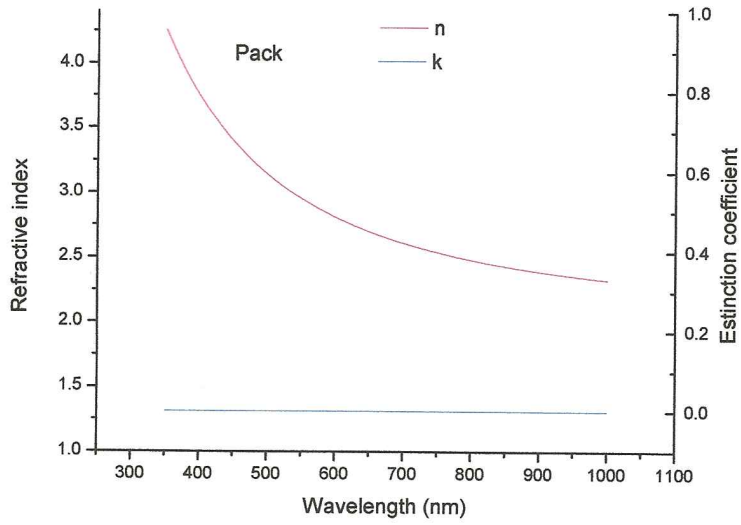

fig.3.2.c

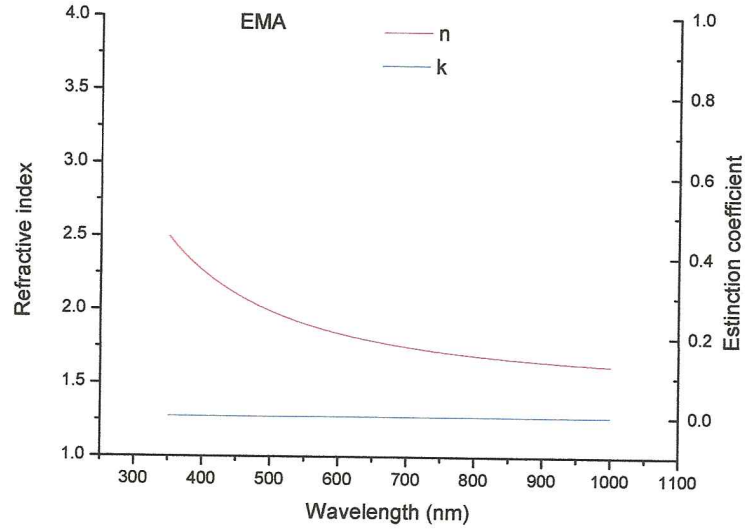

fig.3.2.d

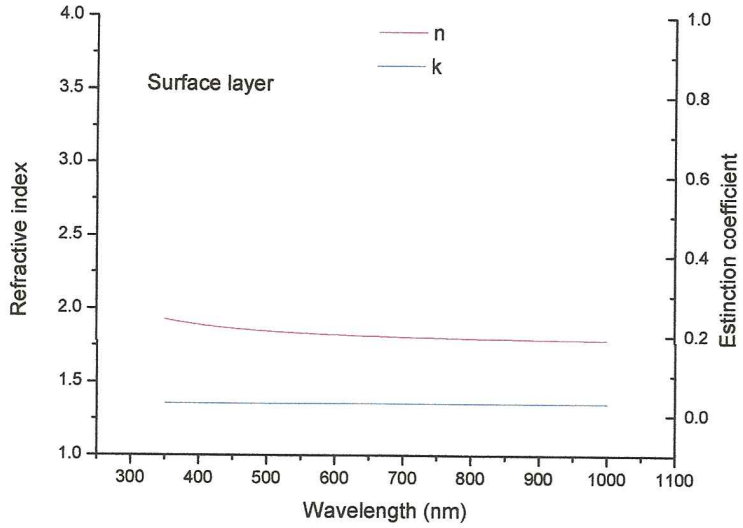

The Transmittance spectrum, annealed and not annealed is clear the change in the absorbance bad, Next heat treatment, TiO_2 are transparently

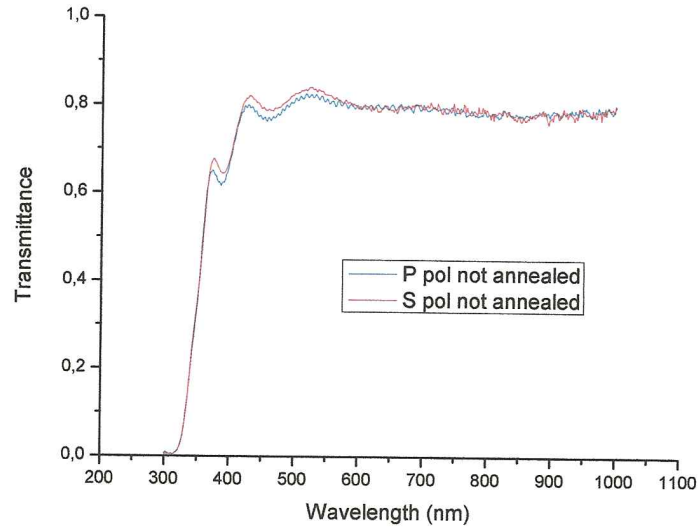

fig.3.2.c

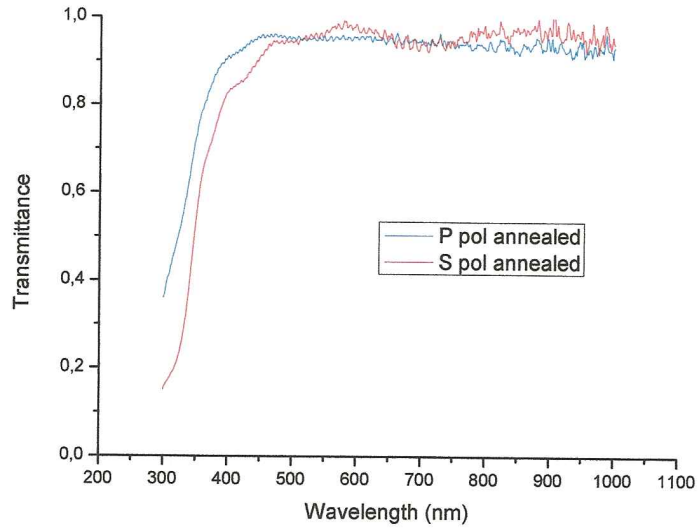

fig.3.2.d

Diameter and length variation depending on temperatures.

	15°C	25°C	30°C	35°C	40°C	45°C	51°	**54°**
d_{in}(nm)	168.25	109	124.32	140.63	121.06	118.9	190.24	**98.24**
d_{ex}(nm)	87	34	54.86	90.4	68.32	75.2	142.93	**33**
length(nm)	**512.87**	**430**	**599.38**	**518.37**	**650**	**668.87**	**601.13**	**644.66**

Table 3.1 variation temperature vs dimension TiO_2 nanotubes

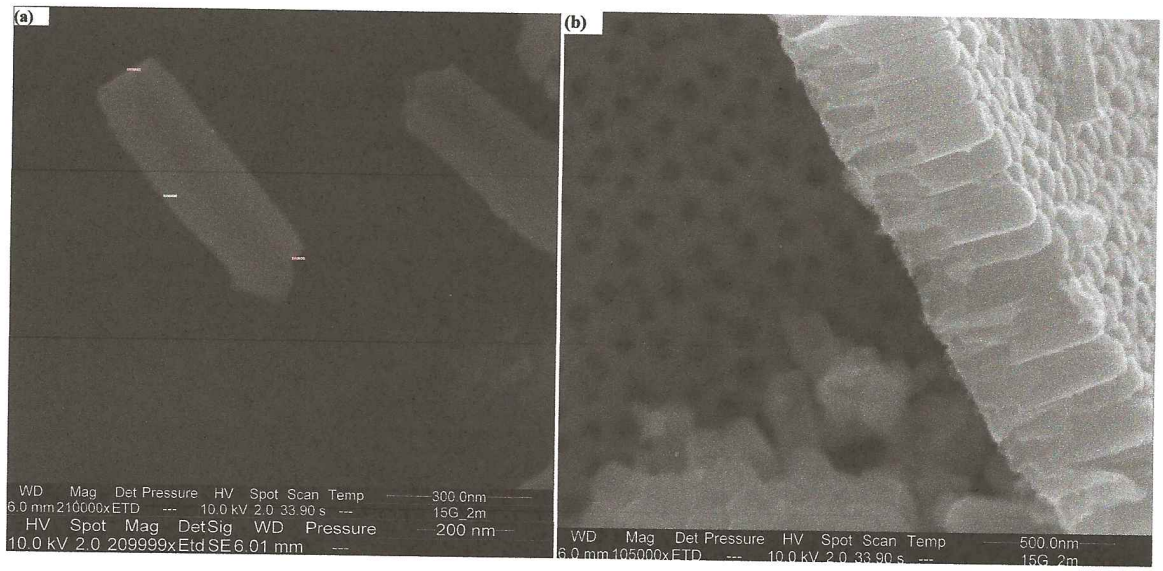

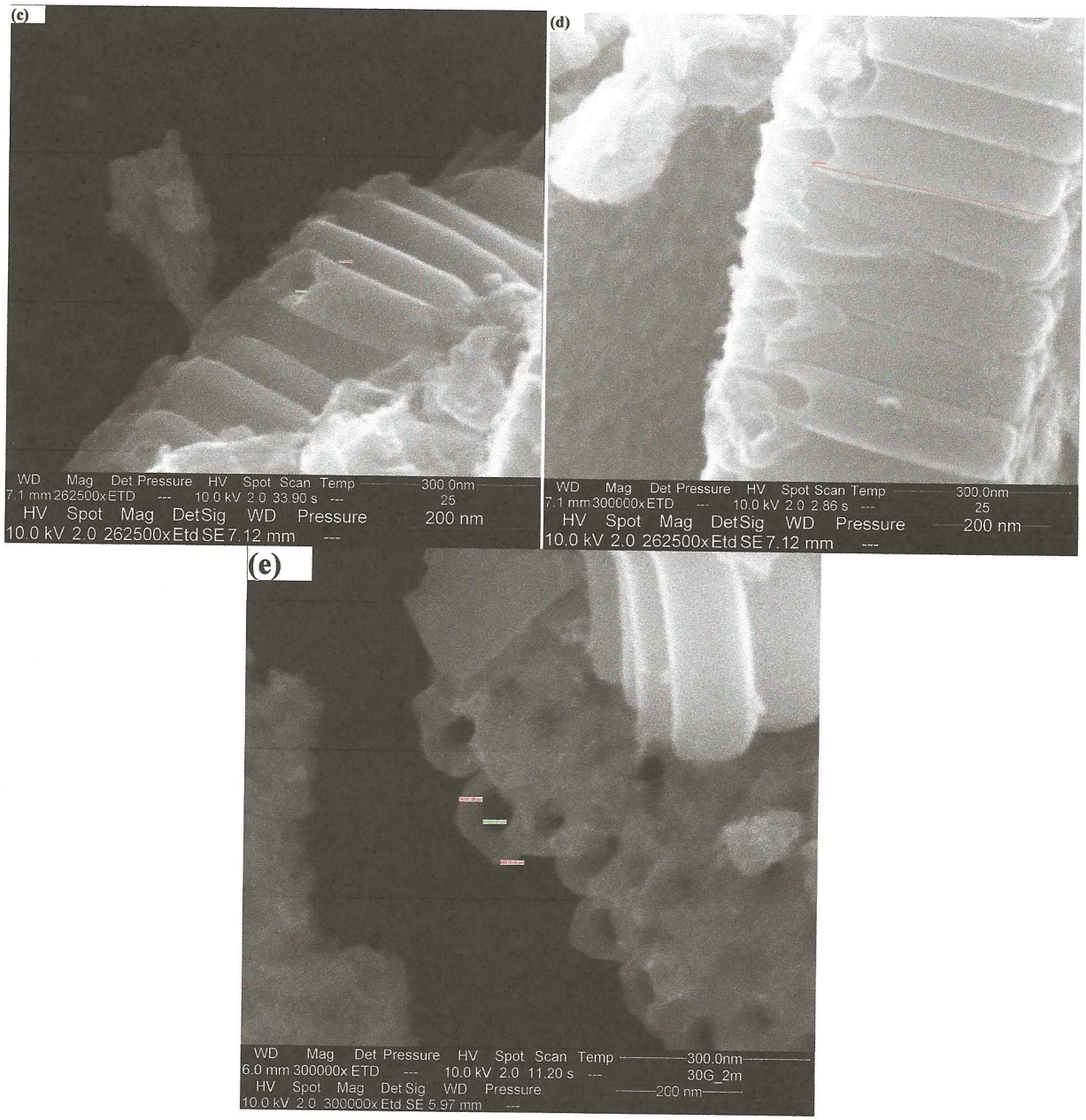
(c)
WD Mag Det Pressure HV Spot Scan Temp 300.0nm
7.1 mm 262500x ETD --- 10.0 kV 2.0 33.90 s --- 25
HV Spot Mag DetSig WD Pressure 200 nm
10.0 kV 2.0 262500x Etd SE 7.12 mm ---
(d)
WD Mag Det Pressure HV Spot Scan Temp 300.0nm
7.1 mm 300000x ETD --- 10.0 kV 2.0 2.86 s --- 25
HV Spot Mag DetSig WD Pressure 200 nm
10.0 kV 2.0 262500x Etd SE 7.12 mm ---
(e)
WD Mag Det Pressure HV Spot Scan Temp 300.0nm
6.0 mm 300000x ETD --- 10.0 kV 2.0 11.20 s --- 30G_2m
HV Spot Mag Det Sig WD Pressure 200 nm
10.0 kV 2.0 300000x Etd SE 5.97 mm ---

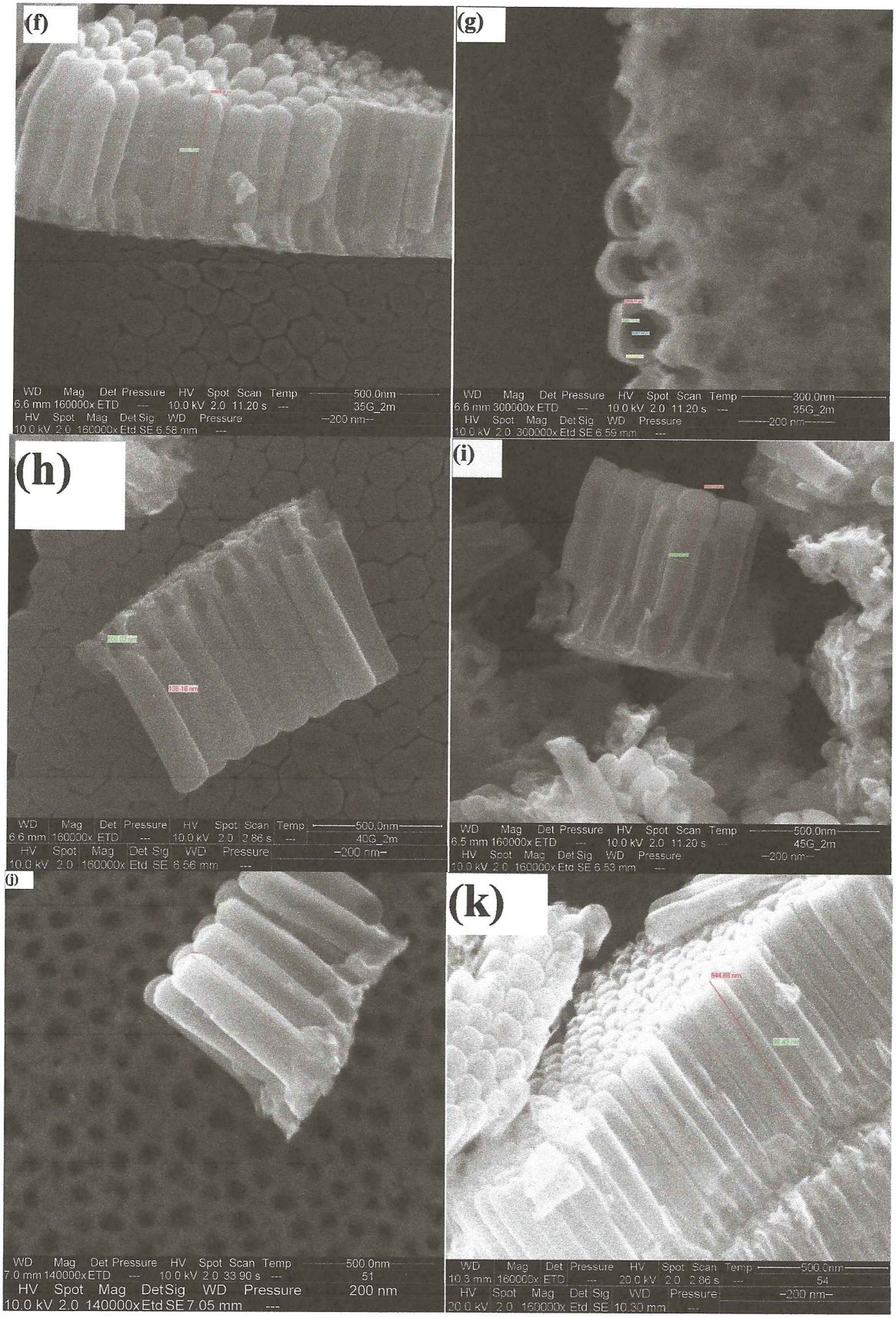

SEM images, we vary the temperature for study the behavior TiO_2 nanotubes, We could see the change, the size variation, high temperature, are longer. But the diameter is short and vice versa.

RX ANALYSIS :

It is known that the as-fabricated nanotube arrays have an amorphous crystallographic structure. Upon annealing at elevated temperatures in an oxygen ambient, the naotubes wall transform into anatase phase[6,96].

The crystallographic properties TiO_2 nanotubes arrays were studied by RX[96] asymmetric geometry and Bragg-Bretano, which reveled presence anatase phase and a very weak rutilo phase, **fig.3.3.1,** that were put in over T=500°C, as was explain in the **Chapter 2.** The principal characteristic are obtained depend which were preparing it, in all experiment the anneling treatment was the same, the interesting discussion about this thermal treatment was published[6] how change the properties, depending as annealing treatment better behavior as crystalline structure.

The XRD results combined with the colour change strongly indicate that the electronic properties of the tubes show differences, whether anneales in Ar or air.

In the spectrums **fig 3.3.2, fig 3.3.3** show peaks TiO_2nanotubes/Au prepared as was explain in the **section 2.7** the TiO_2 nanotubes, were prepared with the same parameters sputtering and anodization, we could see only in the TiO_2 nanotubes/Au rutile phase at θ=39.2° and θ=69.18°. Due to presence of the metals Au, Ag the enhanced anatase and rutile phases.

Only a few items have been written[110,124] about this research, my idea may be is possible apply As metamaterials, but in this field TiO_2 nanotubes don't exist currently research.

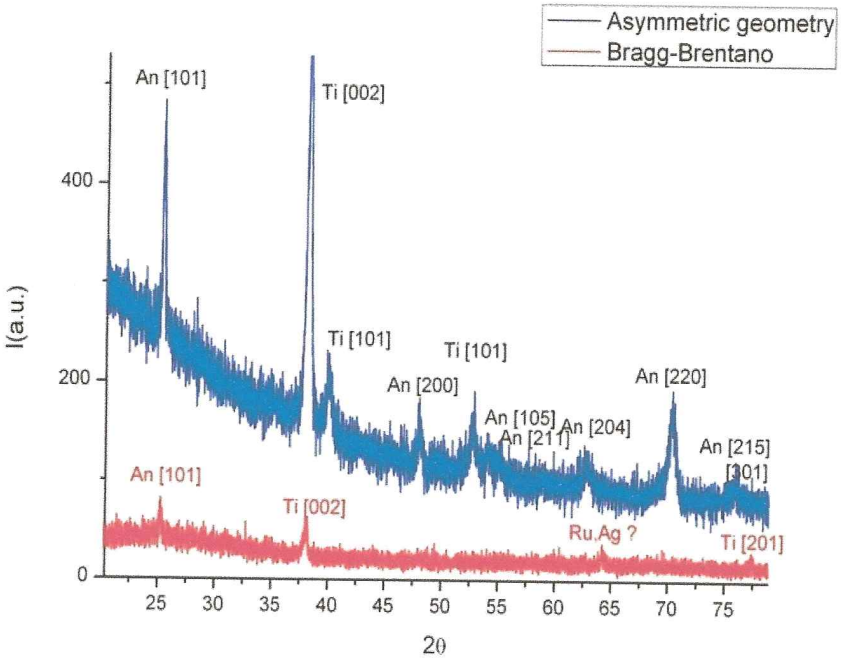

Fig.3.3.1 RX patterns TiO_2 nanotubes annealed at 500°C

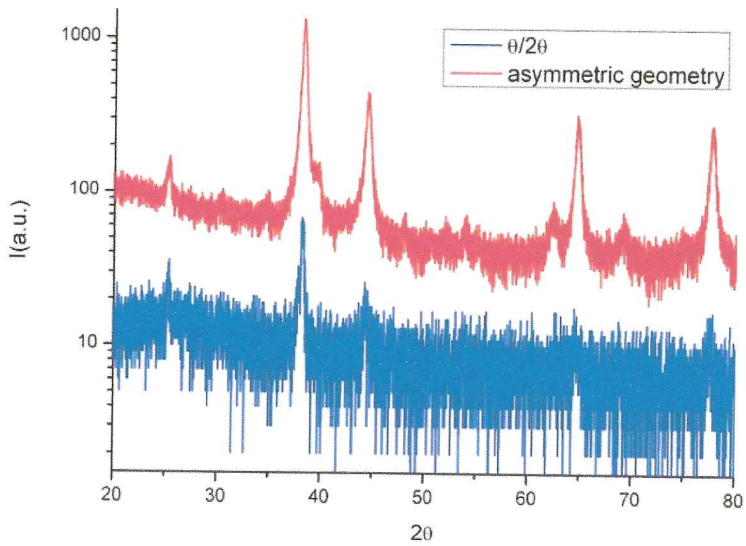

Fig3.3.2 RX: TiO_2 nanotubes/Au,
sputtering at 350°C 5sec.

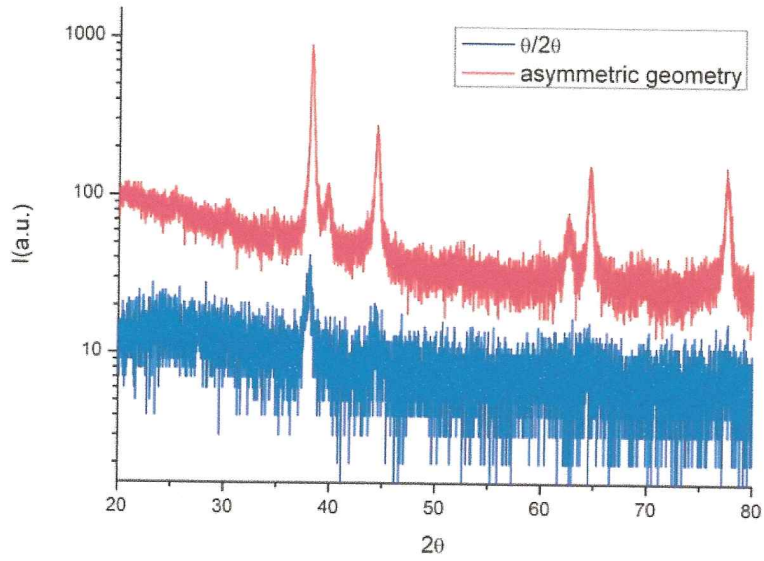

Fig.3.3.3 RX:TiO_2/Ag, Ag sputtering at 350°C, 5sec.

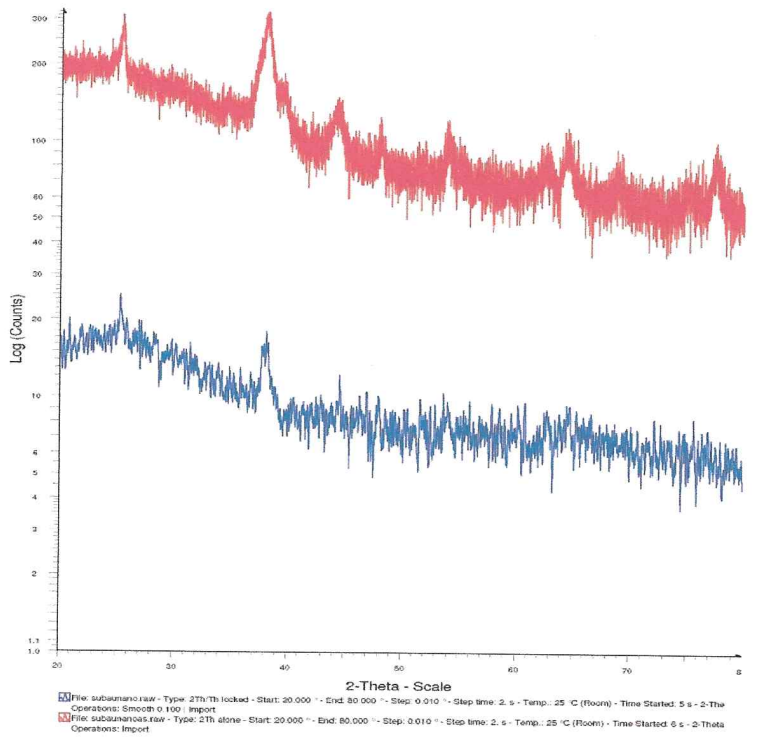

XR. fig.3.3.4 Au(20nm)/TiO_2 nanotubes

The Raman Study.

The samples (a) glass/TiO_2 nanotubes, (b) glass/ITO/TiO_2 nanotubes, (c) glass/ITO/TiO_2 nanotubes/Au, (d) glass/Au(20nm)/TiO_2 nanotubes obtained as described in **Chapter 2** have been investigated by SEM, XRD and Raman Spectroscopy [126,127,128,129,130]. The formation of nanotubes structures on the different substrates can be view by the SEM images shown in figure 3.3.4.

FIG.3.3.4

As it can be seen in **figure 3.3.4** no relevant differences between the nanotubes obtained on the different substrates can be detected.

It is interesting to observe the Raman spectra shown in **Figure 3.3.5.**

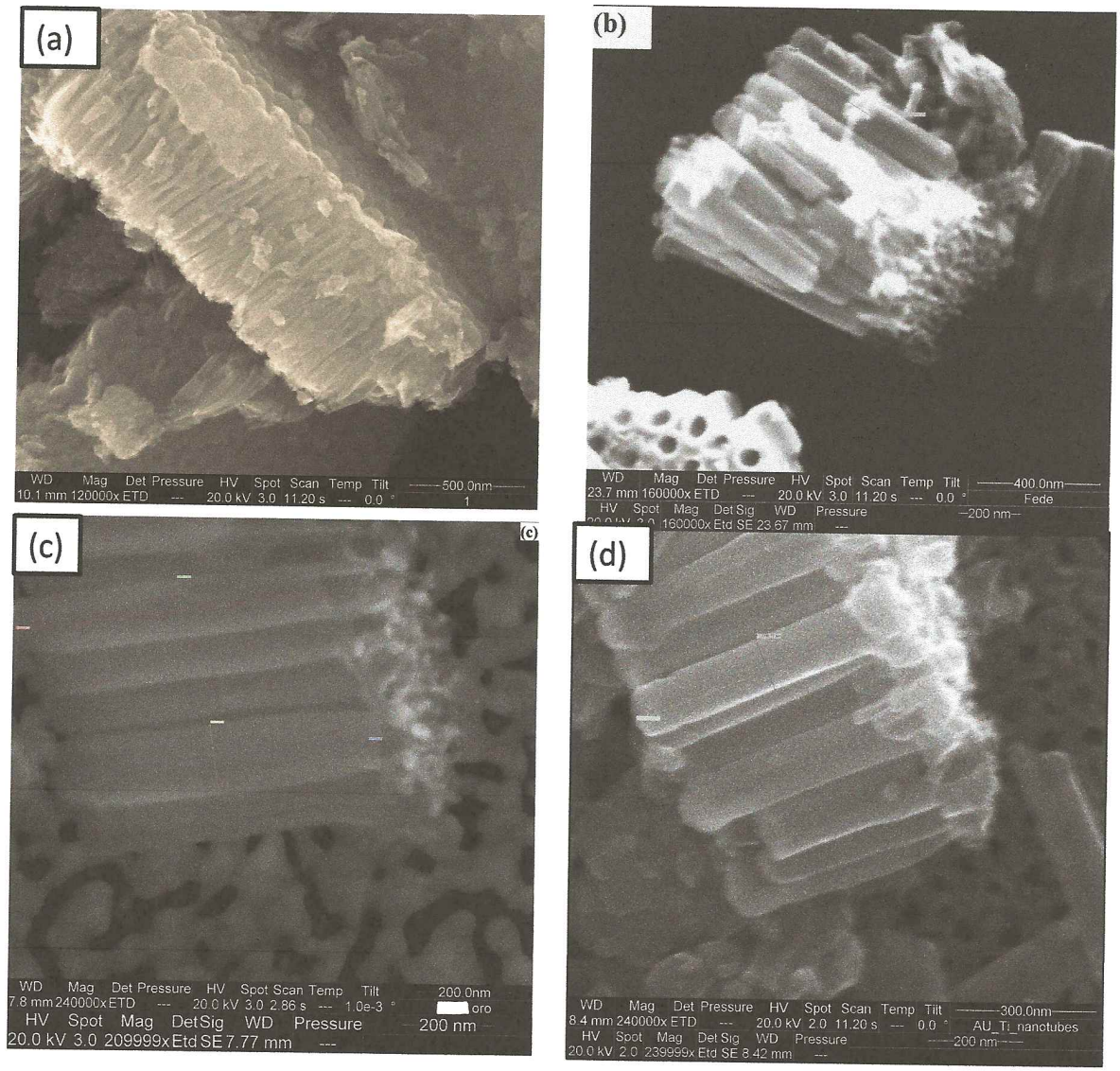

Fig 3.3.4 SEM images

As it can be seen in **figure 3.3.4** no relevant differences between the nanotubes obtained on the different substrates can be detected.

It is interesting to observe the Raman spectra shown in **Figure 3.3.5.**

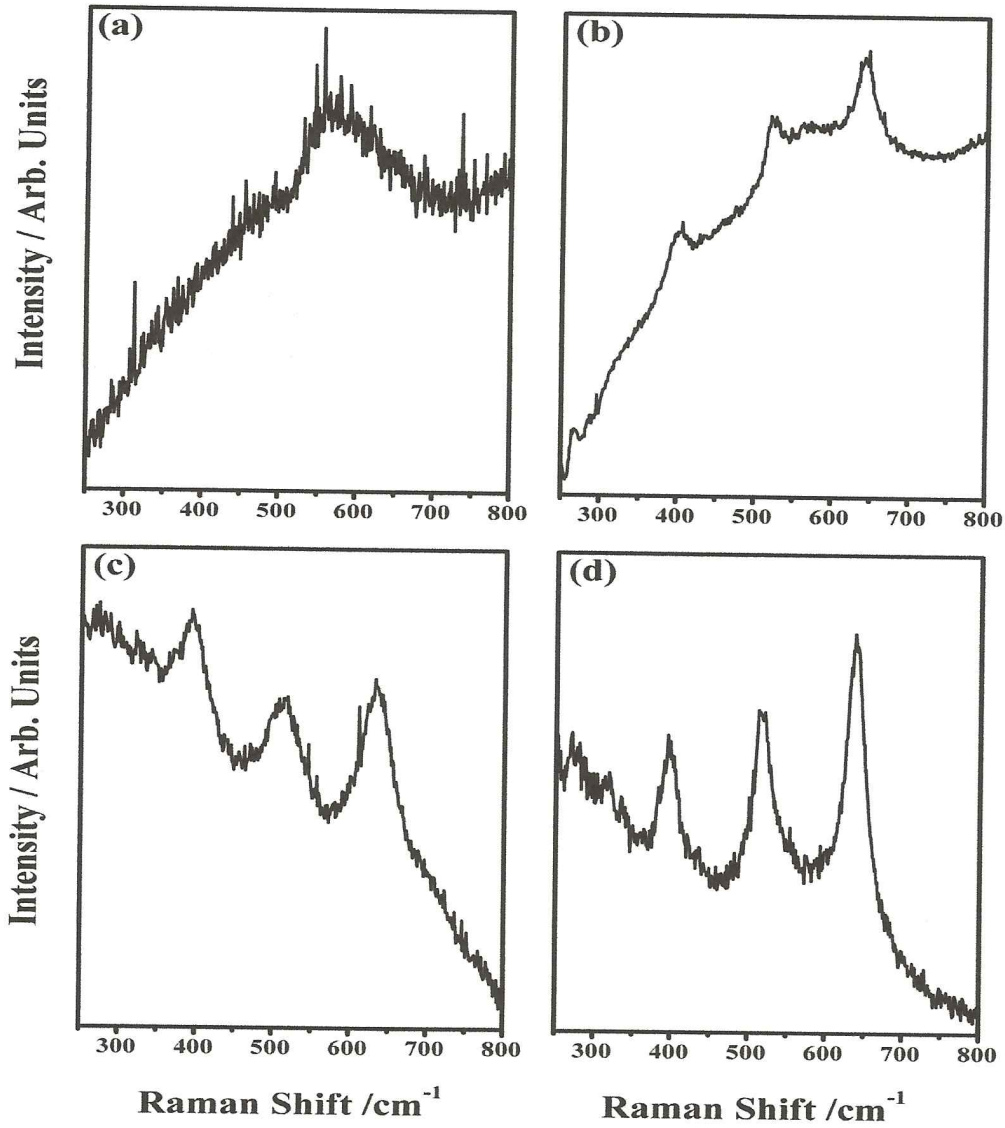

FIG.3.3.5

It can be seen that nanotubes obtained on glass substrates (**Fig. 3.3.5.a**) have been not detected by Raman spectroscopy. The main Raman features at about 396cm^{-1}, 514cm^{-1} and 638cm^{-1} assigned to the TiO_2 anatase can be detected on the samples with ITO substrate and become still more evident when the gold particles were sputtered above the NT (**Fig.3.3.5.c**). Raman spectra it is very interesting when such nanotubes, in anatase form, are obtained on the gold substrate. It can be seen (**fig. 3.3.5**) as the intensity ratios of the Raman bands increase in the sample d and the trend of the intensity ratios as function of the different substrates seems to indicates the presence of a SERS (Surface Enhanced Raman Spectroscopy) effect induced by the gold particles to the TiO_2 "nanotubes". In figura 3.3.6 it has been shown a particular Raman spectra collected on the samples (d).

FIG.3.3.6

As it can be seen with respect to the spectra shown in **fig. 3.3.5** in **fig. 3.3.6** there is the presence of one more Raman bands at about 285 cm^{-1} assigned to the present of sodium ions coming from the glass substrates [122] which could be the reason because the nanotubes obtained on the gold substrates results shorter than those obtained on the others substrates.

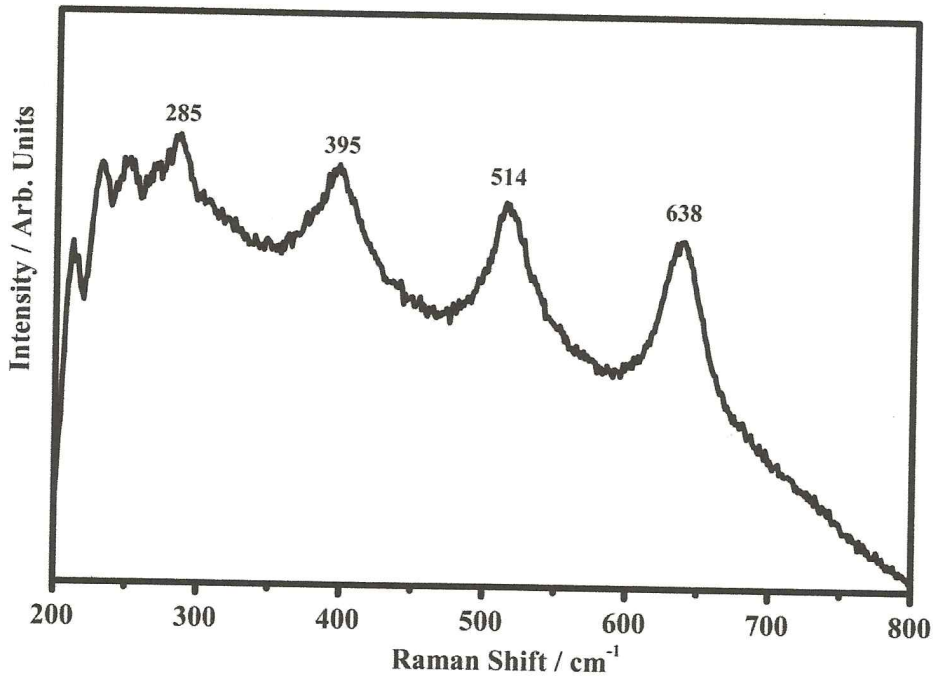

fig. 3.3.6

3.4 Plasmonics - opportunities and challenges

The possibility to confine light to the nanoscale and the ability to tune the dispersion relation of light has raised large interest and led to rapid growth of the field of plasmonic research. The parallel development of nanoscale fabrication techniques like electron beam lithography or focused ion beam milling, has opened up new ways to structure metals surfaces and control SPP propagation and dispersion at the nanoscale.

The large field enhancement of SPPs localized at the metal surface makes SPPs very sensitive to changes in the permittivity of the adjacent dielectric. By functionalizing the metal surface, biological molecules or chemicals can be selectively bound to the surface, shifting the wavelength of the SPP resonance [90,91,92,105]. Research in this field is far advanced and sensors relying on the effect of the surface plasmon resonance.

Similarly, SPPs can be used to efficiently couple sunlight into waveguide modes of thin semiconductor layers. The strong field enhancement and guiding properties of SPPs increase in this case the light absorption and thereby the efficiency of thin-film semiconductor solar cells [105]. So far, the excitation of SPPs is mostly performed using far-field optical techniques which have a resolution that is larger than plasmonic phenomena under investigation. However, for true nanoscale plasmonic studies a SPP point source with nanoscale dimensions is required.

To manipulate SPPs on a surface, reflectors are needed. So far, macroscopic Bragg reflectors structured into the surface have been used. For true nanoscale integration, nanoscale SPP mirrors are required and a question is, how these can be made. Once these are realized, nanoscale cavities to confine SPPs can also be designed. The limits to the plasmonic cavity mode volumes and quality factor are not yet known.

And finally, the use of a particle beam rather than a light beam to excite SPP raises questions and novel opportunities regarding the selectivity with which surface plasmon modes with different symmetry can be excited.

We obtained Au, Al Plasmon, using the samples describes in the **section 2.8.**

However there are under investigation, we can see in **fig 3.4.3.**

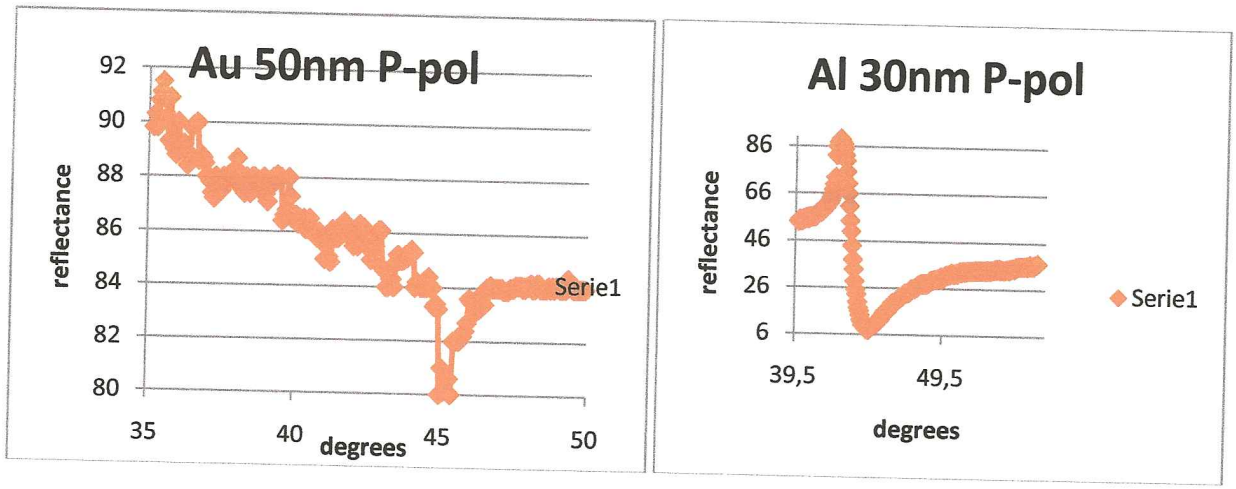

Fig.3.4.1 Au Plasmon obtained by Kretschman configuration **Fig.3.4.2** Al Plasmon obtained by Kretschman configuration

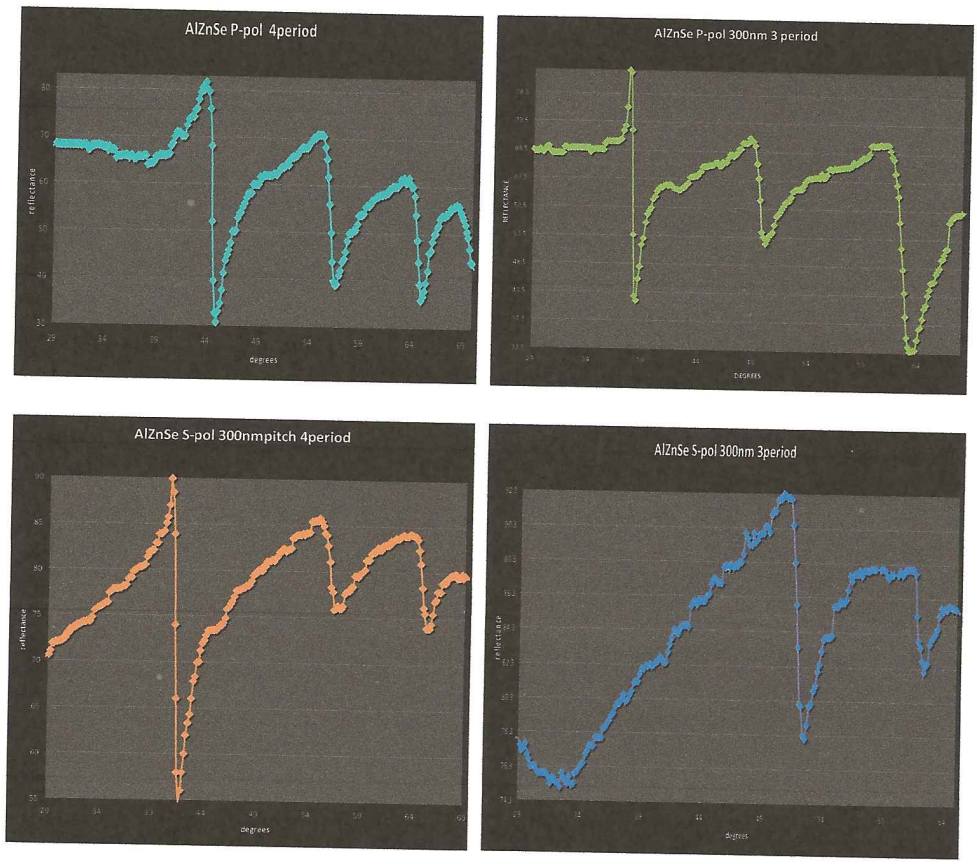

Fig.3.4.3 We obtained the similar dip in the same angle, only for 4period in P-pol and for first time S-pol the hypothesis, we obtained a surface multiple plasmonics, but this is still under study

AKNOWOLEDGMENTS:

Ringrazio infinitamente **all'UNIVERSITA' DELLA CALABRIA** per darmi l'opportunità di continuare a crescere, al carissimo Giovanni Desiderio per la sua pazienza tutto questo tempo,
A Carlo Vena, Marco Castriota per i suo consigli, ad Angela Fasanella per il lavoro accurato che ha fatta per me in Raman, a Federica Ciuchi per il carissimo appoggio nel mio lavoro in RX.
E finalmente a CARLO VERSACE.

REFERENCE

[1] V.Zwiling, M. Aucuoturier, E. Darque-Ceretti. Anoidc oxidation of titanium and TA6V alloy in chromic media. An electrochemical approach, Electrochimica Acta 45(1999) 921-929

[2] Proceeding of world academy of science and technology volume 30 July 2008 1307-6984.

[3] J.M. Macak, H. Tsuchiya , A. Ghicov, K. Yasuda , R. Hahn, S. Bauer, P. Schmuki. TiO_2 nanotubes: Self-organized electrochemical formation,
properties and applications. Solid State and Materials Science 11 (2007) 3-18

[4] Sergiu P. Albu, D. Kim, and P. Schmuki. Growth of Aligned TiO2 Bamboo-Type Nanotubes and Highly Ordered Nanolace. Angew. Chem. Int. Ed 2008 47 1916-1919.

[5] Sergiu P. Albu, Andrei Ghicov, Jan M. Macak, and Patrik Schmuki. 250 μm long anodic TiO_2 nanotubes with hexagonal self-ordering p hys.stat. sol. (RRL) 1, No. 2, R65–R67 (2007) / DOI 10.1002/pssr.200600069.

[6] A. Ghicov, H. Tsuchiya, J. M, and P. Schmuki. Annealing effects on the photerresponse of TiO_2 nanotubes Phy. stat. sol. (a) 203,N 4 R28-R30 (2006)

[7] E. Balaur, J. M. Macak, L. Taveira, P. Schmuki. Tailoring the wettability of TiO_2 nanotube layers Electrochemistry Communications 7 (2005) 1066–1070.

[8] D. Kim, Andrei Ghicov, S. P. Albu, and P. Bamboo-Type TiO_2 Nanotubes: Improved Conversion Efficiency in
Dye-Sensitized Solar Cells Schmuki.J. AM. CHEM. SOC. 2008, *130*, 16454–16455

[9] I. Paramasivam, A. Avhale, A Inayat, A. Bosmann2, P. Schmuki. And W Schwieger. MFI-type (ZSM-5) zeolite-filled TiO_2 nanotubes for enhanced photocatalytic activityNanotechnology 20 (2009) 225607 (5pp)

[10] A. Valota, D.J. LeClere, P. Skeldon, M. Curioni, T. Hashimoto, S. Berger , J. Kunze, P. Schmuki, G.E. Thompson. Influence of water content on nanotubular anodic titania formed in fluoride/glycerol electrolytes Electrochimica Acta 54 (2009) 4321–4327

[11] C. A. Grimes. Synthesis and application of highly ordered arrays of TiO_2 nanotubes.J. Mater. Chem., 2007, 17, 1451–1457

[12] O. K. Varghese, M. Paulose and C. A. Grimes. Long vertically aligned titania nanotubes on transparent conducting oxide for highly efficient solar cells, NATURE NANOTECHNOLOGY September 2009

[13] D. Gong, Craig A. Grimes, and O. K. Varghese. Titanium oxide nanotube arrays prepared by anodic oxidation J. Mater. Res., Vol. 16, No. 12, Dec 2001 3333

[14] M. Paulose, H. E. Prakasam, O. K. Varghese, L. Peng, Ketul C. Popat, G. K. Mor, T. A. Desai, and C. A. Grimes. TiO_2 Nanotube Arrays of 1000μm Length by Anodization of Titanium Foil: Phenol Red Diffusion. *J. Phys. Chem.* C 2007, *111,* 14992-14997

[15] M. Paulose, Lily Peng, Ketul C. Popat, O. K. Varghese, T. J. LaTempa, N. Bao, Tejal A. Desai, C. A. Grimes.Fabrication of mechanically robust, large area, polycrystalline nanotubular/porous TiO_2 membranes Journal of Membrane Science 319 (2008) 199-205

[16] Prashant V. Kamat. Meeting the Clean Energy Demand: Nanostructure Architectures for Solar Energy Conversion Prashant J. Phys. Chem. C, Vol. 111, No. 1, 2007

[17] K. Shankar, J. I. Basham, N. K. Allam, Oomman K. Varghese, Gopal K. Mor, Xinjian Feng, Maggie Paulose, Jason A. Seabold, Kyoung-Shin Choi, and Craig A. Grimes. Recent Advances in the Use of TiO2 Nanotube and Nanowire Arrays for Oxidative Photoelectrochemistry. *J. Phys. Chem. C* 2009, *113,* 6327–6359

[18] Gopal K. Mor , Oomman K. Varghese , Maggie Paulose , Keat G. Ong , Craig A. Grimes.Fabrication of hydrogen sensors with transparent titanium oxide nanotube-array thin films as sensing elements.Thin Solid Films 496 (2006) 42-48

[19] MOR G K, VARGHESE O K, PAULOSE M, GRIMES C A. Transparent highly ordered TiO_2 nanotube arrays via anodization of titanium thin films. Adv Funct Mater, 2005, 15(8): 1291-1296.Adv.

[21] J.C. Manifacier, J. P.Fillard.A simple method for the determination of the optical constants n, k and thethickness of a weakly absorbing thin film. J. Phys. E. 1976, 9, 1002 .

[22] Wilaiwan Chanmanee,Apichon Watcharenwong,C. Ramannair Chenthamarakshan, Puangrat Kajitvichyanukul, Norma R. de Tacconi,, and Krishnan Rajeshwar, Formation and Characterization of Self-Organized TiO_2 Nanotube Arrays by Pulse Anodization.J. AM. CHEM. SOC. 2008, 130, 965-974

[23]S. Yoriya, M. Paulose, O. K. Varghese,Gopal K. Mor, andC. A. Grimes, Fabrication of Vertically Oriented TiO_2 Nanotube Arrays Using Dimethyl Sulfoxide Electrolytes.J. Phys. Chem. C 2007, 111, 13770-13776

[24] Karthik Shankar, Gopal K Mor, Haripriya E Prakasam,Sorachon Yoriya, Maggie Paulose, Oomman K VargheseandCraig A Grimes.Highly-ordered TiO_2nanotube arrays up to 220μm length: use in water photoelectrolysis and dye-sensitized solarcells.Nanotechnology 18 (2007) 065707 (11pp)

[25] A. ALADJEM. Anodic oxidation of titanium and its alloys Journal of Materials Science, vol. 8, issue 5, pp. 688-704.

[26] P. PASCAL, "Nouveau Trait6 de Chimie Minerale",14 (Masson & Cie, Paris 1963).

[27] V. ANDREEVA and v. KAZARIN, "Proc. Internat. Conf. Met. Corrosion. 1966" ("Mir Moscow, 1969) pp. 464-472.

[28] V. ANDREEVA and N. SHISHAKOV, Z. Fiz. Khim. 32 (1958) 1671.

[29] S. MORIOKA and A. UMEZONO, Nippon Kinzoku Gakkaishi 20 (1956) 403.

[30] A. VHH, Electrochimica Acta 14 (1969) 921.

[31] D. FRANZ H. GOEHR, Ber. Binsenges. Physik Chem. 67(7) (1963) 680.

[32] A. BOGOYAVLENSKII. BORODINA, pp. 440.

[33] YA. KOLOTYRKIN and V. STRUNKIN, Zashchita Metallov 6 (1970) 511

[34] L. DZHAPARIDZE, D. OTIASHVILI, A. SHAKARISHV1LI, V. PRUIDZE, ARID R. CHAGUNAVA,Pererabotka Margan. Polimet. Rud. Gruz. (1970) 130.

[35] A. KRASIL'SHCHIKOV, "Proc. III Inter. Conf. Met.Corrosion 1966" ("Mir", Moscow, 1968) pp. 327-335

[36]W. DORNELAS, Thesis, University of Paris, 21Metallov 4(6) (1968) 656.

[37] J. COTTON, "Proc. III Internat. Conf. Met.Corrosion, 1966" ("MW', Moscow, (1969) pp. 334-5

[38] A. ALADJEM, M. AUCOUTURIER, andP. LACOMBE, J. Mater. Sci. 8 (1973).

[39] L. Young, Anodic Oxide Films, Academic Press, London,1961.

[40] G.E. Thompson, Thin Solid Films 297 (1997) 192.

[41] Young L. Anodic oxide films. New York: Plenum; 1961.

[42] Vermilyea DA. Anodic films. In: Advances in electrochemistry and electrochemical engineering. London: Wiley; 1963. p. 248.

[43] Marchenoir JC, Loup JP, Masson J. Thin Solid Films 1980;66:357.J. E´ tude des couches poreuses forme´es par oxydation anodique du titane sous fortestensions. Thin Solid Films 1980;66:357–369.

[44] Marchenoir J-C, Gautron J, Loup JP. Metaux Corrosion-industrie 1977:83.

[45] Beranek R, Hildebrand H, Schmuki P. Self-Organized Porous Titanium Oxide Prepared in H2SO4/HF Electrolytes. Electrochem. Solid-State Lett., Volume 6, Issue 3, pp. B12-B14 (2003)

[46] Bauer S, Kleber S, Schmuki P. TiO_2 nanotubes: Tailoring the geometry in H3PO4/HF electrolytes. Electrochemistry Communications 8 (2006) 1321–1325.

[47] J.M. Macaka, H. Hildebranda, U. Marten-Jahnsa and P. SchmukiMechanistic aspects and growth of large diameter self-organized TiO_2 nanotubes. Journal of Electroanalytical Chemistry 621 (2008) 254–266.

[48] Varghese OK, Gong D, Paulose M, Grimes CA, Dickey EC. J.Crytallization and high-temperaturestructural stability of titanium oxide nanotubes arrays. DOI: 10.1557 /JMR.2003.0022

[49] Ghicov A, Tsuchiya H,Jan M Macak , Schmuki P. Annealing effects on the photoresponse of TiO_2 nanotubes. Physica Status Solidi A: Applications and Materials Science (2006), 203(4), R28-R30 CODEN: PSSABA; ISSN: 0031-8965.

[50] J. Zhao, X. Wang, T. Sun and L.Li.In situ templated synthesis of anatase single-crystal nanotube arrays. Nanotechnology 16 (2005) 2450–2454.

[51] Albu SP, submitted for publication.

[52] S. Funk, B. Hokkanen, U. Burghaus, A. Ghicov, and P. Schmuki "Unexpected adsorption of oxygen on TiO_2 nanotube arrays: Influence of crystal structure" Nano Letters 7 (2007) 1091.

[53] B. Hokkanen, S. Funk, U. Burghaus, A. Ghicov, and P. Schmuki "Adsorption kinetics of alkanes on TiO_2 nanotubes array – structure–activity relationship", Surface Science 601 (2007) 4620–4628.

[54] O'Regan B, Gra¨tzel M. A low-cost, high-efficiency solar cell based on dye-sensitized colloidal TiO_2 films Nature 1991;353:737.

[55] M Grätzel , "Photoelectrochemical Cells" Nature 414, 338-344 (2001).

[56] Amy L. Linsebigler, Guangquan Lu, and John T. Yates, Jr. Photocatalysis on TiO_2 Surfaces: Principles, Mechanisms, andSelected Results.Chem Rev 1995;95735.758

[57] M. R. Hoffmann, S. T. Martin, W. Choi, and D.W. Environmental Applications of Semiconductor Photocatalysis.Chem. Rev. 1995, 95, 735-758.

[58] Asahi R, Morikawa T, Ohwaki T, Aoki A, Taga Y. Visible-light photocatalysis in nitrogen-doped titanium oxides. Science2001;293:269.

[59] J. Siejka, C. Ortega, An O18 Study of Field-Assisted Pore Formationin Compact Anodic Oxide Films on Aluminum J. Electrochem. J. Electrochem. Soc., Volume 124, Issue 6, pp. 883-891 (1977)

[60] G.E.Thompson.Porous anodic alumina.Solid Films 297 (1997) 192.

[61] A. Pakes, G.E. Thompson, P. Skeldon, P.C. Morgan, Corros. Sci. 45 (2003) 1275.

[62] Gopal K. Mor, Oomman K. Varghese, Maggie Paulose. Solar Energy Materials & Solar Cells 90 (2006) 2011–2075

[63] A. Taflove, Computational Electrodynamics: The Finite-Difference Time-Domain Method, Artech HouseInc., Boston, 1995.

[64] K.G. Ong, O.K. Varghese, G.K. Mor, C.A. Grimes, Water-Photolysis Properties of Micron-Length Highly-Ordered Titania Nanotube-Arrays.Volume 5, Number 7, July 2005 , pp. 1158-1165(8).

[65] J.A. Roden, S.D. Gedney, Microwave Opt. Technol. Lett. 14 (1997) 71.

[66] A. Z. Sadek,, H. Zheng, Kay Latham, W. Wlodarski, and
K. Kalantar-zadeh, Anodization of Ti Thin Film Deposited on ITO. Langmuir 2009, Vol. 25, N 1 509-514

[67] W. Chanmanee, A. Watcharenwong, C. Chenthamaraskshan, P. Kajitvichyanukul, Norma R. de Tacconi, and K. Rajeshwar.Formation and Characterization of Self-Organized TiO_2 Nanotube. J. AM. CHEM.SOC. 2008,130 965-974.

[68] X. Yu, Y. Li, W. Wlodarski. Fabrication of nanostructured TiO2 by anodization:A comparison between electrolytes and substrates. Sensors and Actuators B 130 (2008) 25–31.

[69] TANG Yu-xin, TAO Jie, ZHANG Yan-yan, WU Tao, TAO Hai-jun, ZHU Ya-rong Preparation of TiO_2 nanotube on glass by anodization of Ti films at room temperature Trans. Nonferrous Met.Soc. China 19(2009) 192-198.

[70] Q. Cai a, L. Yang , Y. Yu.Investigations on the self-organized growth of TiO_2 nanotube arrays by anodic oxidization. Thin Solid Films 515 (2006) 1802–1806

[71] H Yin, H Liu and W Z Shen. The large diameter and fast growth of self-organized TiO_2 nanotubes arrays achieved via electrochemical anodization. Nanotechnology 21 (2010) 035601 (7pp)

[72] Srimala Sreekantan , Roshasnorlyza Hazan, Zainovia Lockman Photoactivity of anatase–rutile TiO_2 nanotubes formed by anodization method.thin Tin Solid Films 518 (2009) 16-21

[73] Kurt W. Kolasinki "SURFACE SCIENCE" Second edition 2008

[74] P. W. Tasker, The stability of ionic crystal surfaces. J. Phys. C, 12 (1979) 4977.

[75] U. Diebold, Surf.Sci. Rep , 48 (2003) 53.

[76] Solid State Chemistry. Synthesis, structure, and properties of Selected Oxides and Sulfides Aaron Wold Kirby Dwight. Chapman and Hall, Inc. New York

[77] LINUS P. THE CHEMICAL BOND, LONDON OXFORD UNIVERSITY PRESS 1967.

[78] Chemical Physics Letters 428 (2006) 421-425

[79] Abu Z. Sadek,, Haidong Zheng, Kay Latham, Wojtek Wlodarski, and Kourosh Kalantar-zadeh Anodization of Ti thin film Deposited on ITO. Lanmuir 2009, 25, 509-514

[80] Gopal K. Mor, Karthik Shankar, Maggie Paulose, Oomman K Varghese, and Craig A. Grimes

Use of Highly-Order TiO_2 Nanotubes Arrays in Dye-Sensitized Solar Cells NANO LETTERS 2006 VOL. 6, N 2 215-218.

[81] Shang-Di Mo and W.Y. Ching. Electronic and properties of three phases of titanium dioxide:Rutile, anatase, and brookite PHYSICAL REVIEW B.

[82Zhongchun. Wang, Ulf.Helmersson, Per-Olov Ka¨ll.Optical properties of anatase TiO_2 thin films prepared by aqueous sol–gelprocess at low temperatureThin Solid Films 405 (2002) 50–54

[83] I. ABDULHALIM,M, ZOUROB, and A, LAKHTAKIA.
Surface Plasmon Resonance for Biosensing: A Mini-ReviewElectromagnetics, 28:214–242, 2008
Copyright © Taylor & Francis Group, LLC

[84] Kretschmann, E., & H. Raether. 1968. Radiative decay of nonradiative surface plasmons excited by light. Z. Naturforsch. A 23:2135–2136.

[85] E. Kretschmann, Die Bestimmung optischer Konstanten von Metallen durch Anregung von Oberflachenplasmachwingungen. Z. Physik 241, 313-324(1971)

[86] A, LAKHTAKIA. R, Messier Sculptured Thin Films, Nanoengineered Morphology and Optics. SPIE PRESS Bellingham, Washington USA 2005.

[87] R. Messier and A. Lakhtakia,Sculptured Thin Films-II. Experiments and applications, Mater Res Innovat (1999), 217-222.

[88] National Research Council, Condensed-matter and materials physics. Basic research for tomorrow's technology, National Academy Press, Washington, DC, USA, 1999.

[89] R. Messier, T. Gehrke, C. Frankel, V.C. Venugopal, W. Otano, andA. Lakhtakia, Engineered sculptured nematic thin films, J Vac Sci Technol A 15 (1997), 2148-2152.

[90] R. Messier, P. Sunal, and V.C. Venugopal, Evolution of sculptured thin films, Engineerend nanostructural films and materials (A. Lakhtakia and R.F. Messier, ads), Proc SPIE 3790, SPIE, Bellingham, WA, USA, 1999, 133-141.

[91] K. Robbie, M. J. Brett, and A. Lakhtakia. CHIRAL SCULPTURED THIN FILMS. NATURE .VOL 384 19/26 DECEMBER 1996

[92] John Polo, Michael Motyka, and Akhlesh Lakhtakia, Multiple Plasmonic modes with sculptured thin films. SPIE, 10.1117/2.1200810.1310 Page2/4

[93] M. M. Hasan, A. S. M. A. Haseeb, R. Saidur, and H. H. Masjuki Effects of Annealing Treatment on Optical Properties of Anatase TiO_2 Thin Films. World Academy of Science, Engineering and Technology 40 2008

[94] K. NARASIMHA RAO, M. A. MURTHY AND S. MOHAN, OPTICAL PROPERTIES OF ELECTRON-BEAM-EVAPORATED TiO2, FILMS. Thin Solid Films, 176 (1989) 181-186

[95] M. Stamate, I. Vascan, I. Lazar, G. Lazar, I. Caraman, M. Caraman. OPTICAL AND SURFACE PROPERTIES TiO2 THIN FILMS DEPOSITED by DC MAGNETRON

SPUTTERINGMETHOD. Journal of Optoelectronics and Advanced Materials Vol. 7, No. 2, April 2005, p. 771 - 774

[96] Craig A. Grimes Gopal K. Mor.TiO_2 Nanotube Arrays.Synthesis, Properties, and Applications,Springer Dordrecht Heidelberg London New York 2009.

[97] J. C. Manifacier, J Gasiot and J P Fillard. A simple method for the determination of the optical constants n, k and the thickness of a weakly absorbing thin film. Journal of Physics E: Scientific Instruments 1976 Volume 9

[98] Vogel R, Meredith P, Kartini I, Harvey M, Riches JD, Bishop A, Heckenberg N, Trau M, Dunlop HR (2003) Mesostructured dye-doped titanium dioxide for micro-optoelectronic applications. Chem Phys Chem 4:595–603

[99] S. CHANDRASEKHAR, F.R.S. LIQUID CRYSTAL CAMBRIDGE UNIVERSITYPRESS 2nded 1992.

[100] P. J. Collings and M. Hird. INTRODUCCION TO LIQUID CRYSTAL. Taylor & Francis Group, Ltd. 1997.

[101] R. Messier,V, C. Venugopal,P. D. Sunal, Origin and evolution of sculptured thin films. J. Vac. Sci. Technol. A, Vol. 18, No. 4, Jul/Aug 2000

[102] E. Balaur, J M. Macak, L. Taveira, P. Schmuki. Tailoring the wettability of TiO_2 nanotube layers. Electrochemistry Communications 7 (2005) 1066–1070

[103] M. Enachi , M. Stevens-Kalceff , I. Tiginyanu, V. Ursaki. Cathodoluminescence of TiO_2 nanotubes prepared by low-temperature anodization of Ti foils. Materials Letters, doi:10.1016/j.matlet.2010.07.028

[104] M. Enachi, M. Stevens-Kalceff, Ion Tiginyanu, V. Ursaki, Cathodoluminescence of TiO_2 nanotubes prepared by low-temperature anodization of Ti foils. http://dx.doi.org/10.1016/j.matlet.2010.07.028

[105] Yue Bing Zheng, and Tony Jun Huang. Surface Plasmons of Metal Nanostructure Arrays:From Nanoengineeringto Active Plasmonics.doi:10.1016/j.jala.2008.03.006

[106] Nageh K. Allam, and Craig A. Grimes. Room Temperature One-Step Polyol Synthesis of Anatase TiO2 NanotubeArrays: Photoelectrochemical Properties. Langmuir 2009, 25(13), 7234–7240

[107] K.S. Raja, T. Gandhi, M. Misra.Effect of water content of ethylene glycol as electrolyte for synthesis.Electrochemistry Communications 9 (2007) 1069–1076.

[108] A. P. Alivisatos. Semiconductor Clusters, Nanocristals, and Quantum Dots. Science VOL 271 16 FEBRUARY 1996.

[109] A. P. Alivisatos. Perspectives on the Physical Chemistry of Semiconductor Nanocrystals J. Phys. Chem. 1996, 100, 13226-13239

[110]Jiaguo Yu, Gaopeng Dai, and Baibiao Huang.Fabrication and Characterization of Visible-Light-Driven Plasmonic Photocatalyst Ag/AgCl/TiO_2 Nanotube Arrays. J. Phys. Chem. C 2009, 113, 16394–16401

[111] Hu JIANGTAO, TERI WANG ODOM, CHARLES M. LIEBER. CHEMISTRY and PHYSICS in one dimension: Synthesis and properties of Nanowires and nanotubes. Acc.Chem. Res.1999, 32, 435-445.

[112] R.S Wagner and W.C Ellis. VAPOR-LIQUID-SOLID MECHANISM OF SINGLE CRYSTAL GROWTH. APPLIED PHISYCS LETTERS Volume 4,Number 5, 89-90

[113] STEPHAN HOFMANN, RENUS SHARMA,CHISTOPH T. WIRTH, FELIPE CERVANTES-SODI, CATERINA DUCAT, TAKESHI KASAMA, RAFAEL E. DUNIN-BORKOWSKI, JEFF DRUCKER, PETER BENNETT AND JOHN ROBERTSON. Ledge-flow-controlled catalyst interface dynamics during Si nanowire growth. Nature materials VOL7 MAY 2008. Doi: 10.1038/nmat2140.

[114] YEWU WANG, VOLKER SCHMIDT,STEPHAN SENZ, ULRICH GUSELE. Epitaxial growth of silicon nanowires using an aluminium catalyst. Nature nanotechnology VOL 1, DECEMBER 2006, DOI:10.1038/nnano.2006.133.

[115] Hengzhong Zhang, Jillian F. Banfield. Phase transformation of nanocrystalline anatase-to-rutile via combined interface and surface nucleation. Materials Research Society Volume: 15 N 2 Pages: 437-448 DOI: 10.1557/JMR.2000.0067

[116] C.A Grimes,O. K. Varghese, S. Ranjan. Light, Water, Hydrogen: The solar production of Hydrogen by water photoeletrolysis. Springer, Norwell, MA. (2007).

[117] Ritchie, R. H. Plasma losses by fast electrons thin films. Phys. Rev. 106, 874-881(1957).

[118] William L. Barnes, Alain Dereux, Thomas W. Ebbesen. Surface Plasmon subwavelength optics. Nature Vol 424 14 August 2003 824-830 doi:10.1038/nature01937

[119] Wood, R. W. On a remarkable case of uneven distribution of light in a diffraction grating spectrum . Phil. Mag. 4 396 1902.

[120] M. Gopal. W. J Moberly Chan. L.C De Jonghe. Room temperature synthesis of crystalline metal oxides. Journal of Materials Science 32 (1997) 6001-6008.

[121] Y. Zheng, E. Shi, Z. Chen, L. Wenjun and H. Xingfang, Influence of solution concentration on the hydrothermal preparation of titania crystallites, *J. Mater. Chem.* 11 (2001) 1547.–1551.

[122] M. Castriota, T. Caruso, A. Policicchio, S. La Rosa, R.G. Agostino, E. Cazzanelli. Anomalous enhancement of Raman scattering of metal oxide film deposited on thermally treated ITO-coated glass substrates. Chemical Physics Letters 478 (2009) 195–199

[123] Jan-Yul Kim, Tohru Sekino, Dong Jin Park. Morphology modification of TiO_2 nanotubes by controlling the starting material crystallite size for chemical synthesis. Springer DOI 10.1007/s11051-010-9990-6.

[124] A. Roguska, A. Kudelski, M. Pisarek, M. Opara, M. Janik-Czachor. Raman investigations of SERS activity of Ag nanoclusters on a TiO_2 -nanotubes/Ti. Doi 10.1016/j.vibspec.2010.07.003

[125] I. Paramasivam, J.M, P.Schmuki. Photocatalytic of activity of TiO_2 nanotubes layers loaded with Ag and Au nanoparticles. Electrochemistry Communications 10 2008 71 75.

[126] Z. Wu, Fan Dong,Weirong Zhao, Haiqiang Wang, Yue Liu and Baohong Guan. The fabrication and characterization of novel carbon doped TiO2 nanotubes, nanowires and nanorods with high visible light photocatalytic activity. **Nanotechnology 20 (2009) 23701.**

[127] J. Xu, C. Jia, B. Cao, W.F. Zhang Electrochemical properties of anatase TiO2 nanotubes as an anode material for lithium-ion batteries. Electrochimica Acta 52 (2007) 8044–8047

[128] T MAIYALAGAN, B. VISWANATHAN and U.V. Varadarju. Fabrication and characterization of uniform TiO_2 nanotubes arrays by sol-gel template method. Bull Mater. Sci, Vol 29 N 7, December 2007 pp 705-708.

[129] K. Legarec, and S. Desgreniers, Raman Study of Single Anatase TiO_2 UP TO 70 Gpa. Solid State Communications,Vol 94 n 7 pp 519-524, 1995.

[130] W. F Zhang, Y. L He, M, S Zhang, Z Yin and Q Chen. Raman scattering study on anatase TiO_2 nanocrystals. J. Phys. D: Apply Phys. 33 2000 912-916.

[131] A. S. Vengurlekar. Extraordinary optical transmission through metal films with subwavelength holes and slits. CURRENT SCIENCE, VOL. 98, NO. 8, 25 APRIL 2010